RIBF Facility Upgrade Project

July 2023

RIKEN Nishina Center for Accelerator-Based Science (RNC)

理化学研究所
仁科加速器科学研究センター

Contents

1 RIBF as an internationally open-accessed leading facility for the low energy nuclear physics

The RIKEN Nishina Center for Accelerator-Based Science promotes science and technology development for “element transmutation” pioneered by Dr. Yoshio Nishina approximately 80 years ago, and is dedicated to answering two questions: “How were elements created by the universe?” and “Can humans change the elements at will?” Since the heavy-ion accelerator facility “Radioactive Isotope Beam Factory (RIBF)” constructed officially started operation in 2007, the facility has become a global center for research on the low energy nuclear physics while playing a global leadership role in the field.

As the name implies, the RIBF is a facility that supplies radioactive isotopes (RIs) as “beams,” and produces RI beams like a “factory.” Its RI beam intensity is famous worldwide, and has gathered users from around the world, and produced a wealth of outstanding research results. The intense RI beams are realized with combination of the high-performance heavy-ion accelerator complex and the large-acceptance inflight-separator. The superconducting ring cyclotron, the energy breeder at the final acceleration stage has delivered the intense primary beams, which are converted to radioactive isotopes via reactions at target. The reaction products of interest are collected and separated at inflight separator and hence are delivered as secondary beams. It would be emphasized that the accelerator system and inflight separator are optimized to obtain high intense fission products as secondary beams. The acceleration scheme was designed to deliver an intense uranium beam at an intermediate energy of 345 MeV/u and momentum and angular acceptance of the separator was fit for momentum and angular spread of fission products.

In addition to the intensity of RI beams, the other uniqueness of RIBF is three magnetic spectrometers equipped, which are complementary each other in terms of resolution and solid angle and are suitable for any styles of reaction studies. A storage ring dedicated to mass measurement is also uniquely designed to storage RI ions produced with continuous beams delivered at the cyclotron-based accelerator complex.

Since 2007, experimental programs with these spectrometers and the ring have been organized under international collaboration. Based on in-kind contributions of users in the world such as detectors or newly developed system, large-size collaborations have been formed to lead to so called “campaign-style” experiments to achieve efficient operation in terms of machine time, data production and manpower.

RIBF has contributed to the expansion of the nuclear chart by producing more than 150 new isotopes and has provided a multitude of opportunities to discover new phenomena originating from high-isospin asymmetry. Very selected research highlights in studying the nuclear structure are the determination of the neutron dripline in the F and Ne isotopes, appearance of a new magic number of N=34, discovery of the deformed halo nuclei ^{29}F, ^{31}Ne and ^{37}Mg, the double magicity in ^{78}Ni. Recently, the tetra-neutron state was observed with the two independent experiments, which has stimulated the community to investigate T=3/2 three-nucleon forces. The world-first heavy ion-collision with RI beams is giving the information on Equation-of-State of asymmetric nuclear matter. RIBF produced the world’s first neutron-rich nuclei involved in the r-process and succeeded in investigating their properties and demonstrated the impacts of experiment data. It is not an exaggeration to say that the RIBF pioneered the r-process research based on experimental results for the first time in history.

It would be emphasized that based on the intense RI beams available at RIBF, a new nuclear engineering program was launched to solve the problem of the high-level radioactive waste from nuclear power plants. In this program long-lived fission products in the waste were delivered as RI beams for reaction studies.

All the highlighted results above have been obtained due to the nice facility performances of RIBF. The success of RIBF has brought the great growth of the low energy physics community and has advanced construction plans of new inflight facilities abroad. FRIB (US) was completed in 2022 and started operation.

RAON (Korea), HIAF (China), and FAIR (Germany) are projects with their budget plan and construction currently underway. The designs of these worthy rival facilities also focus on the production of RI beams via fission reaction with a uranium beam.

Considering the uniqueness of RIBF and competitiveness with other facilities, we are proposing an RIBF upgrade project. The target region newly accompanied with the upgrade is proton-rich and heavy mass region at $Z>50$, where dynamical phenomena in nucleus such as alpha-clustering and fission will be studied with reactions. Such nuclear physics research aims to bring safe and nuclear-waste free energy source in the society 50-100 years later. The region will be accessed via projectile fragmentation not via fission with a more intense uranium beam. Not only the accelerator complex but also the inflight separator and detector systems are being upgraded to access the heavy region.

2 Progresses and prospects of physics

In this chapter, we will present the achievements of physics obtained at the RIBF since 2007 to present and the future perspective with the upgraded RIBF.

2.1 Programs FY2007 – 2022

2.1.1 New knowledge from newly observed isotopes

Since the RIBF started to provide beams, more than 150 new isotopes are produced using a variety of heavy-ion primary beams. Among them, discoveries of ^{31}F, ^{34}Ne [AHN19], ^{39}Na [AHN22] result in extension of the neutron dripline from previous Z = 8 (N = 16) to Z = 9 (N = 22), 10 (N = 24), and 11 (N = 28), which provides us with invaluable information on nuclear stability in the region between N=20 and 28 magic numbers. Discovery of the doubly magic ^{60}Ca [TAR18] also impacts theoretical mass models and implies existence of another doubly magic ^{70}Ca isotope.

On the neutron deficient side, it is found that ^{72}Rb with odd-number protons (Z = 37) and odd-number neutrons (N = 35) exists, while ^{73}Rb with even-number neutrons is unbound [SUZ17]. This contradicts, at least at a glance, a common sense of traditional nuclear physics which tells that a nucleus with even-number neutrons is more stable than one with odd-number neutrons, and hints existence of an unknown mechanism to stabilize nuclei near the proton dripline.

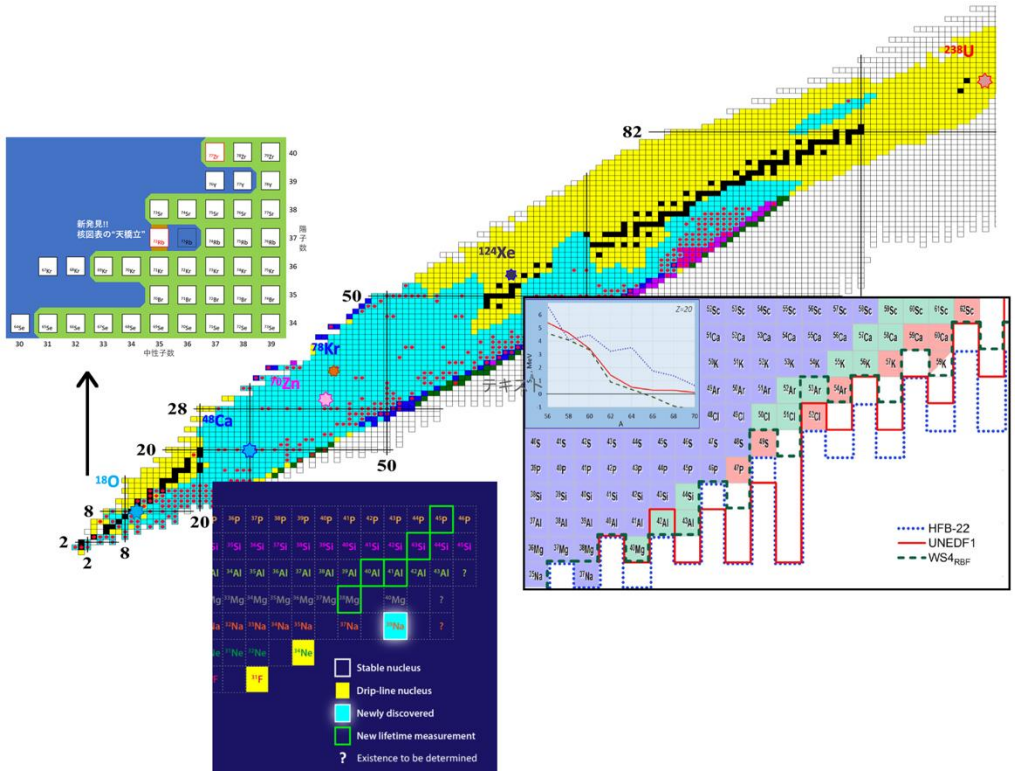

2.1.2 Shell evolution and universality of level inversion

One of the subjects focused during the last 15 years is shell evolution in the region far from the stability line, in particular appearance and disappearance of magic numbers. RIBF has discovered that 1) the island of inversion, known to be localized around Z = 12 and N = 20, has an extended structure covering N = 28 to east, and Z ~ 8/N = 20 to south [^{29}F: DOR17, ^{28}F: REV20]. It was also found the mechanism similar to the island of inversion is responsible for nuclear structure around Z ~ 28, N = 40. 2) A new magic number of N = 34

appears in the neutron-rich calcium isotopes [STE13]. 3) The Z = 28, N = 50 magicity in ^{78}Ni is persistent [TAN19].

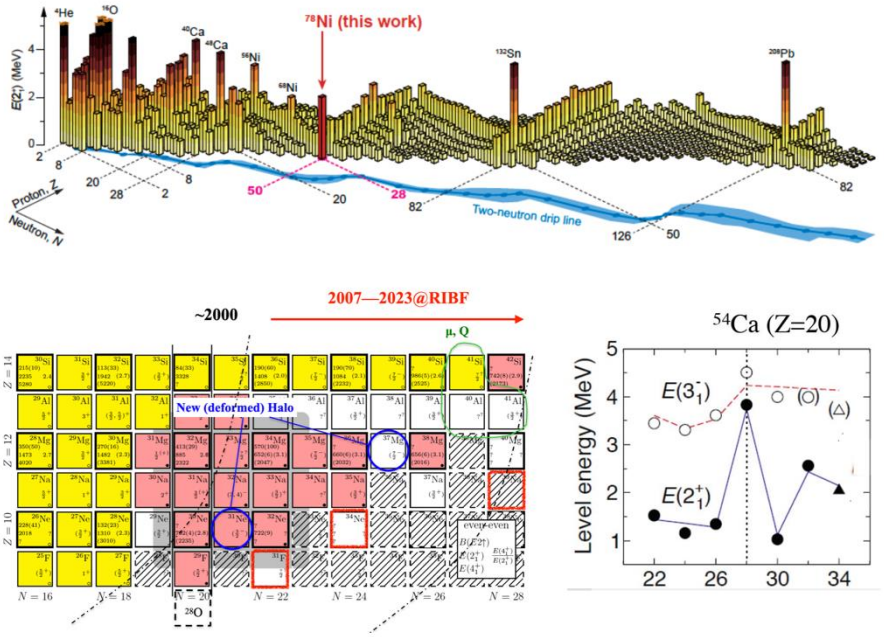

2.1.3 New forms of existence around the neutron drip-line

High-intensity neutron-rich beams from RIBF have been used to reveal new forms of existence near and beyond the neutron drip-line. Coulomb and nuclear breakup experiments at SAMURAI show that a new mechanism leading to occurrence of a neutron halo with a deformed core stabilize ^{31}Ne [NAK14] and ^{37}Mg [KOB14].

The (*p,pn*) knockout reaction experiment clarified previously-unknown feature of dineutron in Borromean nuclei, namely localization of the dineutron in ^{11}Li around the surface of the ^{9}Li core [KUB20]. This dineutron localization seems to be universal and occurs in ^{14}Be and ^{17}B, too [COR23].

The most remarkable outcomes relevant to the physics are discoveries of a tetraneutron state. A clear peak slightly above the four neutron threshold was first found in the double charge exchange ^{4}He(^{8}He,^{8}Be)^{4}n experiment at SHARAQ [KIS16]. Existence of the same structure was successfully confirmed in the recent SAMURAI experiment using ^{8}He(*p,pα*)^{4}n reaction [DUE22].

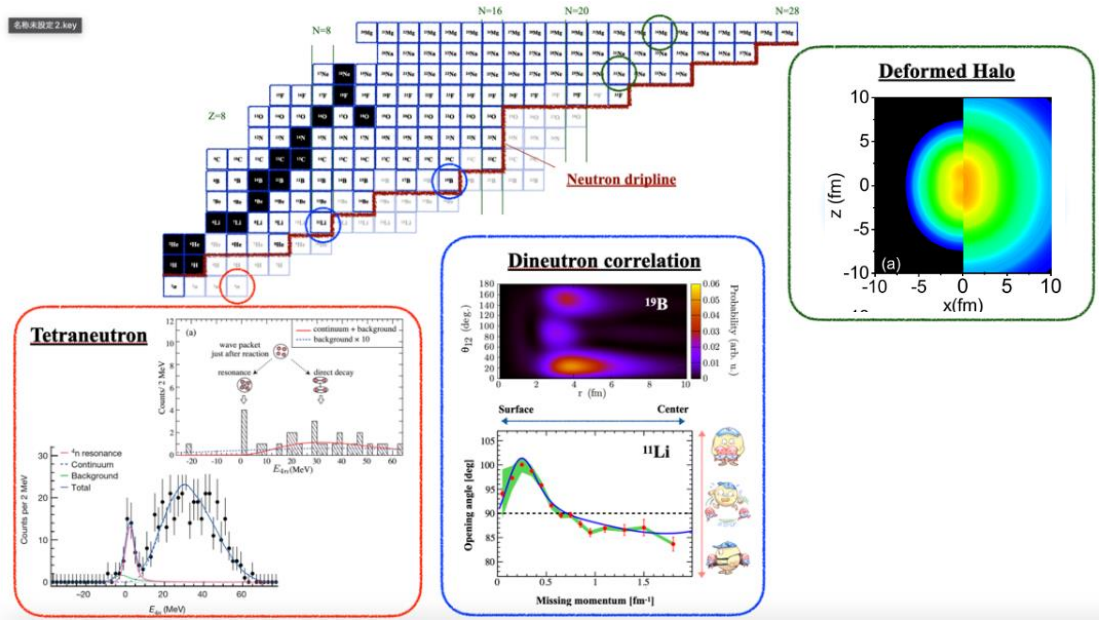

2.1.4 Nuclear data to ground the r-process research

RIBF is the first accelerator facility that enables access to r-process nuclei. Using inflight fission of ^{238}U, nuclei along and close to r-process paths are produced and provided to experiments. RIBF r-process studies started with lifetime measurements with the EURICA setup. From the EURICA campaign, 150 new half-life data and 326 improved half-life data have been obtained [XU14, LOR15]. It is followed by decay branching ratio measurements using high-efficiency neutron detectors under the BRIKEN collaboration. BRIKEN has succeeded in measuring one or two neutron emission branching ratio data after β-decays for 80 nuclides.

Now mass measurements of r-process nuclei are starting. Combined use of MR-TOF [IIM23], Rare RI Ring [LI22], and SHARAQ-OEDO [MIC18] when necessary will open broad research opportunities at RIBF.

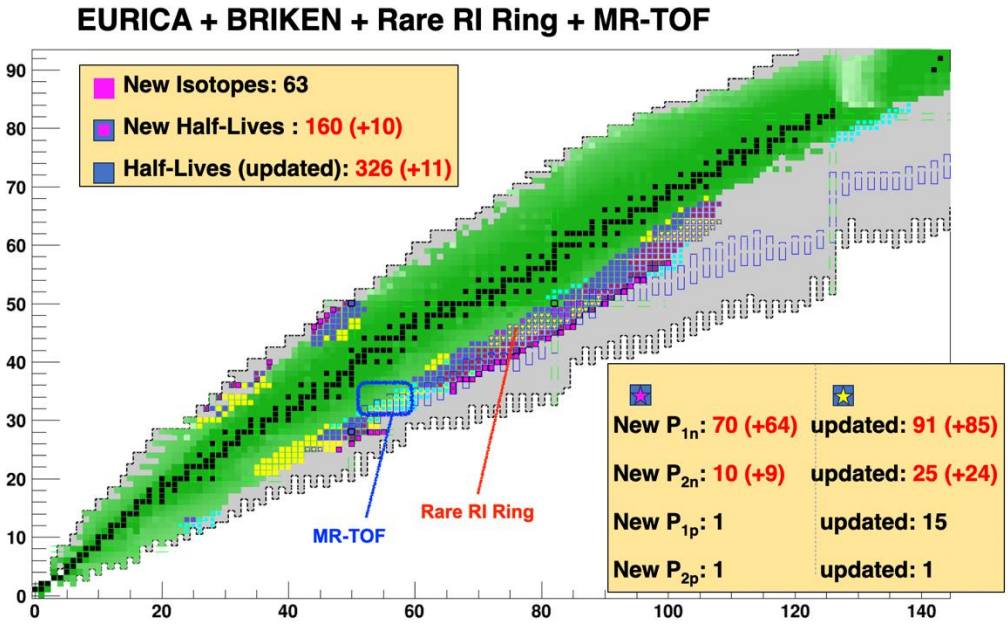

2.1.5 Properties of neutron-rich matter

Evolution of nuclear matter properties with an increasing neutron to proton ratio is another focused subject

at RIBF and has been investigated in a variety of viewpoints.

SπRIT at SAMURAI is the heavy-ion collision program at 200 to 300 MeV/u aiming at determination of the equation of state of neutron matter. The collaboration set up a large-volume time projection chamber in the gap of the SAMURAI magnet and observed particle emission from the collision of neutron-rich Sn isotopes. The measured π^+/π^- [EST21] and t/p [KAN21] ratios clearly support smaller values of L of 40 to 60 when compared with results of the recent transport theories.

Direct reactions also shed new lights on the properties of neutron-rich matter: The first observation of Gamow-Teller giant resonances in an unstable ^{132}Sn nucleus [YAS18] indicates the Landau-Migdal parameter g' doesn't significantly change with the neutron excess and gives a new constraint on occurrence of the pion condensation in dense neutron-rich matter. Quasi-free knockout reaction study of single particle strengths in neutron-rich and deficient oxygen isotopes shows a weak dependence of the reduction factor on the neutron-proton separation energy difference [KAW18]. Other direct reaction programs such as the active-target measurements of isoscalar monopole strengths in ^{132}Sn, the proton elastic scattering experiments to determine proton- and neutron-density distributions in ^{132}Sn are ongoing. Recently, the SCRIT collaboration has succeeded, for the first time, in performing the electron elastic scattering experiment for an unstable ^{137}Cs [TSU23]. The neutron and proton density distributions determined by the proton and electron elastic scatterings, respectively, will provide us with accurate data of the neutron-skin thickness in neutron-rich nuclei.

2.1.6 The first step towards transmutation of nuclear waste

Nishina Center initiated a basic science program aiming at reduction of high-level radioactive waste through nuclear transmutation, in particular, on fission products. Taking full advantages of high-intensity RI beams produced from in-flight fission of a uranium beam and methodologies of inverse-kinematics reaction, the collaboration took cross section data for spallation reactions induced by proton and deuteron in a wide range of incident energies. The data clearly show that long-lived fission products can be efficiently transmuted to stable or short-lived radioactive nuclides by the reactions.

2.1.7 References

[AHN19] D.S. Ahn et al., Phys. Rev. Lett. 123, 212501 (2019)
https://doi.org/10.1103/PhysRevLett.123.212501
[AHN22] D.S. Ahn et al., Phys. Rev. Lett. 129, 212502 (2022)
https://doi.org/10.1103/PhysRevLett.129.212502
[COR23] A. Corsi et al., Phys. Lett. B 840, 137875 (2023)
https://doi.org/10.1016/j.physletb.2023.137875
[DOR17] P. Doornenbal et al., Phys. Rev. C 95, 041301 (R) (2017)
https://doi.org/10.1103/PhysRevC.95.041301
[DUE22] M. Duer et al., Nature 606, 678 (2022)
https://doi.org/10.1038/s41586-022-04827-6
[EST21] J. Estee et al., Phys. Rev. Lett. 126, 162701 (2021)
https://doi.org/10.1103/PhysRevLett.126.162701
[IIM23] S. Iimura et al., Phys. Rev. Lett. 130, 012501 (2023)
https://doi.org/10.1103/PhysRevLett.130.012501
[KAN21] M. Kaneko et al., Phys. Lett. B 822, 136681 (2021)
https://doi.org/10.1016/j.physletb.2021.136681

[KAW18] S. Kawase et al., Prog. Theor. Exp. Phys. 2018, 021D01 (2018)
https://doi.org/10.1093/ptep/pty011
[KIS16] K. Kisamori et al., Phys. Rev. Lett. 116, 052501 (2016)
https://doi.org/10.1103/PhysRevLett.116.052501
[KOB14] N. Kobayashi et al., Phys. Rev. Lett. 112, 242501 (2014)
https://doi.org/10.1103/PhysRevLett.112.242501
[KUB20] Y. Kubota et al., Phys. Rev. Lett. 125, 252501 (2020)
https://doi.org/10.1103/PhysRevLett.125.252501
[LI22] H.F. Li et al., Phys. Rev. Lett. 128, 152701 (2022)
https://doi.org/10.1103/PhysRevLett.128.152701
[LOR15] G. Lorusso et al., Phys. Rev. Lett. 114, 192501 (2015)
https://doi.org/10.1103/PhysRevLett.114.192501
[MIC18] S. Michimasa et al., Phys. Rev. Lett. 121, 022506 (2018)
https://doi.org/10.1103/PhysRevLett.121.022506
[NAK14] T. Nakamura et al., Phys. Rev. Lett. 112, 142501 (2014)
https://doi.org/10.1103/PhysRevLett.112.142501
[REV20] A. Revel et al., Phys. Rev. Lett. 124, 152502 (2020)
https://doi.org/10.1103/PhysRevLett.124.152502
[STE13] D. Steppenbeck et al., Nature 502, 207 (2013)
https://doi.org/10.1038/nature12522
[SUZ17] H. Suzuki et al., Phys. Rev. Lett. 119, 192503 (2017)
https://doi.org/10.1103/PhysRevLett.119.192503
[TAN19] R. Taniuchi et al., Nature 569, 53 (2019)
https://doi.org/10.1038/s41586-019-1155-x
[TAR18] O.B. Tarasov et al., Phys. Rev. Lett. 121, 022501 (2018)
https://doi.org/10.1103/PhysRevLett.121.022501
[TSU23] K. Tsukada et al., Phys. Rev. Lett. in press.
[XU14] Z.Y. Xu et al., Phys. Rev. Lett. 113, 032505 (2014)
https://doi.org/10.1103/PhysRevLett.113.032505
[YAS18] J. Yasuda et al., Phys. Rev. Lett. 121, 132501 (2018)
https://doi.org/10.1103/PhysRevLett.121.132501

2.2 Prospects for the next 20 years

In this section, we will present the long-term goals of physics that will be pursued in the upgraded RIBF.

The goal of the upgraded RIBF in a long-term perspective will be the understanding of the structure and dynamics of heavy element RIs, especially in the region accessed by the projectile fragmentation reaction of a uranium beam. The upgraded RIBF will offer great opportunities to investigate the north area of the nuclear chart, which presently remains an unreached territory for the RIBF. The richness in the structure and dynamics expected in this region, as described below, will be fascinating in terms of the physics of many-body nuclear systems and far-reaching on other disciplines such as astrophysics, medical application, or energy resources.

This ultimate goal, defined as Pilar 3 in this report, will require the totality of the knowledge on atomic nuclei and of the theoretical and experimental techniques that have been developed at the RIBF. Therefore, Pillar 3 will be based on other two Pillars that represent evolutional extensions of the research initiatives practiced at the present RIBF; Pillar 1, the understanding of the nuclear force, especially the three-nucleon force (3NF), and Pillar 2, the understanding of the physics of the continuum. Pillar 1 (3NF) and Pillar 2 (continuum) are of utmost importance in low-energy nuclear physics today, and closely linked to various phenomena expected in

heavy element RIs, thus providing a foundation to challenge Pillar 3.

In the following, we will overview three Pillars with physics interests and envisioned experiments at the upgraded RIBF.

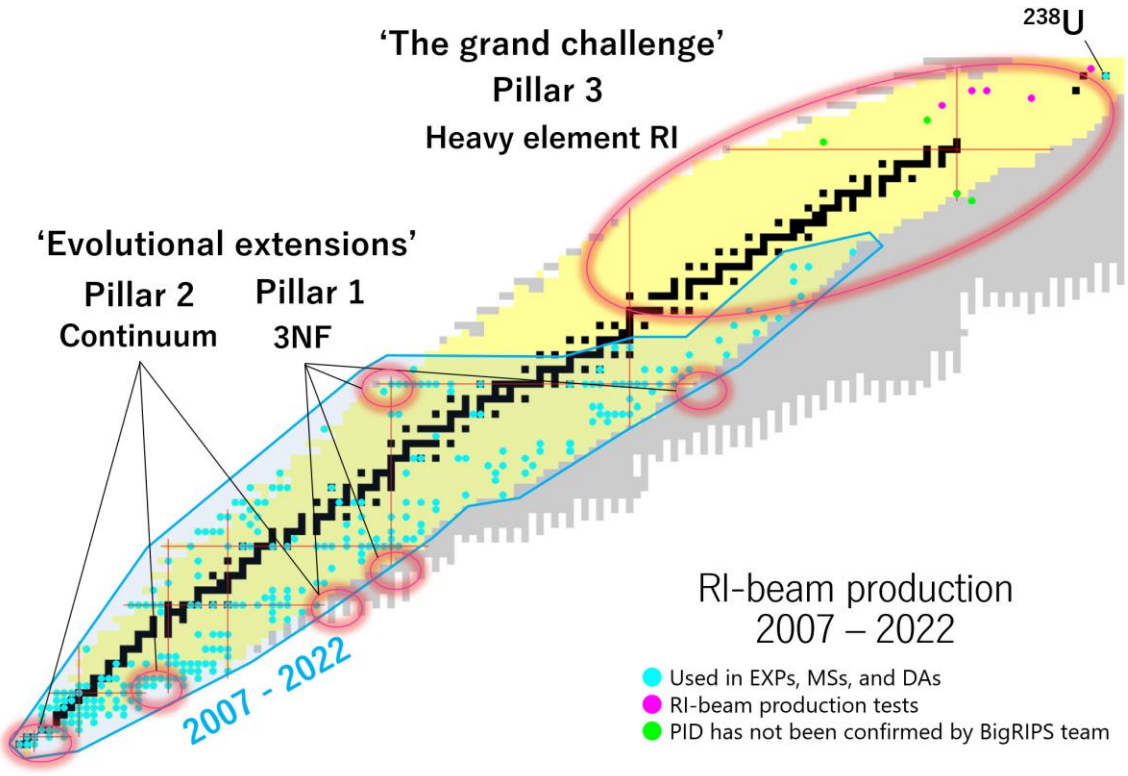

Figure 41 Summary of three Pillars of physics in the upgraded RIBF. The nuclear chart is taken from Chapter 3.

2.2.1 Pillar 1: How does the three-body force organize nuclear many-body systems?

Understanding the nature of nuclear forces, particularly the properties of three-body forces, and how they manifest in the properties of nuclear many-body systems is a crucial task that remains in nuclear physics. Obviously, high-precision theoretical and experimental studies of the scattering and resonances of few-nucleon systems are indispensable.

Furthermore, three-body forces have a significant impact on the properties of finite mass nuclei, for example, the position of the dripline. RIBF can provide such valuable information. It is also important to promote the theoretical studies that make use of the data from RIBF to reveal the nature of 3NF and predict the properties of nuclei in a broader area in the nuclear chart.

Deeper understanding of the three-body forces will shed light on the properties of the unstable nuclei as well as the EOS of nuclear matter at high densities. For example, we have an intriguing question of how much three-body forces influence the magnitude of LS splitting. This question will be answered through the research of the mass region beyond ^{78}Ni and ^{132}Sn.

Short to long-term future

A. Nature of (sub-)shell closures at ^{100}Sn ($Z = 50$, $N = 50$), ^{140}Sn ($Z = 50$, $N = 90$) and ^{60}Ca ($Z = 20$, $N = 40$)

   These RIs with (semi-)magic numbers are currently at the limit of production for spectroscopy and will be more available in the upgraded RIBF. Most of the data obtained so far supports that the shell gaps persist in these nuclei. Nonetheless, the shell closures have not yet been tested directly with these nuclei lacking

the level scheme information. The direct observation of their first 2^+ states by in-beam γ-ray spectroscopy will be very important. A comprehensive data of RIs in each region will help quantify the detailed properties of the shell closures, such as the shell gap energies.

B. Island of Inversion in the region beyond doubly-magic ^{78}Ni (Z = 28, N = 50)

The Ni isotopes are now within reach for ab-initio methods such as Coupled Cluster and Valence Space In-Medium Renormalization Group (VS-IMSRG). Yet, the most important features of the region of ^{78}Ni are seemingly picked up only by effective interactions, such as PFSDG-U. This interaction, using a ^{60}Ca inert core, the *pf*-shell for protons and the *sdg*-shell for neutrons, strikingly reveals a rapid change in the shell structure in form of low-lying intruder configurations in ^{78}Ni, which may lead to deformed ground states in ^{76}Fe, and ^{74}Cr.

The possible breakdown of the shell closures at Z = 28 and N = 50 would create an Island of Inversion in the region beyond ^{78}Ni, where the deformed ground states dominate. This would impact not only the structural characteristics of RIs in this region, but also the nuclear ground state masses. The latter governs the r-process path running across the region beyond ^{78}Ni. The consequence would thus be far-reaching.

The even-even ^{76}Fe, ^{74}Cr or ^{80}Ni nuclei beyond ^{78}Ni will be available in the upgraded RIBF for in-beam γ-ray spectroscopy with the new scintillators array. The information of the first 2^+ states will be critical to establish the onset of the fifth Island of Inversion, if it occurs.

2.2.2 Pillar 2 : How do nuclear many-body systems get organized in continuum?

The advancement of experimental techniques has enabled the exploration of continuum across highly excited states and driplines. These are governed by many-body correlations rather than average single-particle behavior, and exhibit rich structures and dynamics, as illustrated by the discovery of the 4n resonance. The physics in this domain is a challenging task for theoretical research, requiring seamless discussions bridging bound and unbound states. Understanding resonances near the neutron drip line and phenomena like 2p decay is crucial for comprehending the multi-particle tunneling effects observed in heavier systems, including α decay and rare cluster decays.

Short to long-term future

A. Next step for tetra neutrons research

Near-future SAMURAI experiments will probe nature of multi-neutron states and their stabilizing mechanisms more deeply from several different angles: 1) Neutron-neutron correlations in multi-neutron states will be investigated through detection of all the decay neutrons. The neutron detection capability of the SAMURAI setup reinforced by addition of NEBULA-Plus arrays from LPC-Caen and HIME arrays from TITech and TU Darmstadt will result in unprecedentedly high statistics multi-neutron data. 2) Multi-neutron states will be produced from different initial states using several cluster knockout reactions. 3) Superheavy hydrogen ($^{7-9}$H), helium ($^{10-12}$He), and litium ($^{13-15}$Li) isotopes , and their decays accompanying multi-neutron emissions will be studied. In all the experiments, newly-developed telescope arrays for charged particles, Straβe-CATANA+ and TOGAXSI, will be introduced to significantly enhance the experimental efficiencies.

B. Multi-neutrons correlations in the vicinity of ^{24}O and ^{60}Ca

In terms of the multi-neutron physics, it is also important to investigate the multi-neutron correlations in atomic nuclei and connect them to the resonances of 4*n* and possibly 6*n* in continuum. The region around the doubly-LS-closed shell nuclei ^{24}O and ^{60}Ca will be ideal playgrounds. For instance, ^{26,28}O with extra neutrons will be interesting for the investigation of 2*n* and 4*n* correlations. The SAMURAI-NEBULA+ system will be powerful for the complete kinematical reconstruction of emitted neutrons.

C. Magnetized nuclear bulk in heavy ion collision

Heavy ion collisions, primarily aimed at the investigation of EOS, are also a tool to create a drip of bulk nuclear matter in the laboratory. For instance, it is predicted that a nuclear bulk by heavy ion collisions generates a very high magnetic field of about 10^{16} Gauss. A similar effect is studied at RHIC-STAR by

measuring the polarization of Λ. It will be interesting to investigate this possible magnetization with RI beam collisions at the SAMURAI-SpiRIT TPC system by measuring, for instance, the spin polarization of neutrons. Studies on the spin degree of freedom in heavy ion collisions may also be important for the understanding of spin-polarized nuclear matters in magnetors.

2.2.3 Pillar 3 : How do nuclear many-body systems get organized heavy element RIs under an extraordinarily high Coulomb field.

The proton-rich nuclei with heavier masses delivered by RIBF has the potential to open new era of modern nuclear physics. Due to the Coulomb barrier, there will be many unbound but long-lived nuclei, which compels us to reassess the concept of the dripline. In this domain, the correlations between nucleons will dominate over single-particle features, and there will be a delicate balance between the Coulomb and nuclear forces. Consequently, we will discover various exotic decays and cluster formations.

We also note that protons and neutrons occupy the closer orbits which will emphasize the shell effect and induce stronger proton-neutron correlations. As a result, we expect coexistence of various nuclear shape and emergence of exotic nuclear deformations. A highlight may be the emergence of the octupole deformation which simultaneously breaks the rotational and reflection symmetries.

Heavy-mass proton-rich nuclei produced through nuclear fragmentation will enable the study of various isomers, including high-spin isomers and shape isomers. For instance, the spin response of high-spin states represents entirely novel physics. It would also be possible to systematically investigate the nuclear fission as a function of proton and neutron numbers, which will reveal the physics behind the symmetric/asymmetric fission processes.

Short to long term future

A. The third peak of r-process and freezeout

The nuclear mass information in the region of N = 126 is essential to understand the third peak of the elemental abundance, which is governed by the (n,γ) equilibrium during the hot phase. Heavy element RIs near N = 126 will be produced more efficiently by the upgraded BigRIPS and by KISS II. As a mass-spectrograph, MRTOF-MS and R3 can be chosen depending on the mass and lifetime ranges.

The neutron capture cross sections play an important role in the freezeout phase. A study by the (d,p) surrogate reaction will be carried out at OEDO for key nuclei, for instance, around ^{132}Sn to understand especially the competition between two types of neutron capture, the direct capture process and the compound process.

It should be noted that both data will not only tune or benchmark theoretical frameworks, but also be used to improve the prediction powers by the machine learning toward the r-process path that is still out of the reach with the upgraded RIBF.

Long term future

The physics of heavy element RIs will be a new challenge for the upgraded RIBF. The availability of heavy element RIs will be enhanced by the primary beam intensity upgrade (Chapter 5) and also by the upgraded BigRIPS separator (Chapter 3). It should also be emphasized that the opportunities of reaction studies using fast RI beams are one of the greatest advantages of the RIBF compared to previous studies in the heavy region often based on the stable beam fusion or decay spectroscopy of actinides. Various reaction probes with different sensitivities, developed also for Pillar 1 and 2, will greatly assist the challenges in Pillar 3.

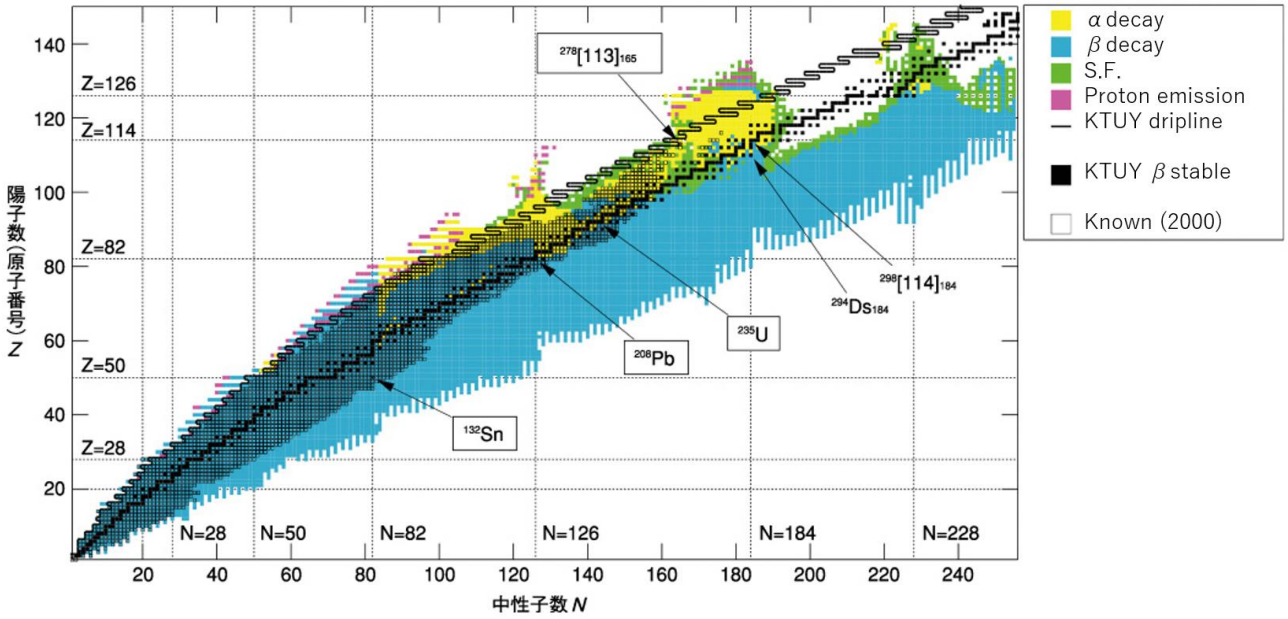

Figure 41 Predicted decay modes mapped over the nuclear chart (by H. Koura of JAEA). The nuclei with the predicted lifetimes longer than 1 ns are plotted in colors.

Below several major cases of physics are listed.

A. Proton dripline without a drip

The proton dripline, especially beyond Pb, is expected to give a very complex landscape due to multiple decay modes (beta, alpha, proton, 2p …) competing with each other and due to the Coulomb barrier which delays proton emissions. As a result, the dripline, defined by the masses, and the existential limit of nuclei, governed by the lifetimes, split apart. The complex dual coast lines should reflect structural and dynamical properties, such as alpha cluster formation, 2p correlation, or multi-dimensional tunneling through the Coulomb potential, providing challenges to both experiments and theories. Experimentally, not only the determination of the dripline, but also measurements of lifetimes and decay modes are required. New isotope searches and decay spectroscopy with the upgrade BigRIPS, and mass measurements by MRTOF or R3 will be instrumental.

B. Rare mode of nuclear decay

Rare decay modes involving charged-particle emissions are phenomena bridging alpha decays to fission. The first of this kind was found in ^{223}Ra decaying by a ^{14}C emission to ^{209}Pb in 1984, and about 30 examples are presently known. Another important decay mode is two or multifold alpha emissions, predicted in 1985, but still elusive. The upgraded BigRIPS allows to directly deliver an RI of interest to the decay station. The beam purity is a key to suppress background radiations, which will be improved by the upgraded first stage of BigRIPS.

The excitation of RI beams by reactions will also be an advantageous method. This allows to measure the rare decay mode in excites states. The decay residue in-flight will be identified by the upgraded ZeroDegree.

C. Shape and clustering

Due to the symmetry breaking or to the emphasized proton-neutron interactions, exotic shapes and clustering are expected in heavy element RIs. In-beam reaction studies by using fast RI beams will be a powerful tool to shed light onto the structural richness of heavy element RIs. In addition to SAMURAI and ZeroDegree adapted to a few hundred MeV/u, low energy reactions are also feasible at the energy degrading beamline OEDO down to 10 MeV/u. The upgraded RIBF will also be equipped with new spectroscopic instruments, for instance, for γ -rays (the new scintillator array and the germanium clusters array GT-5) or for knockout particles (TOGAXI or STRASSE).

Examples include:

- Octupole deformation. Higher-order shapes beyond the quadrupole are expected due to the breaking of the reflection symmetry. Nuclei around N = 134 and Z = 88 are predicted to favor the octupole deformation. In-beam γ-ray spectroscopy with inelastic scattering, knockout reactions or Coulomb excitations will be essential to characterize the deformation.

- Shape coexistence. A variety of coexistence phenomena involving various deformation types are foreseen. A special interest goes to the magicity region near Pb and the north area with N = 126.

- Alpha cluster formation. It is a longstanding question as to whether and how an alpha particle is formed prior to the alpha decay. It is also interesting whether multiple alpha clusters are formed and possibly condensed at the nuclear surface. Alpha knockout reaction studies can be carried out by using TOGAXI for various alpha-decaying RIs. The upgraded ZeroDegree will serve to identify the knockout residue.

D. Isomerism

Isomerism is another interesting subject in the heavy element region. Extremely high spin states (e.g. ^{151}Er 67/2$^-$ state at 10.3 MeV with a lifetime of 420 ns; ^{178}Hf 16$^+$, 2.45 MeV, 31 y), highly-deformed fissile states (^{235}U J$^\pi$ unknown, 2.5 MeV, 3.5 ms), or extremely low energy states (^{229}Th 3/2$^+$, 8.2 eV, 7 μs) represent extreme conditions that are not often met in ground states. The upgraded BigRIPS and KISS II with MRTOF-MS will offer great opportunities to extensively survey still unknown isomeric states up to the region of actinides from the proton dripline towards very neutron-rich side.

The isomer RI beam filter based on R3 is an innovative technology envisioned at the upgraded RIBF. This instrument will deliver isomeric RI beams for reaction studies. The R3 storage ring will serve to tag (for the states with lifetimes greater than 50 μs) and/or physically filter (＞50 ms) RIs in isomeric states and extract them in-flight toward the reaction station. Spectroscopy of isomeric states by reaction probes will help shed light onto the structure or nuclear properties in extreme conditions. For instance, the extremely large deformative nature of fission isomers, so far inferred only indirectly or theoretically, can be characterized by Coulomb excitations or inelastic scattering to measure quadrupole transition strengths or giant dipole strengths. High-spin isomers, if regarded as a state more magnetized than ordinally ground states, would offer interesting playgrounds to investigate the spin response of nuclear matters. Gamow-Teller giant resonances can be investigated by the (p,n) reaction.

E. Fission factory

Induced fission studies by various fast RI beams will be feasible at the upgraded BigRIPS. An advantage of the RIBF is that the fission fragments are moving in-flight and can be analyzed by the upgraded SAMURAI or ZeroDegree to obtain a complete set of information (the particle identity and momentum). This allows not only to evaluate the symmetry or asymmetry in fragment mass distributions, but also to analyze correlations in the multi-dimensional parameter space. Systematic data of this kind for nuclei with different proton and neutron numbers, close to and away from N = 126, will be important to further our understanding of nuclear dynamics. This will also give a feedback to related phenomena such as the fission recycling at the r-process termination, albeit still difficult to directly access.

F. RI beam reactions toward the next-next phase beyond the perspective of 20 years

The regions beyond uranium, for instance, related to the Island of Stability or to the fission recycling, will remain inaccessible even at the upgraded RIBF. It is important to continue the efforts to investigate new reaction techniques to produce RIs. The two-step RI beam production method, where an RI beam is bombarded onto a secondary production target, is promising. The understanding of reaction dynamics of RI beams, especially at low energies, is especially important. For instance, nuclear fusion or deep inelastic scattering with RI beams are interesting in terms of understanding the dynamics, such as the fusion hindrance, the cross-section enhancement with side collisions, or the spin distributions in compound states. The energy degrading OEDO beamline can be used for reaction studies down to the beam energy of about 10 MeV/u. The future RUNBA recycling ring facility is an innovative luminosity booster for low-energy reactions, where target thicknesses are limited. Reaction studies with low-rate RI beams will be facilitated.

3 Accelerator Complex

3.1 Performances FY2007-2022

This section gives an overview of the RIBF accelerators, followed by description of some technical developments since 2007 through 2022, and present status of the accelerator system.

3.1.1 Overview of RIBF

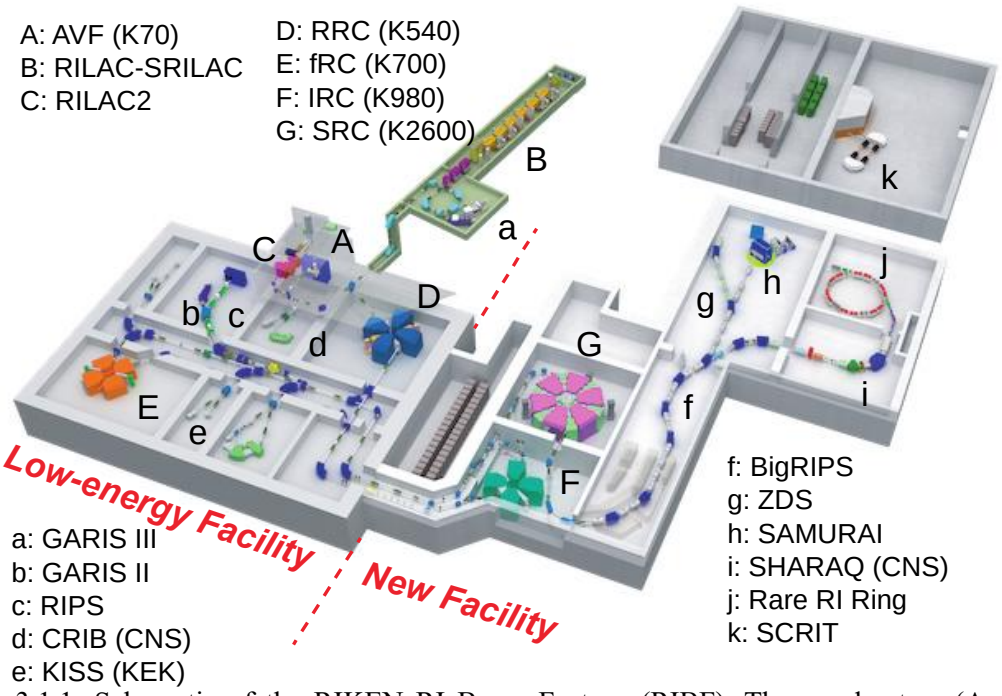

Figure 3.1.1: Schematic of the RIKEN RI Beam Factory (RIBF). The accelerators (A–G) and experimental devices (a–k) are presented.

The Radioactive Isotope Beam Factory (RIBF) at RIKEN is a cyclotron-based accelerator facility that uses fragmentation or fission reactions of intense heavy-ion beams to produce RI beams over the entire atomic mass range[3.1.1]. The RIBF started beam delivery in 2007, after the commissioning of the three ring cyclotrons, namely, fRC (fixed-frequency Ring Cyclotron), IRC (Intermediate-stage Ring Cyclotron), and SRC (Superconducting Ring Cyclotron)[3.1.3.1.2, 3]. These cyclotrons were constructed to boost the energies of the beams accelerated by RRC (RIKEN Ring Cyclotron) as shown in Fig. 3.1.1. The main specifications of the four ring cyclotrons are summarized in Table 3.1.I. Currently, there are three injectors, AVF, RILAC (RIKEN Linear ACcelerator), and RILAC2, that provide a wide variety of heavy-ion beams.

Table 3.1.I: Specifications of the RIBF ring cyclotrons.

	RRC	fRC	IRC	SRC
Sectors	4	4	4	6
K [MeV]	540	700	980	2600
R_{inj} [cm]	89	156	278	356
R_{ext} [cm]	356	330	415	536
Weight [t]	2400	1300	2900	8300
Trim coils/ main coil	26	10	20	4 (SC) + 22 (NC)
RF system	2	2 + FT	2 + FT	4 + FT
Freq. [MHz]	18–38	54.75	18–38	18–38

The most important feature of the RIBF accelerator system is the ability to accelerate all ions from hydrogen to uranium up to 70% of the speed of light. To make this possible, three acceleration modes are used in the RIBF accelerators, as shown in Fig. 3.1.2(a). The first mode is the fixed-energy mode, originally designed for accelerating very heavy ions such as xenon and uranium. This mode uses the RILAC2 injector with a powerful 28-GHz superconducting electron-cyclotron-resonance ion source (SC-ECRIS), and boosts the beam energy up to 345 MeV/u with the four booster ring cyclotrons (RRC, fRC, IRC, and SRC). Two charge strippers are used for

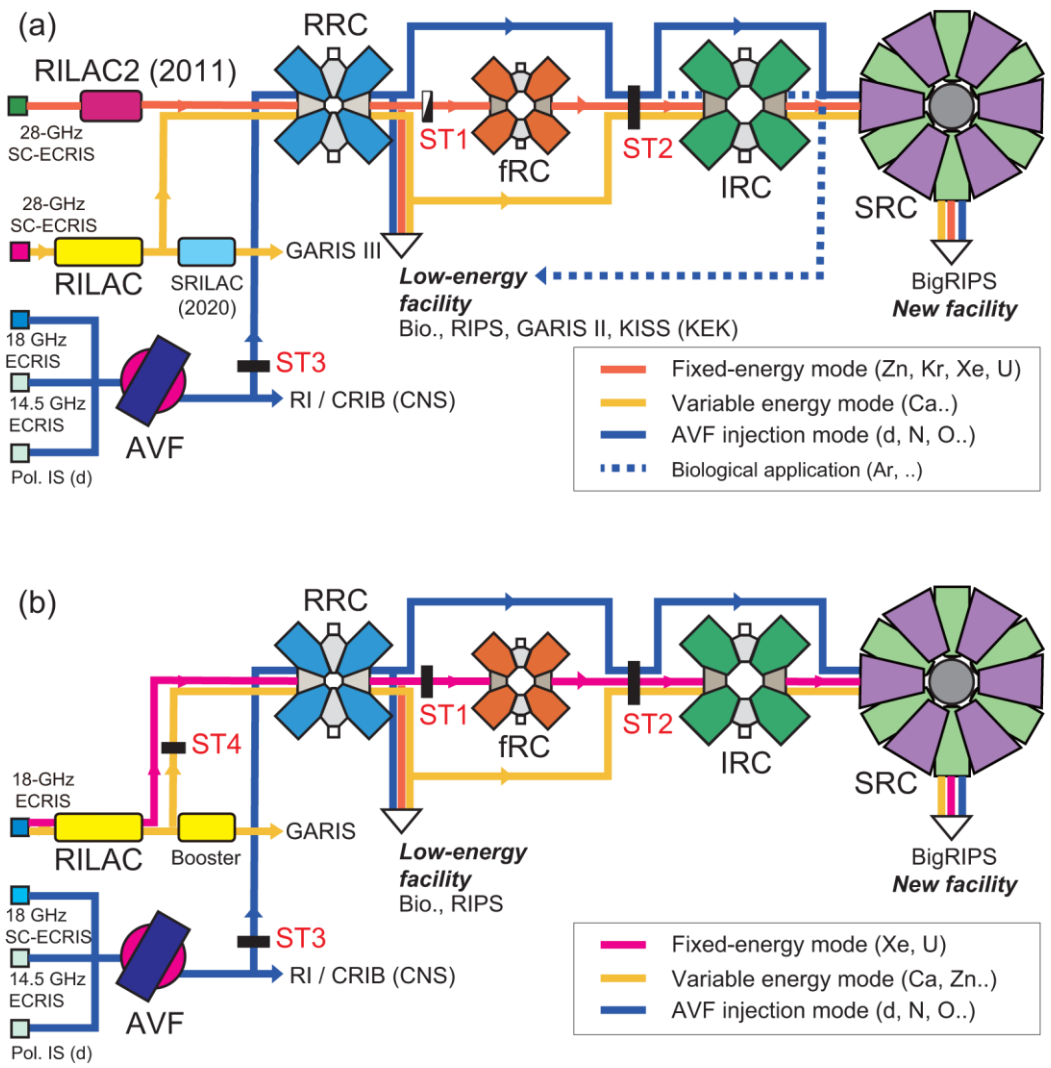

Figure 3.1.2: Accelerator chain of RIBF today (a) and that in 2007 when RIBF started (b). The injectors, RILAC, RILAC2, and the AVF cyclotron are followed by four booster cyclotrons, RIKEN Ring Cyclotron (RRC), fixed-frequency Ring Cyclotron (fRC), Intermediate-stage Ring Cyclotron (IRC), and Superconducting Ring Cyclotron (SRC)[3.1.4]. The charge strippers are indicated by labels in red text (ST1−ST4). The superconducting linac booster, SRILAC, has been operational since 2020[3.1.5]. The dotted line in (a) represents the return beam line dedicated to the biological applications[3.1.6].

the uranium beam. One is a helium gas stripper located at the exit of RRC (E=11 MeV/u), and the other is a rotating graphite-sheet stripper located between fRC and IRC (E=50 MeV/u). Recently, due to the high performance of ion sources, it has become possible to accelerate zinc and krypton beams in this mode using only the second charge stripper.

The second acceleration mode is a variable energy mode that uses RILAC, RRC, IRC, and SRC to accelerate medium-mass ions such as calcium. The beam energy from SRC can be changed in a wide range below 400 MeV/u by changing the RF frequency. The third acceleration mode uses the AVF cyclotron as an injector and two boosters, RRC and SRC. This mode is dedicated for light ions such as deuterons, nitrogen, and oxygen. By changing the RF frequency, the beam energy from SRC can also be changed in the range below 440 MeV/u.

3.1.2 Technical Development during 2007-2022

Among heavy ion beams, the uranium beam is the most effective because it can produce medium-mass RI beams far from the stability line through fission reactions. For this reason, our research and development efforts to date have focused mainly on increasing the intensity of uranium beams. This subsection gives some examples related to these efforts.

RILAC2 Injector

As shown in Fig. 3.1.2(b), we used RILAC for the uranium beam injection in the early stage of RIBF operation. This linac, consisting of six variable-frequency cavities, was commissioned in 1981, and is capable of the total acceleration voltage of 16 MV. We first intended to provide $^{238}U^{14+}$ from the 18-GHz electron-cyclotron-resonance ion source (ECRIS), which had been operational since 1996, and strip it into $^{238}U^{35+}$ at the exit of RILAC in the design stage around 2001. This scheme was found to be unrealistic[3.1.7], and we had accelerated $^{238}U^{35+}$ directly with RILAC since the beam commissioning[3.1.8]. However, RILAC was not suited for accelerating highly charged ions. First, the beam current of $^{238}U^{35+}$ from the ion source was too low to meet the demand of RIBF. Second, this linac was designed to accelerate low charged ions, and the vacuum level was not so good. Moreover, we encountered various difficulties caused by the RF instability in the low-frequency and low-voltage operation. Furthermore, the total voltage required for $^{238}U^{35+}$ is only 4.7 MV, while the voltage gain of 16 MV of RILAC was too high.

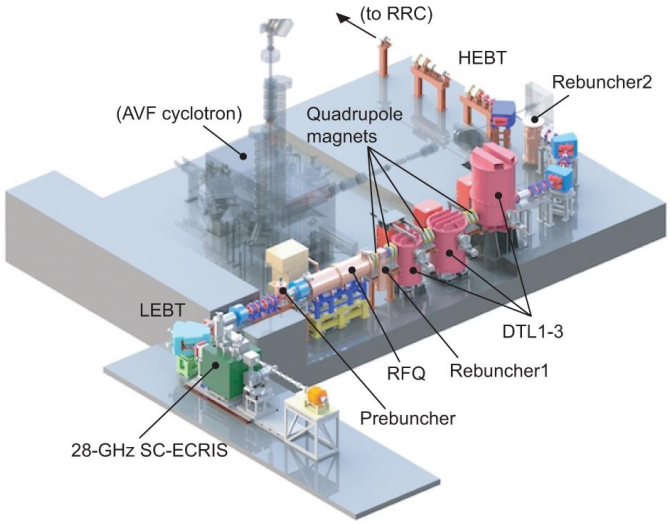

Figure 3.1.3: Schematic drawing of RILAC2.

Therefore, a new injector that could deliver more intense and highly charged uranium beams was required, and a basic design study had been conducted by 2006[3.1.9]. The new injector, which was named "RILAC2", was designed to accelerate ions with a mass-to-charge ratio of 7; this was targeted towards very heavy ions such as $^{136}Xe^{20+}$ and $^{238}U^{35+}$, up to an energy of 680 keV/u in the continuous-wave (CW) mode. As shown in Fig. 3.1.3, RILAC2 consists of the 28-GHz SC-ECRIS, a low-energy beam-transport (LEBT) line including a pre-buncher, an RFQ linac, and three Drift Tube Linac (DTL) cavities (DTL1−3). A rebuncher is located between the RFQ and DTL1, and another rebuncher is positioned in the high-energy beam-transport (HEBT) line after DTL3. The RF cavities (excluding the pre-buncher) are operated at a fixed resonant frequency of 36.5 MHz, whereas the pre-buncher is operated at 18.25 MHz. Strong quadrupole magnets are placed in the beam line between the DTL cavities. The RFQ and DTL design parameters are listed in Table 3.1.II. Owing to the high performance of the new SC-ECRIS, it was possible to reduce the total length of the linac structure to less than 8 m, and we decided to place the new injector in the AVF cyclotron vault as shown in Fig. 3.1.3. The length of the beam transport line to RRC could be reduced to 36 m, which is less than half that required for the RILAC injector.

Table 3.1.II: Main parameters of the RILAC2 cavities for the acceleration of ions with M/q=7. All the cavities are operated at 36.5 MHz in the CW mode. For the RFQ, the cell number and the mean radius r_0 are listed as "Gap number" and "Gap length".

	RFQ	DTL1	DTL2	DTL3
E_{in} (keV/u)	3.3	100	220	450
E_{out} (keV/u)	100	220	450	680
Gap number	(93)	10	10	8
Gap length (mm)	(8)	20	50	65
Gap voltage (kV)	42	110	210	260
Power (kW)	18	7	13	20

We achieved the first beam from RILAC2 in December 2010, and the uranium beam was accelerated through SRC in May 2011[3.1.10-14]. Since then, this injector has been working very stably. A side effect of RILAC2 is that more time can be spent on the experiments for synthesizing super-heavy elements using RILAC. This contributed to the observation of the third event of the element 113 in 2012[3.1.15], later named nihonium[3.1.16]. There is another side effect of the introduction of the new injector. Now intense ion beams of 6−10 MeV/u are available in the low-energy facility behind RRC, where KISS and GARIS II are under operation.

28-GHz Superconducting ECR Ion Source

Before the RILAC2 project started, the construction of a powerful ECRIS was initiated in 2007. This source was designed to operate at 28-GHz microwave power using fully superconducting magnets with a plasma volume as large as 1,100 cm^3[3.1.17]. The coil assembly consists of a set of sextupole coils and six solenoids, which are used to generate a confinement magnetic field. All coils use a niobium-titanium conductor and are bath-cooled in liquid helium. The maximum magnetic field on the coils is 7.4 T. A large radial magnetic field due to this solenoid configuration is provided on the sextupole coils, and an inhomogeneous, strong expansion force is generated on the coils. Note that this renders the design and fabrication of the sextupole coil assembly difficult.

After the coil assembly was fabricated, excitation tests were performed at the manufacturing company facility in June 2008. However, quenching occurred in the sextupole coils at approximately 85% of the design current, when the solenoids and sextupole were excited simultaneously. As the cause of this quenching was attributed to coil motion, the sextupole-coil supporting structure was modified to fix the coils in position more firmly. Following this modification, the design currents were successfully achieved in October 2008[3.1.18]. The ion source was then moved to RIKEN in December 2008, where it was installed on the high-voltage platform of the RILAC pre-injector. Then, initial beam tests and beam delivery were performed using an 18-GHz microwave power source. However, the beam intensity extracted from SRC in 2009 was as low as 0.8 pnA. One of the reasons for this was that the transmission efficiency through RILAC was relatively poor.

Because the budget for the new injector was approved in late 2008, it was decided to move this ion source to RILAC2, and the operation with the 28-GHz microwave power source was initiated in August 2011. During the first few years, a sputtering method with a metallic uranium rod was used to generate uranium ions, and a $^{238}U^{35+}$ beam of approximately 100 eμA could be extracted from the ion source during the beam time. However, the beam stability was not satisfactory.

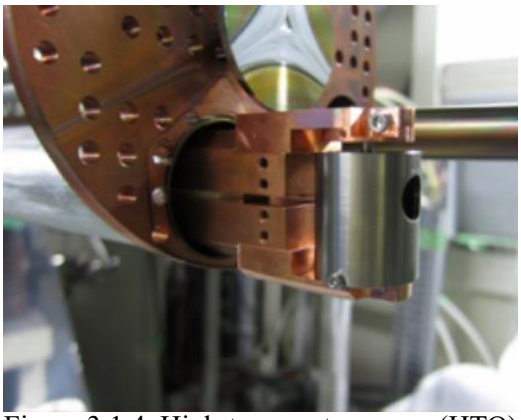

Figure 3.1.4: High-temperature oven (HTO) used in the 28 GHz superconducting ECR ion source (SC-ECRIS)[3.1.19].

In 2013, we started the development of a high-temperature oven (HTO) method, because this method was expected to control the amount of vapor supplied to the ion source plasma. Figure 3.1.4 shows the HTO in the SC-ECRIS. The HTO is equipped with a pure tungsten crucible loaded with uranium oxide. The crucible is supported by a pair of copper rods that act as bus bars carrying DC current to heat the crucible directly. A temperature of 2000 ℃ is required for the crucible to bring the vapor pressure of uranium oxide to 0.1−1 Pa. The HTO has been used in the uranium beam time since autumn 2016. In the first beam time, the $^{238}U^{35+}$ beam was successfully supplied for 34 consecutive days with a current of 120 eμA or more. The uranium beam intensity supplied to the RILAC2 injector are now kept at 100−130 eμA at the ion source for more than one month[3.1.19].

First Stripping Section

As shown in Fig. 3.1.2, two charge strippers are used in the acceleration of uranium beams. The first stripper is located behind RRC, where the beam energy is 11 MeV/u. In the early stage of the RIBF operation, carbon foils with an thickness of 300 μg/cm^2 have been used for this stripping section, and they convert U^{35+} into U^{71+} at an efficiency of 18%. Intensive study has been made for making the lifetime of carbon foils longer since 2008[3.1.20-22]. In the beam time of 2011, carbon-nanotube/sputter-deposited carbon (CNT-SDC) foil, which has been newly developed in RIKEN, was used as this stripping stage[3.1.23]. The foil, having a shape of a disk of 100 mmϕ, was attached to a cylinder rotating with a speed of 1/20 rpm. The longer lifetime of the CNT-SDC foils, typically 30 hours at the intensity of 13 eμA, made the beam delivery fairly successful. The maximum instantaneous current was 3.6 pnA at the exit of SRC. However, the beam quality was not satisfactory due to the inhomogeneous thickness in the foil. Our goal is 5 pμA at this section, and it was obvious that an innovative stripper was necessary to achieve this goal.

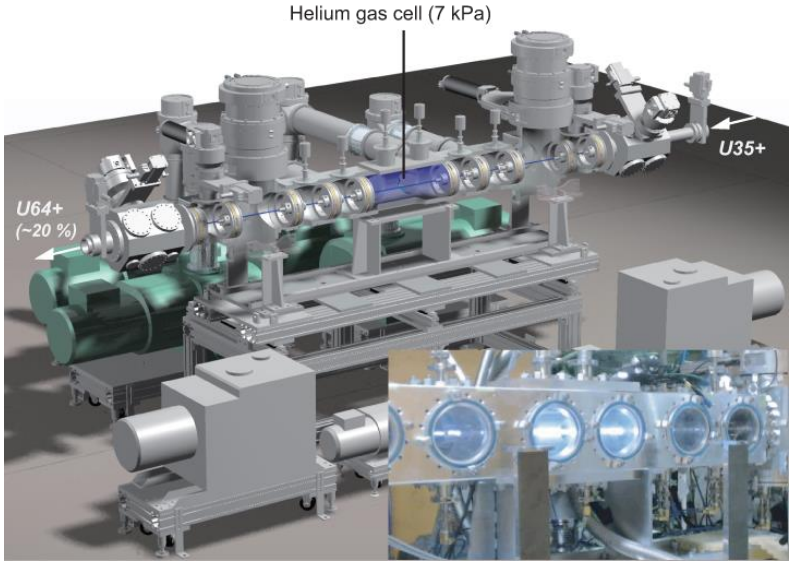

Figure 3.1.5: Schematic drawing of the helium gas stripper and fluorescence of helium gas by uranium beam[3.1.26].

Therefore, we started the development of gas strippers started in 2010. We first measured the equilibrium charge state of ^{136}Xe and ^{238}U beams in nitrogen gas at 11 MeV/u[3.1.24], and found that the nitrogen gas works as the stripper for the xenon beam; sufficient amount of 41+ state, which is acceptable by fRC, has been obtained. In contrast, the equilibrium charge state of the uranium beam was found to be 56+, which is far below the acceptable charge state of 69+.

The turning point was the measurement of electron stripping and electron capture of uranium ions in helium gas at 11 MeV/u[3.1.25]. The result was remarkable; the equilibrium charge state is estimated to be 66+, which is not so far from the acceptable charge state in fRC. Then, based on a careful design of differential pumping systems, we successfully measured the charge evolution for the uranium ions through window-less helium gas cells of 8 m and 0.5 m in length, respectively[3.1.26-27]. The measured mean charge reached up to about 65+, which is consistent with that estimated from the measured cross sections for electron loss and capture. Thus, the use of helium gas seemed promising, but the central issue remained to accumulate a sufficiently thick helium gas in the beamline without a window.

This problem was finally solved by a novel helium-gas stripper in January 2012[3.1.28-29]. It is based on a five-stage differential pumping system, as shown schematically in Fig. 3.1.5. The target cell of the stripper contains helium gas at approximately 7 kPa, while the gas leaked into the next stages is re-circulated to the target cell with the help of mechanical booster pumps. This helium-gas stripper has played an essential role in increasing the uranium beam intensity and stability. In fact, the present intensity of uranium beams injected into the stripper has reached 2.5 pμA, and the system is working stably.

Bending Power Upgrade of fRC

The fRC was originally designed to accelerate $^{238}U^{73+}$ ions using a 0.6-mg/cm^2-thick carbon foil at 10.8 MeV/nucleon. Beam commissioning of the fRC started in 2006, and we immediately recognized that insufficiently uniform thickness of the carbon foil produced a momentum spread outside the tolerance for the fRC. Hence, we reduced the carbon foil thickness to 0.3 mg/cm^2 and modified the injection radius of the fRC. The most probable charge state is 71+ and the operating magnetic field of the fRC is 1.69 T in this case. This modification resulted in satisfactory transmission efficiency of the uranium beam: >90%.

The helium gas stripper described above expected that the equilibrium charge mean was 65+ at first. The required magnetic field exceeded the capacity of the original design: the maximum rise in the cooling water temperature was 10 degrees for the main coils of the sector magnets, and the tolerance was sufficient for increasing the magnetic field up to the 1.85 T required for 65+ ions. Design studies performed from May to early July 2011 identified the devices to be upgraded. The existing power supply system for exciting the fRC sector magnets consisted of one main power supply and four current-bypassing power supplies to compensate for small differences between the four sector magnets. The maximum current of the system is 650 A, corresponding to $^{238}U^{69+}$ ions. Hence, capacity should be upgraded to the 830 A expected for $^{238}U^{65+}$. The current setting precision of the new main power supply was designed to be 1 mA, taking into account the low-magnetic-field operation for the xenon beam. In addition, the injection bending magnet (BM), the magnetic inflection channel 2 and its power supply, and the extraction BM (EBM) required upgrading because their maximum magnetic fields were insufficient. All these devices were newly built except for the EBM, for which replacement of its iron cores was sufficient to generate the required magnetic field. A drawback of the new iron cores is that magnetic field uniformity is worse than it was with the old cores, though the uniformity remains within the permissible range. Finally, two new beam steering magnets were introduced in the beam

injection line to compensate for the much stronger stray magnetic fields expected for $^{238}U^{65+}$ in comparison with $^{238}U^{71+}$. The manufacture of these devices was completed in March 2012. The installation work and magnetic field measurements were performed during the first three months of FY2012 coinciding with tightly scheduled beam services for users. We measured magnetic fields for various excitation currents along the centerline of each sector magnet. It is challenging to skip the two-dimensional magnetic field mapping for large-scale ring cyclotrons such as the fRC, but we gained experience doing this during commissioning of the fRC. An acceleration test of $^{238}U^{65+}$ ions was performed in July 2012 and completed in one night. We successfully extracted a $^{238}U^{65+}$ beam from the upgraded fRC with transmission efficiency of 80%[3.1.30].

It was found thet the newly developed helium gas stripper had stripping efficiency that was higher for $^{238}U^{64+}$ (27%) than for $^{238}U^{65+}$ (21%) with a 0.7-mg/cm2-thick helium gas, owing to the atomic shell effect of the uranium ion [3.1.26]. The used thickness is thinner than that required for charge state equilibrium. Thus 64+ ions were accelerated on 28 October by exploiting the design margin of the new power supply system for the fRC sector magnets. The isochronous magnetic fields obtained for the 64+ and 65+ uranium ions are shown in Fig. 3.1.6. Other quantities, such as transmission efficiency and acceleration turn pattern, exhibited no performance decline after the upgrade of the fRC. The beam transport system from the RRC and the fRC was also upgraded to alleviate difficulty in beam tuning caused by an insufficient number of quadrupole magnets[3.1.30].

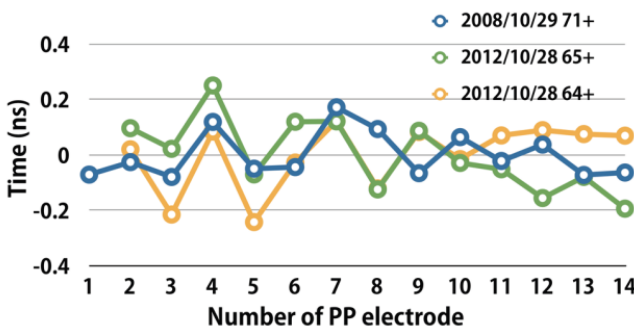

Figure 3.1.6: Isochronous magnetic fields of the fRC.

Second Stripping Section

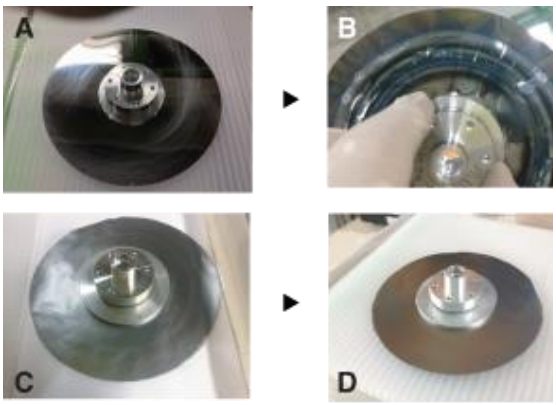

Figure 3.1.7: Charge strippers for uranium beams at 50 MeV/u[3.1.31]. A: Beryllium disk stripper (16 mg/cm^2) before use. B: Beryllium disk stripper after irradiation with approximately 10^{18}uranium ions. C: Graphite sheet stripper (2×7 mg/cm^2) before use. D: Graphite disk stripper after irradiation with approximately 1.4×10^{18} uranium ions. Each stripper has an outer diameter of approximately 100 mm.

The second stripper section is located behind fRC at the energy of 50 MeV/u. In 2007, the charge state of the uranium ions was converted into 86+ with carbon foils of 17 mg/cm^2 at an efficiency of 28%. Owing to the heat load by the intense beams, these efficiency values decreased with an increased beam dose. The typical lifetime made from commercially available foils was 12 hours at an intensity of 1 eμA.

Therefore, we decided to replace the carbon-foil stripper with an alternative. In November 2012, the carbon-foil stripper was replaced with a 19 mg/cm^2 beryllium disk stripper rotated at 300−1000 rpm as shown in Fig. 3.1.7 A. However, as shown in Fig. 3.1.7 B, the disks were found to have many tiny cracks and were heavily distorted following irradiation of approximately 10^{18} uranium ions, which corresponded to a twenty-days beam time.

This final bottleneck problem was successfully overcome through the introduction of a new type of stripper composed of a “highly-oriented graphite sheet”, which was manufactured by a Japanese company, Kaneka Corporation, shown in Fig. 3.1.7 C. This material, which was fabricated from a polymer sheet under high pressure and temperature, has high thermal conductivity of 1500 W/m K in the planar direction. This value is more than three times that of copper. We employed a pair of graphite sheets, each of which had 7 mg/cm^2 thickness, to form the second stripper. For the uranium beam delivery performed in March−May 2015, we achieved a final intensity of 39.5 pnA at the exit of SRC using this stripper. The carbon sheets werenot damaged at all, as shown in Fig. 3.1.7 D, even following irradiation with 1.4×10^{18} uranium ions at a 200 W heat load. The corresponding temperature on the stripper was estimated to be 600 K via a computer simulation using the ANSYS software. This graphite-sheet stripper has been used consistently up to date[3.1.31-32].

RRC Cavity

The RIKEN Ring Cyclotron (RRC) has two acceleration cavities based on variable-frequency, half-wavelength resonator, constructed more than 30 years ago[3.1.33]. The resonant frequency of this cavity is varied by moving two boxes vertically. The inner height of the cavities could be made as small as 2.1 m, while keeping a wide range of resonant frequency from 20 to 45 MHz. However, the frequency for uranium acceleration is 18.25 MHz, which is outside the designed range. The gap length between the dee electrode and the movable box had to be made as small as 20 mm, as shown in Fig. 3.1.8. During the acceleration of the uranium beam, the narrow gap between the dee electrode and the movable box caused a bottleneck problem limiting the cavity voltage to a maximum of 80 kV. In addition to frequent discharges during operation, this narrow gap increases the capacitance in the cavity, thus lowering the shunt impedance. Furthermore, due to the low acceleration voltage, the uranium beam current reached a space charge limit in the RRC[3.1.34].

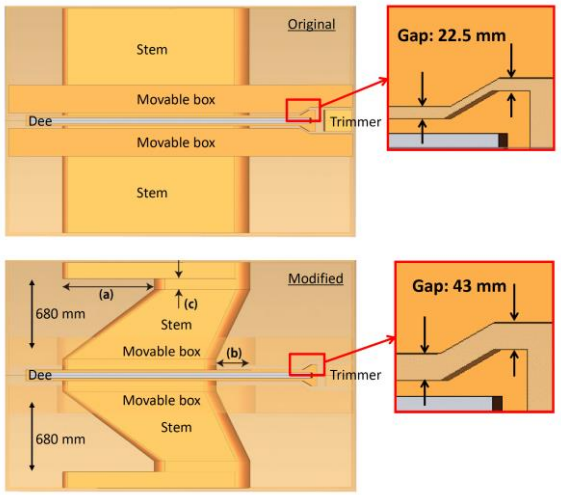

Figure 3.1.8: Calculation models for the original cavity (upper panel) and the modified cavity (lower panel). The gap length required for a resonant frequency of 18.25 MHz is shown in each panel.

Therefore, as shown in Fig. 3.1.8, the internal components of the cavity, the stems and the dee electrode, were replaced, leaving the external box and movable box of the cavity unchanged. The frequency range of the RRC cavity is shifted downward by the insertion of a notch into the stem, which was originally straight. Since the RRC cavities have not operated at frequencies above 39 MHz in recent years, the frequency range was set to 16−38 MHz after remodeling. The shunt impedance, voltage distribution, and frequency range were optimized by changing the notch size based on 3D electromagnetic calculations using the computer code Microwave Studio (MWS). The new cavities have been used in beam time since May 2018 and show good operational performance from 18.25 to 32.6 MHz. In particular, stable operation was achieved at a voltage of 120 kV at 18.25 MHz. This is due to an improvement in shunt impedance and an increase in the gap length between the dee and the movable box. In fact, the frequency of voltage breakdown has decreased significantly. The bottleneck problem during uranium acceleration was solved in this way.

3.1.3 Present Status

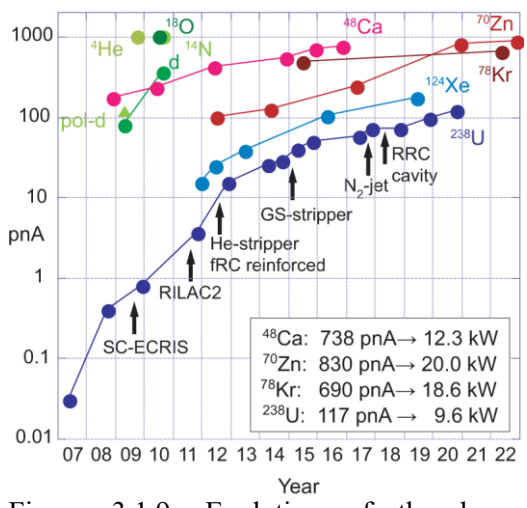

Figure 3.1.9: Evolution of the beam intensity at the exit of SRC since the start of operation of RIBF in 2007. The main R&D items for increasing the uranium beam are also indicated.

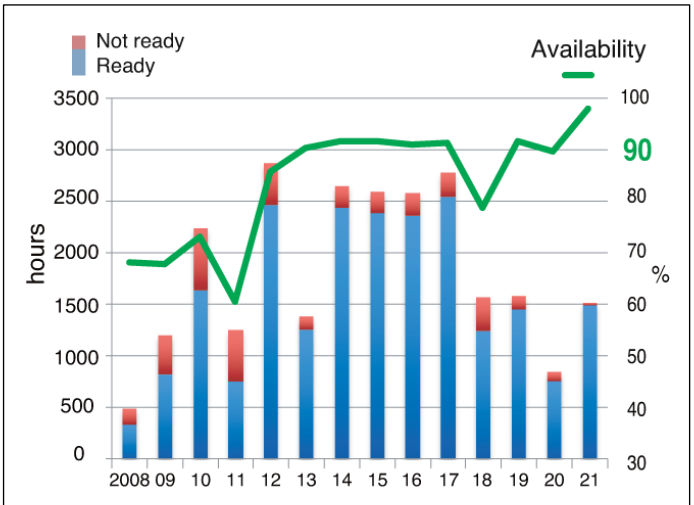

Figure 3.1.10: Availability of RIBF accelerator complex delivering beams to BigRIPS experiments.

The evolution of the maximum beam intensity for the ion beams accelerated at RIBF is shown in Fig. 3.1.9[3.1.35]. Through our continuous efforts including the research and development described above, the uranium intensity is now 117 pnA and the beam power has reached 9.6 kW, which exceeded goal of this mid-term plan of Nishina Center. As mentioned above, the first stripper shown as ST1 in Fig. 3.1.2 became unnecessary for medium-mass ions such as zinc and krypton, owing to the high performance of the 28-GHz SC-ECRIS. The beam power of these ion beams has now reached 20 kW, as shown in Fig. 3.1.9.

Figure 3.1.10 shows the availability of the RIBF accelerator supplying the beam to the BigRIPS target. The figure shows that the availability has significantly improved since 2012, when the helium gas stripper was installed. The availability of the accelerator has also exceeded 90% in these years. In addition to the developments mentioned above, members of our group have made continuous efforts to improve the stability of the RIBF accelerator, especially the injector section built in the 1980s. Some of these efforts are described in the reference[3.1.36].

References

[3.1.1] Y. Yano, “The RIKEN RI Beam Factory Project: A status report”, Nucl. Instrum. Methods Sec. B, vol. 261, pp. 1009−1013, 2007.

[3.1.2] A. Goto *et al*., “Commissioning of RIKEN RI Beam Factory”, in Proc. 18th Int. Conf. on Cyclotrons and their Applications (Cyclotrons'07), Giardini Naxos, Italy, Oct. 2007, pp.3−8.

[3.1.3] N. Fukunishi *et al*., “Present Performance and Commissioning Details of RIBF Accelerator Complex”, in Proc. 18th Int. Conf. on Cyclotrons and their Applications (Cyclotrons'07), Giardini Naxos, Italy, Oct. 2007,, pp.21−23.

[3.1.4] H. Okuno *et al*., “The Superconducting Ring Cyclotron in RIKEN”, IEEE Trans. Applied Superconductivity, vol. 261, pp. 1009−1013, 2007.

[3.1.5] Accelerator Group of RIKEN Nishina Center, “First Beam from SRILAC”, RIKEN Accelerator Progress Report, vol. 54, 2021, p. S1.

[3.1.6] N. Fukunishi *et al*., “New High-energy Beam Transport Line Dedicated to Biological Applications in RIKEN RI Beam Factory”, Proc. HIAT'15, Yokohama, Japan, Sep. 2015, paper MOPA04, pp. 42−44.

[3.1.7] H. Ryuto *et al*., “Charge Stripping Plan of the RIKEN RI-Beam Factory”, in Proc. Cyclotrons'04, Tokyo, Japan, Oct. 2004, paper 19P25, pp. 307−309.

[3.1.8] N. Fukunishi *et al*., “Acceleration Tests of Uranium Beam in RIBF (I)”, RIKEN Accelerator Progress Report, vol. 41, 2008, pp. 79−80.

[3.1.9] O. Kamigaito *et al*., “Design of New Injector to RIKEN Ring Cyclotron”, in Proc. 3rd PASJ and 31st LAM in Japan, Sendai, Aug. 2006, paper WP78, pp. 502−504.

[3.1.10] K. Yamada *et al*., “Construction of New Injector Linac for RI Beam Factory at RIKEN Nishina Center”, in Proc. IPAC'10, Kyoto, Japan, May 2010, paper MOPD046, pp. 789−791.

[3.1.11] K. Suda *et al*., “Design of Coupler for Direct Coupled Amplifier to Drift Tube Linac Cavities of the Injector RILAC2 for RIKEN RI Beam Factory”, in Proc. LINAC'12, Tel Aviv, Israel, Sep. 2012, paper TUPB095, pp. 684−686.

[3.1.12] K. Suda *et al*., “Design and construction of drift tube linac cavities for RIKEN RI Beam Factory”, Nucl. Instrum. Methods Sec. A, vol. 722, pp. 55−64, 2013.

[3.1.13] K. Yamada *et al*., “Beam Commissioning and Operation of New Linac Injector for RIKEN RI-beam Factory”, in Proc. IPAC'12, New Orleans, LA, USA, May 2012, paper TUOBA02, pp. 1071−1073.

[3.1.14] N. Sakamoto *et al*., "Commissioning of a New Injector for the RIKEN RI-Beam Factory", in Proc. LINAC'12, Tel Aviv, Israel, Sep. 2012, paper MO3A02, pp. 125−129.

[3.1.15] K. Morita *et al*., "New Result in the Production and Decay of an Isotope, ^{278}113, of the 113th Element", J. Phys. Soc. Jpnin Proc, vol. 81, 103201, 2012.

[3.1.16] P. J. Karol, R. C. Barber, B. M. Sherrill, E. Vardaci and T. Yamazaki, "Discovery of the elements with atomic numbers Z = 113, 115 and 117 (IUPAC Technical Report)", Pure Appl. Chem., vol. 88, pp.139−153, 2016.

[3.1.17] T. Nakagawa, "New 28 GHz SC-ECRIS for RIKEN RI Beam Factory Project", in Proc. ECRIS'08, Chicago, IL, USA, Sep. 2008, paper MOCO−B01, pp. 8−12.

[3.1.18] T. Nakagawa *et al*., "First Results from the new RIKEN superconducting electron cyclotron resonance ion source", Rev. Sci. Instrum., vol. 81, 02A320, 2010.

[3.1.19] J. Ohnishi, Y. Higurashi, and T. Nakagawa, "Practical Use of High-Temperature Oven for 28 GHz Superconducting ECR Ion Source at RIKEN", in Proc. ECRIS'18, Catania, Italy, Sep. 2018, pp. 180−184.

[3.1.20] H. Hasebe *et al*., "Polymer coating method developed for carbon stripper foils", Nucl. Instrum. Methods Sec. A, vol. 590, pp. 13−17, 2008.

[3.1.21] H. Hasebe *et al*., "Development of long-life carbon stripper foils for uranium ion beams", Nucl. Instrum. Methods Sec. A, vol. 613, pp. 453−456, 2010.

[3.1.22] H. Hasebe *et al*., "Development of the carbon foils as charge strippers for high-intensity uranium ion beams", Nucl. Instrum. Methods Sec. Ain Proc, vol. 655, pp. 57−60, 2011.

[3.1.23] H. Hasebe *et al*., "Development of a new foil compounded from carbon nanotubes and sputter-deposition carbon", J Radioanal Nucl Chem vol. 299, pp. 1013−1018, 2014.

[3.1.24] H. Kuboki *et al*., "Charge-state distribution of ^{238}U and ^{136}Xe in nitrogen gas and carbon foil at 11 MeV/nucleon using gas charge stripper", Phys. Rev. ST Accel. Beams, vol. 13, 093501, 2011.

[3.1.25] H. Okuno *et al*., "Low-Z gas stripper as an alternative to carbon foils for the acceleration of high-power uranium beams", Phys. Rev. ST Accel. Beams, vol. 14, 033503, 2011.

[3.1.26] H. Imao *et al*., "Charge Stripping Of Uranium-238 Ion Beam with Helium Gas Stripper", in Proc. IPAC2012, New Orleans, Louisiana, USA, paper THPPP084, Aug. 2012, pp.3930−3932.

[3.1.27] H. Imao *et al*., "Charge stripping of ^{238}U by helium gas stripper", Phys. Rev. ST Accel. Beams, vol. 15, 123501, 2012.

[3.1.28] H. Imao *et al*., "R&D of Helium Gas Stripper for Intense Uranium Beams", in Proc. Cyclotrons'13, Vancouver, Canada, Sep. 2013, paper TU3PB03, pp. 265−268.

[3.1.29] H. Imao, "Development of Gas Stripper at RIBF", in Proc. IPAC'18, Vancouver, Canada, Apr.−May 2018, pp. 41−46.

[3.1.30] N. Fukunishi *et al*., "Acceleration of Intense Heavy Ion Beams in RIBF Cascaded-Cyclotrons", in Proc. Cyclotrons'13, Vancouver, Canada, Sep. 2013, paper MO1PB01, pp. 1−6.

[3.1.31] H. Hasebe *et al*., "History of Solid Disk Improvement for Rotating Charge Stripper", in Proc. HIAT'15, Yokohama, Japan, Sep. 2015, paper MOA1C01, pp. 17−19.

[3.1.32] H. Hasebe *et al*., "Development of a high-density highly oriented graphite stripper", EPJ Web of

Conferences, vol. 229, 01004, 2020.

[3.1.33] T. Fujisawa *et al*., “The Radiofrequency System of the RIKEN Ring Cyclotron”, Nucl. Instrum. Meth. A, vol. 292, pp. 1−11, Jun. 1990.

[3.1.34] K. Yamada *et al*., “Upgrade and current status of high-frequency systems for RIKEN Ring Cyclotron”, in Proc. 23rd Int. Conf. on Cyclotrons and their Applications (Cyclotrons'22), Beijing, China, MOAI2, Dec. 2022.

[3.1.35] O. Kamigaito *et al*., “High Beam Power Operations at RIKEN RIBF: Technical Developments, Challenges and Resolutions”, in Proc. HIAT'22, Darmstadt, Germany, Jun.−Jul. 2022, MO4I.

[3.1.36] H. Okuno, N. Fukunishi, and O. Kamigaito, “Progress of RIBF accelerators”, Prog. Theor. Exp. Phys., vol. 2012, pp. 03C002, 2012.

3.2 Upgrade plan

The RIBF accelerator upgrade plan aims to dramatically increase the output intensity of primary heavy-element ion beams, such as uranium, which are particularly important in unstable nuclear physics research in the midst of global research competition. The targeted RI-beam production ability by the upgrade plan will exceed the targeted ability of the latest facility, FRIB [3.2.1] in the U.S., which started user operation in 2022, as well as the next generation facilities with construction costs over $1 billion such as FAIR [3.2.2] in Germany, RAON [3.2.3] in Korea, and HIAF [3.2.4] in China, which are scheduled to start operation within the next decade. The upgrade plan will allow RIBF to continue to maintain the leadership in this field of science in the world. We believe that this is in line with the national strategy in the field of science that our center should promote.

The upgrade plan is feasible and realistic enough based on the accelerator technology accumulated at the RIBF. It is designed to be upgraded in stages with a reasonable total construction period of ~8 years and relatively low budget of approximately 17.3 billion JPY, which is less than half of the construction cost of the RIBF. In particular, we believe that the intensity of the uranium beam can be increased by a factor of 20 by introducing a revolutionary ring, the charge stripper ring (CSR) [3.2.5-6]. An important feature of CSR is that it recycles the beam, which allows a 20-fold increase in intensity to be achieved with only a 6 MW increase in electrical power (the current operating electrical power is approximately 17 MW for uranium acceleration).

Although CSR is a very unique and unprecedended accelerator component, the technology required for the realization is based on the cyclotron and stripper technology that has matured at RIBF. For more than a decade, the basic design and the development of elemental technologies of CSRs have been proceeded by the accelerator group at the RIBF. Such studies of CSRs were presented in some papers [3.2.7-9] and conferences [3.2.5-6] and well recognized by domestic and international accelerator societies. Recently, a detailed technical design report (TDR) has been prepared for CSR1 and a technical advisory committee (TAC) meeting was held on June 15-16, 2023. We have had strong support from TAC in moving forward with the project with CSR1. There are no intrinsic problems with the feasibility of CSR, which is well suited for our facility. From an accelerator physics perspective, CSR is an attractive device with a wide range of possible applications, and the realization will have an immeasurable impact on the accelerator industry.

The recycling beam technology to be established in this project with CSRs has great scalability for the future. Further future upgrading with various CSR-like rings for a high-intensity injector, efficient energy upgrade and efficient secondary beam productions are conceivable at the RIBF. The present upgrade plan with CSRs will also be important cornerstone of such applications possible in the future.

General description of upgrade plan with CSR

As mentioned above, heavy-ion accelerator facilities are being operated or constructed around the world to follow the RIBF. Among them, the FRIB project in the U.S., which aims to accelerate a uranium beam to 200 MeV/u using a long superconducting linear accelerator, started operation in 2022. The acceleration scheme involves a single charge conversion process. Because it is a linear accelerator, it can accelerate ions in multiple charge states simultaneously [3.2.10], and the final target beam intensity is set at 8400 pnA (400 kW).

To compete with the FRIB project, the intensity of the uranium beam at RIBF must be significantly increased, but the current acceleration scheme is limited to the intensity of around 200 pnA (16 kW). The main bottleneck for the intensity upgrade is two charge conversion processes. The present acceleration scheme for the ^{238}U beam at the RIBF is shown in Fig. 3.2.1(a). A He gas stripper was the first stripper to convert the charge states from U^{35+} to U^{64+} at an energy of 11 MeV/u. During the second stage, a rotating graphite sheet disk stripper is used to convert U^{64+} into U^{86+} at an energy of 51 MeV/u. Although the two types of strippers are advanced strippers that can withstand the highest-intensity uranium beams, the first and second charge conversion efficiencies are 20% and 25%, respectively, thus the overall charge conversion efficiency is only 5%. In other words, in the current acceleration scheme for uranium beams, 95% of the beam is discarded.

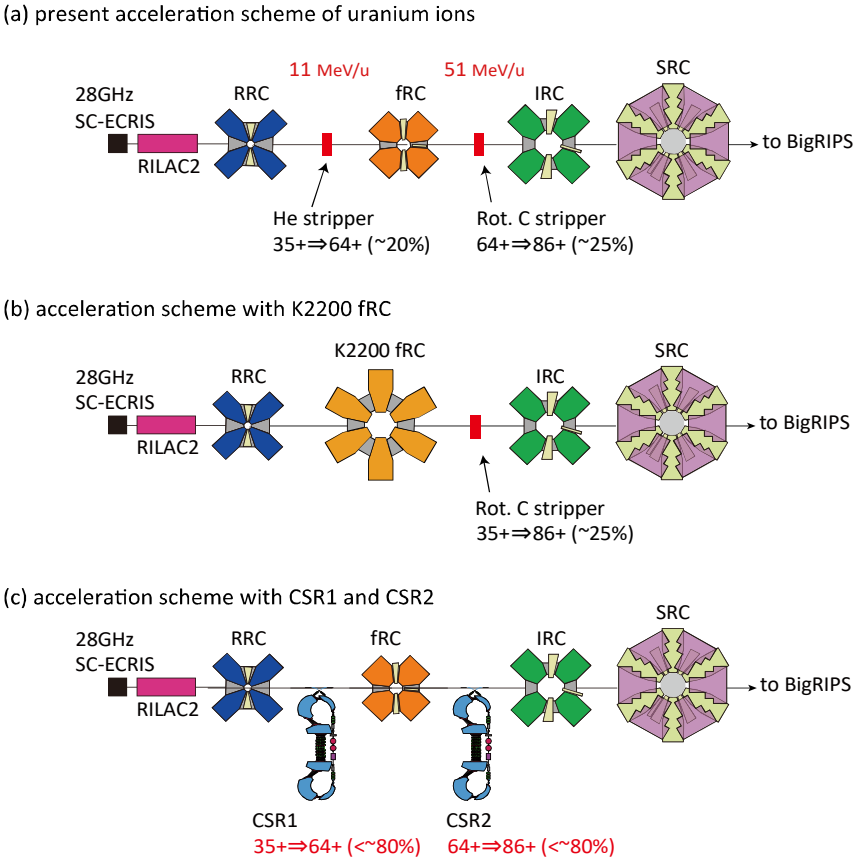

Figure 3.2.1. Schematic view of the present acceleration scheme of ^{238}U beam at the RIBF (a). Two strippers, a He stripper at 11 MeV/u and a rotating graphite sheet stripper at 51 MeV/u, are used in the acceleration with four ring cyclotrons (RRC, fRC, IRC, and SRC). The charge stripping efficiencies are approximately 20% and 25%, respectively. Schematic views of possible new acceleration schemes to enhance the total charge stripping efficiency with (b) a normal conducting K2200 cyclotron and (c) CSRs are also shown.

A simple way to increase the total charge stripping efficiency of the RIBF is to remove the He stripper and rebuild the fRC to accelerate a U^{35+} beam without the stripper (Fig. 3.2.1(b)). A new normal conducting ring cyclotron (K = 2200 MeV) will increase the intensity by a factor of 5, although such a huge cyclotron would be extremely expensive and large, almost the same size as the SRC.

We proposed using a charge stripper ring (CSR) to recycle the beams discarded during the charge conversion process as shown in Fig. 3.2.1(c). The estimated iron weight and main coil power consumption for a normal conducting K2200 cyclotron are approximately 7000 t and 2.2 MW [3.2.11], respectively. In contrast, those for CSR1 as a replacement for the first He stripper are approximately 300 t and 0.3 MW (Fig. 3.2.2). The CSR1 is superior in terms of manufacturing cost, running cost and small building modification. The technology of CSR can be applied to the second stripper (CSR2) as well. As shown in the Fig. 3.2.3, CSR1 and CSR2 will be located in the existing Nishina Building without building expansion.

The first charge conversion efficiency will be increased from 20% to 77%, and the second charge conversion efficiency will be increased from 25% to 63%, thereby increasing the overall charge conversion efficiency

from 5% to 50% (10 times of the current level) with CSRs. This upgrading would allow a final beam intensity of 2000 pnA (160 kW). Although this target is lower in beam intensity than FRIB, it does not lose its advantage in the ability to produce RI beams, since the energy per nucleon is more than 1.5 times higher. We note that there is a room in CSR for applying other ions in the mass region between Xe and U, although CSR has been designed primary for uranium.

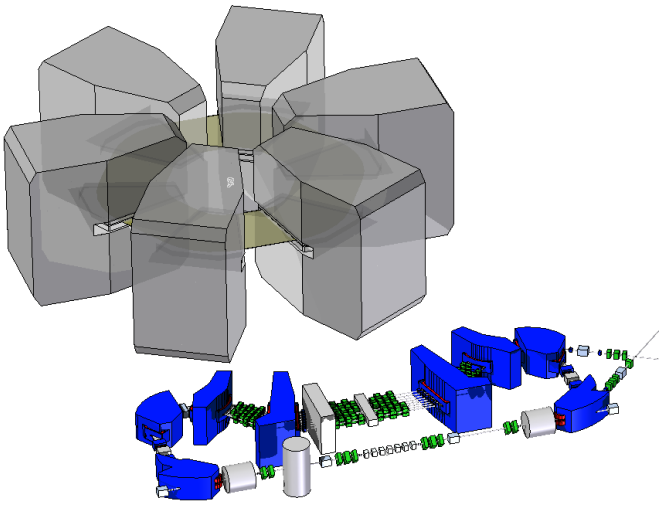

Figure 3.2.2. Comparison of the size of the K2200 cyclotron and the CSR1: The K2200 cyclotron weighs more than 7000 tons and is expected to consume more than 4 MW of electricity during operation. On the other hand, the CSR1 weighs about 300 tons and is estimated to consume only 1.5 MW of electricity during operation.

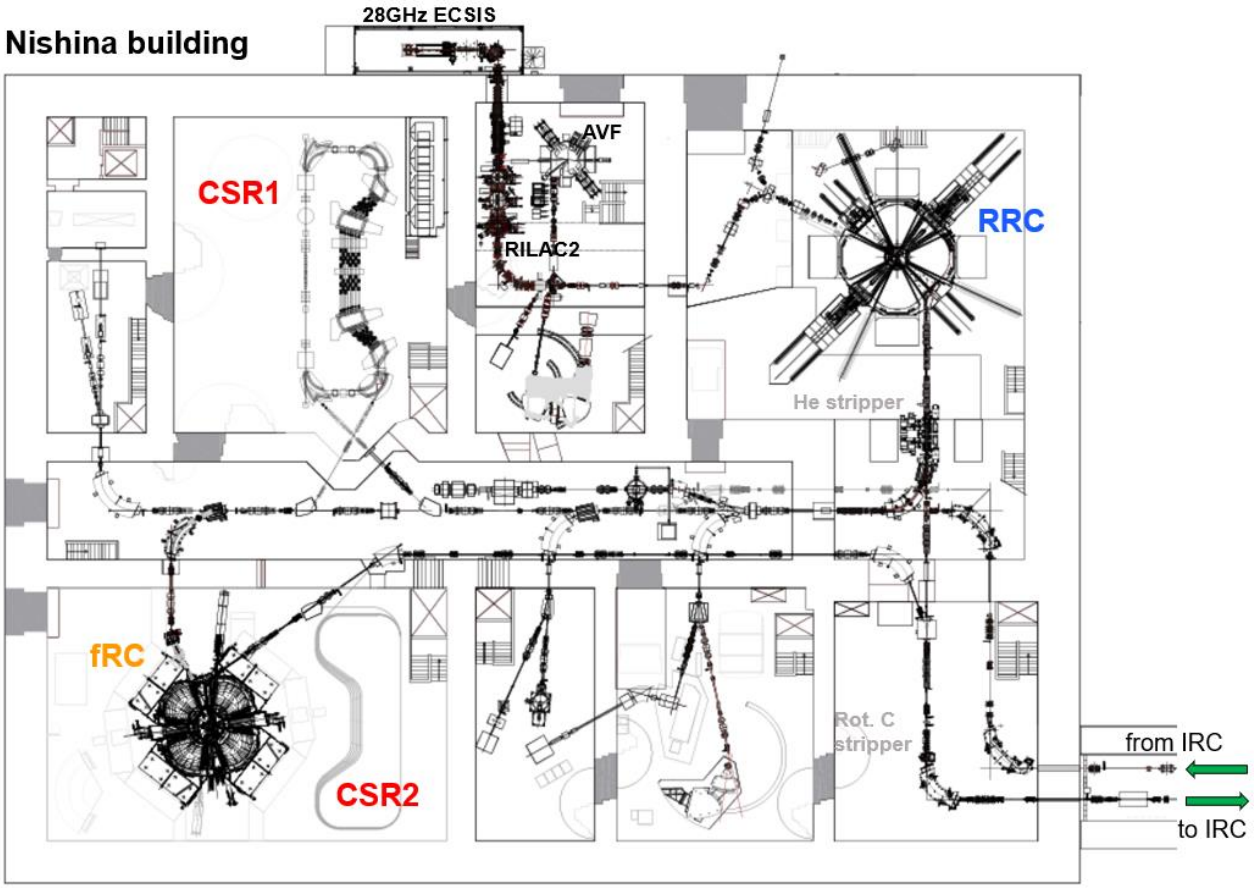

Figure 3.2.3. Proposed construction sites for CSR1 and CSR2 at Nishina Building.

Effective upgrading of existing accelerators is also essential to enable the acceleration of intensity-enhanced beams by CSR. The major items for upgrading existing accelerators include: ion source enhancement, SRC-RF system enhancement, SRC extraction system enhancement, fRC-RF system enhancement, IRC injection system modification and upgrade of infrastructures (Fig. 3.2.4). The following sections provide an overview of each task.

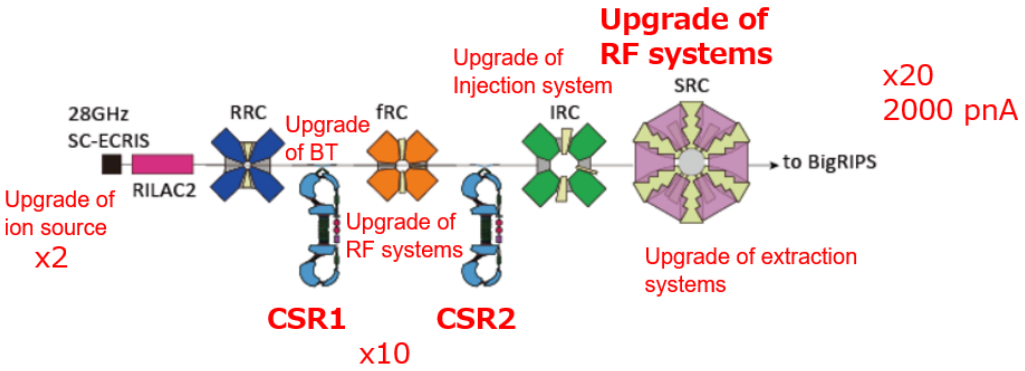

Figure 3.2.4. CSRs and upgrade of existing accelerators at the RIBF

Design work of CSR1

The CSR is a new concept ring with a built-in charged stripper, unprecedented worldwide. Here the CSR scheme is explained as shown in Fig. 3.2.5, using the first ring CSR1 as an example and comparing it with the present scheme with the He stripper. In the present charge stripping scheme for the first stripper at the RIBF, the $^{238}U^{35+}$ beam (10.8 MeV/u, 18.25 MHz) passes through the He stripper with a thickness of approximately 0.7 mg/cm^2, and only the $^{238}U^{64+}$ beam is selected by the subsequent bending magnets. As a result, the charge stripping efficiency is approximately 20%. This means that 80% of the beam is dumped into the beam dump in the bending magnet.

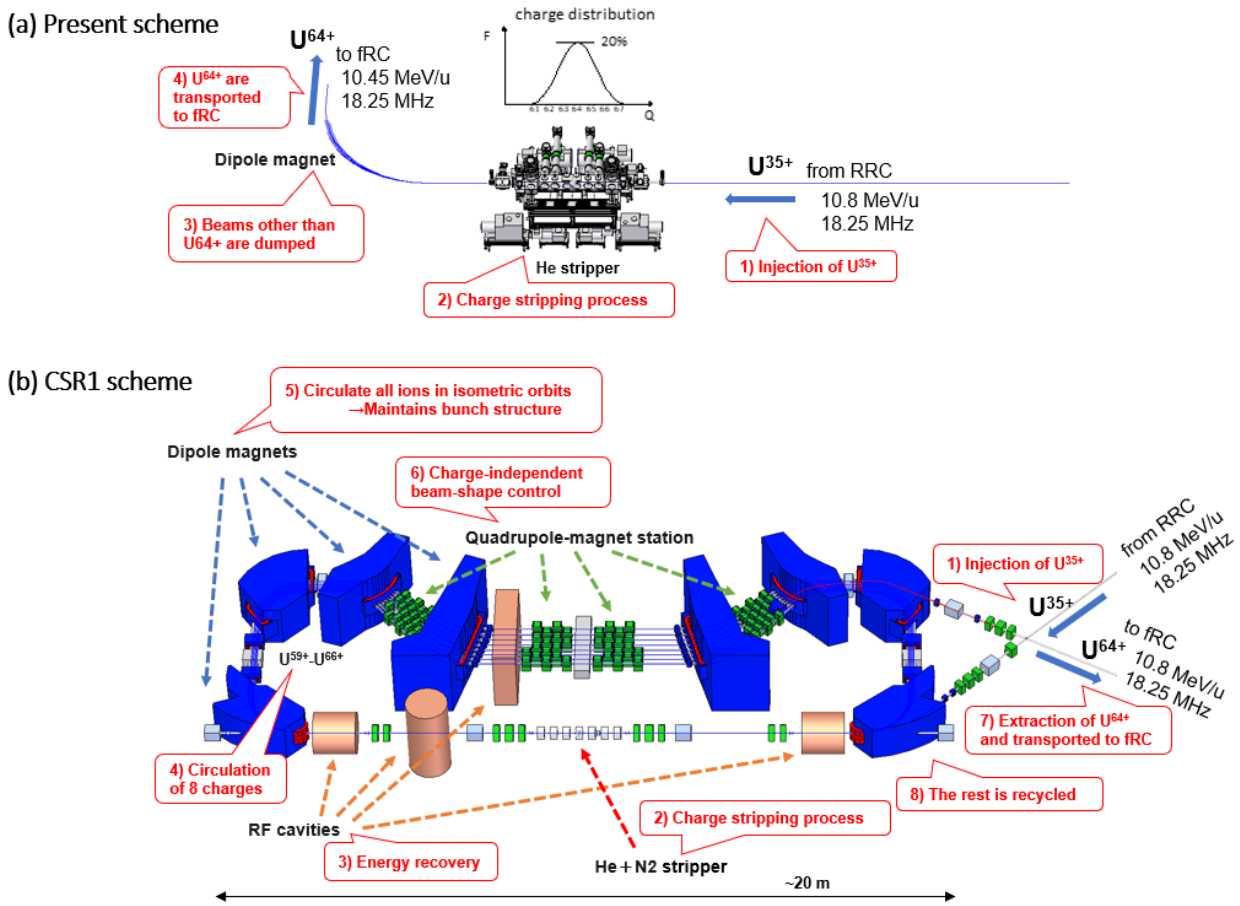

Figure 3.2.5. Comparison of the current charge conversion scheme using the He gas stripper alone (a) and for CSR1 (b).

For CSR scheme, the U^{35+} beam bunches are injected simultaneously into CSR1 with a frequency of 18.25 MHz using the charge exchange injection method. The charge state is converted at the 2-stage stripper (He and N_2 stripper) and the energy lost in the charge stripper is recovered by the acceleration cavity. The beams other than the selected U^{64+} beams are circulated and reenter the stripper. The phase spread during the circulation is suppressed by the buncher cavities. The recycling cycles are repeated, and only the U^{64+} beams are continuously extracted using a static magnetic kicker.

The most important property required for CSRs is that all orbit lengths of the orbiting beams (e.g., $U^{59\text{-}66+}$ for CSR1) are equal (isometricity). Forming such isometric orbits by eight special bending magnets, the bunch structure of the orbiting beams can be maintained. The spatial shape of bunchs for all charge states are also matched at the stripper by controlling the oscillation of the beams using a charge-independent focusing system (quadrupole-magnet stations). We have performed lattice designs and beam simulations of CSR1 as shown in Fig. 3.2.6 and confirmed that the bunch structure and shape at the stripper can be maintained and matched almost perfectly. The results of beam calculations considering emittance growth due to the stripper show that the charge conversion efficiency up to 80% can be obtained for CSR1.

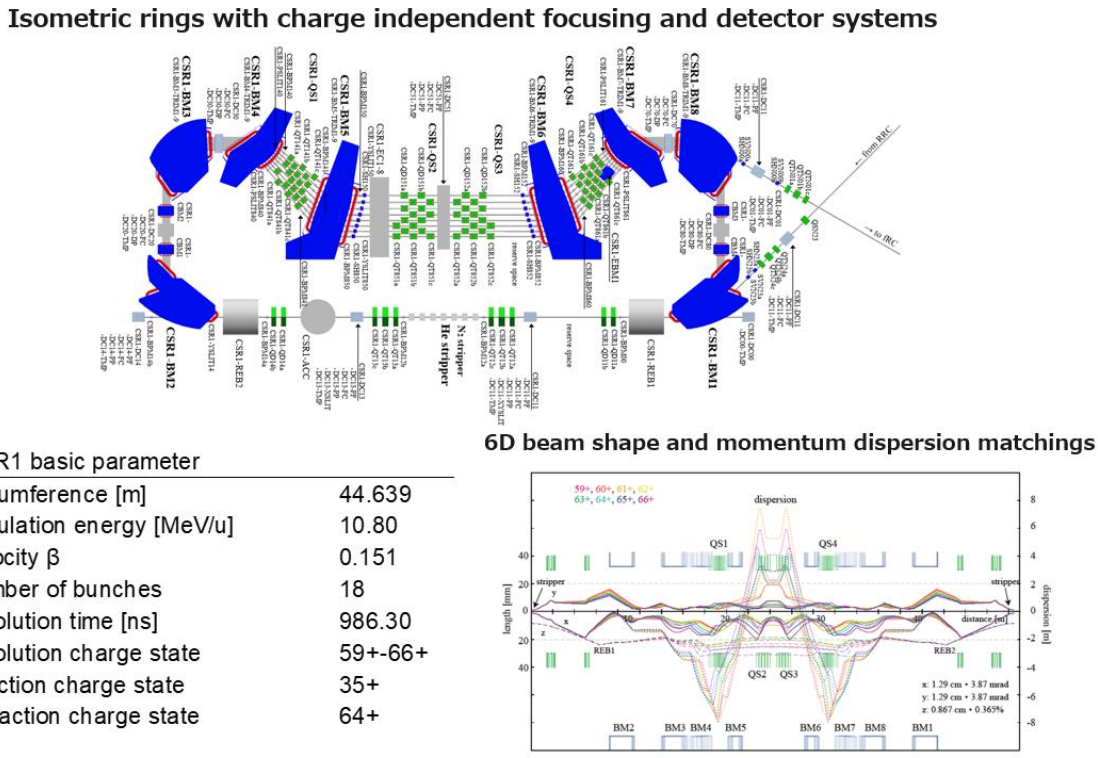

CSR1 basic parameter	
circumference [m]	44.639
circulation energy [MeV/u]	10.80
velocity β	0.151
number of bunches	18
revolution time [ns]	986.30
revolution charge state	59+-66+
injection charge state	35+
extraction charge state	64+

Figure 3.2.6. Basic design works for CSR1.

In parallel, we have been developing elemental technologies to realize CSR1. The magnets, in particular, are important development elements that determine the feasibility of CSR1, and has been proceeded as shown in Fig. 3.2.7. The 3D magnetic field calculations have been almost completed for the eight main bending magnets, which define isometric orbits. The mechanical design including trim coils for fine tuning of the magnetic field, is also progressing sequentially. Concerning about the quadrupole-magnet station, which is the key to controlling beam oscillation, the magnetic field calculations, prototype fabrication and magnetic field measurements have been completed for the quadrupole magnets and beam extraction bending magnets, which are the main components of the quadrupole-magnet station. Although this is an unprecedented magnet configuration, we have confirmed that the required performance can be obtained, and we are already well prepared to move on to the fabrication of the actual magnets.

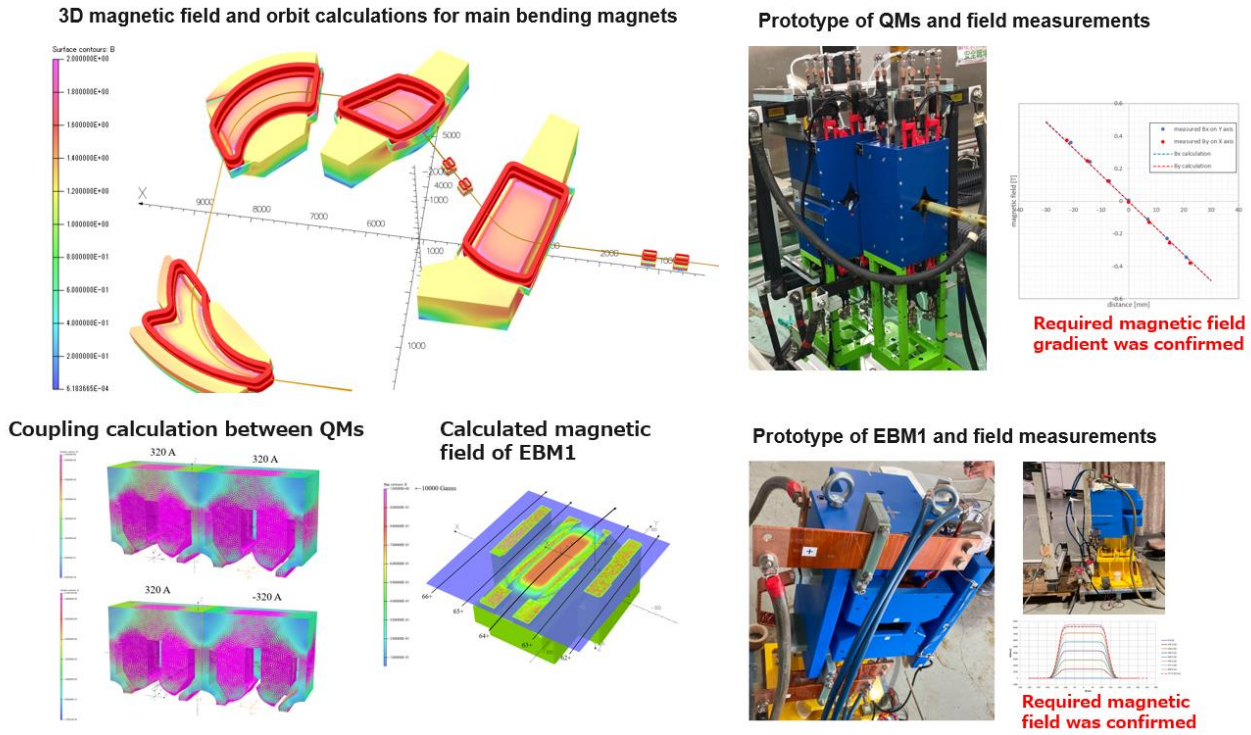

Figure 3.2.7. Magnet design and development works for CSR1.

Other necessary tasks have been almost completed, including calculation of interactions in the stripper and 2-stage stripper design, RF cavities design and optimization, beam position monitor (BPM) design calculations [3.2.12], design of beam transport (BT) systems before and after CSR1, and their beam-matching methods (Fig. 3.2.8).

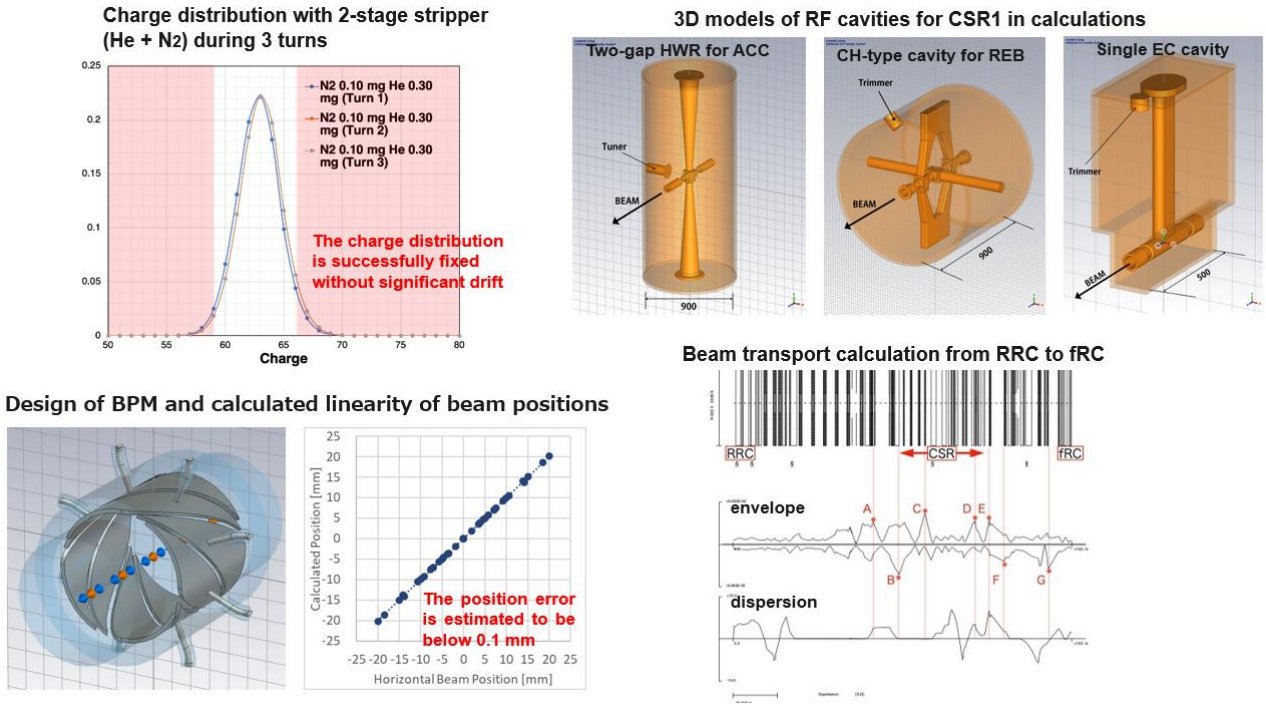

Figure 3.2.8. Component design works for CSR1.

As mentioned above, a technical advisory committee (TAC) meeting was held on June 15-16, 2023. We have had strong support and 20 recommendations (R1-20) from TAC in moving forward with the project with CSR1. The items of the 20 recommendations can be categorized as follows.

1. Recommendations on how to proceed with the project (R1-2, R20).
2. Recommendations related to essential system design (R4-6).
3. Recommendations related to understanding beam interaction (R8, R10, R12).
4. Recommendations on beam tuning (R3, R7, R14).
5. Recommendations for detailed mechanical design and prototype fabrication (R9, R11, R13, R15-19).

The recommendations in category 1 are very reasonable, and we will proceed with the upgrade plan in accordance with the recommendations. Category 2, the system-related recommendations, is the most important, and for R4, we have already completed a study for a 10-charge circulation. The number of circulating charges can be adapted to meet budgetary requirements. We have also decided to place dedicated steerers for closed orbit distortion (COD) compensations in accordance with the R5 recommendation. In category 3, especially R10 is important and will be studied by a dedicated research team. For the category 4, we will build a realistic beam simulator of CSR1 according to R7. Concerning about category 5, mechanical design and prototyping have been concentrated on the main magnets, but will be progressed for all components in sequence. The concentration of recommendations on category 5 indicates that the development of this unprecedented device, CSR1, is entering a phase of actual fabrication in all directions.

CSR2 and modification of injection system for IRC

As mentioned above, we have already started the detailed design and element development of CSR1, and it is possible to design CSR2 with the same equipment configuration as CSR1. For CSR2, we are also proceeding with the determination of basic parameters, lattice design and orbit calculation, and have shown that CSR2 is feasible with the same instrument design as CSR1.

Prior to the introduction of CSR2, the IRC injection radius will be modified to be variable within a range of 5 %. Currently, the injection energy of IRC is 10% lower than the extraction energy of fRC due to energy loss at the second stripper. Since the CSR is a machine with equal injection and extraction energies, these energies need to be matched in the use of CSR2.

We note that the 10% energy difference is too large even for the current acceleration scheme. This is due to the lack of data on the equilibrium charge of the uranium beam during the design and construction phase of the RIBF. In the current scheme, a thicker stripper than the optimum thickness to obtain U^{86+} required for IRC acceleration is used, which leads to unnecessary emittance growth of the beam. The data obtained at the RIBF shows that the U^{86+} can be obtained with an energy loss of about 5%. The energy loss required for non-uranium acceleration is also less than 5%. If the injection radius of the IRC can be made variable to accommodate injection with energy loss within 5%, CSR2 can be used in the future and strippers with optimal thickness can be used in the current acceleration scheme without CSR2. This is important to reduce the heat load on the stripper and improve beam quality. The feasibility of the moving mechanism of the IRC injection devices (MIC1, MIC2 and EIC) to change the injection radius has been confirmed, and detailed calculation and optimization of the injection trajectory is in progress.

RF system upgrade for SRC and fRC

The beam intensity to be extracted from the SRC is planned to be 160 kW in this upgrading project. Unfortunately, the current RF accelerator for the SRC is not powerful enough to handle this high beam power. It is necessary to enhance the RF system of the SRC and increase the acceleration voltage V_{acc} by a factor of about 2 (~1 MV/unit) before the beam intensity upgrade by CSR2 is completed. The upgrade will increase the beam turn separation during extraction and suppress the space-charge effect ($\propto V_{acc}^{3}$) of the beam during acceleration in the SRC. We can increase the extraction efficiency of the 160-kW beam and suppress the heat load on the beam extraction equipment such as the EDC to an appropriate value. We will modify the inside of the RF accelerating cavity and install a new RF power amplifier, RF coaxial waveguide, and couplers with a power output of about 500 kW. At the same time, we will improve the extraction system of the SRC such as EDC. Optimization calculations for the RF accelerator cavity for the SRC are already underway (Fig. 3.2.9).

Furthermore, for the RF system of the fRC, the acceleration voltage will be increased and the frequency will be changed to suppress the space-charge effect. The current fixed acceleration frequency of the fRC is 54.75

MHz, but it can be lowered to 36.5 MHz, the same frequency as that of the later cyclotrons (IRC and SRC), to increase the phase acceptance. Furthermore, beam frequency conversion from 18.25 MHz to 36.5 MHz can be performed in CSR1 to fill the beam bunch with 36.5 MHz. This will strongly suppress the space-charge effect in CSR1 and subsequent cyclotrons. Optimization calculations for the RF accelerator cavity of the fRC are also in progress (Fig. 3.2.9).

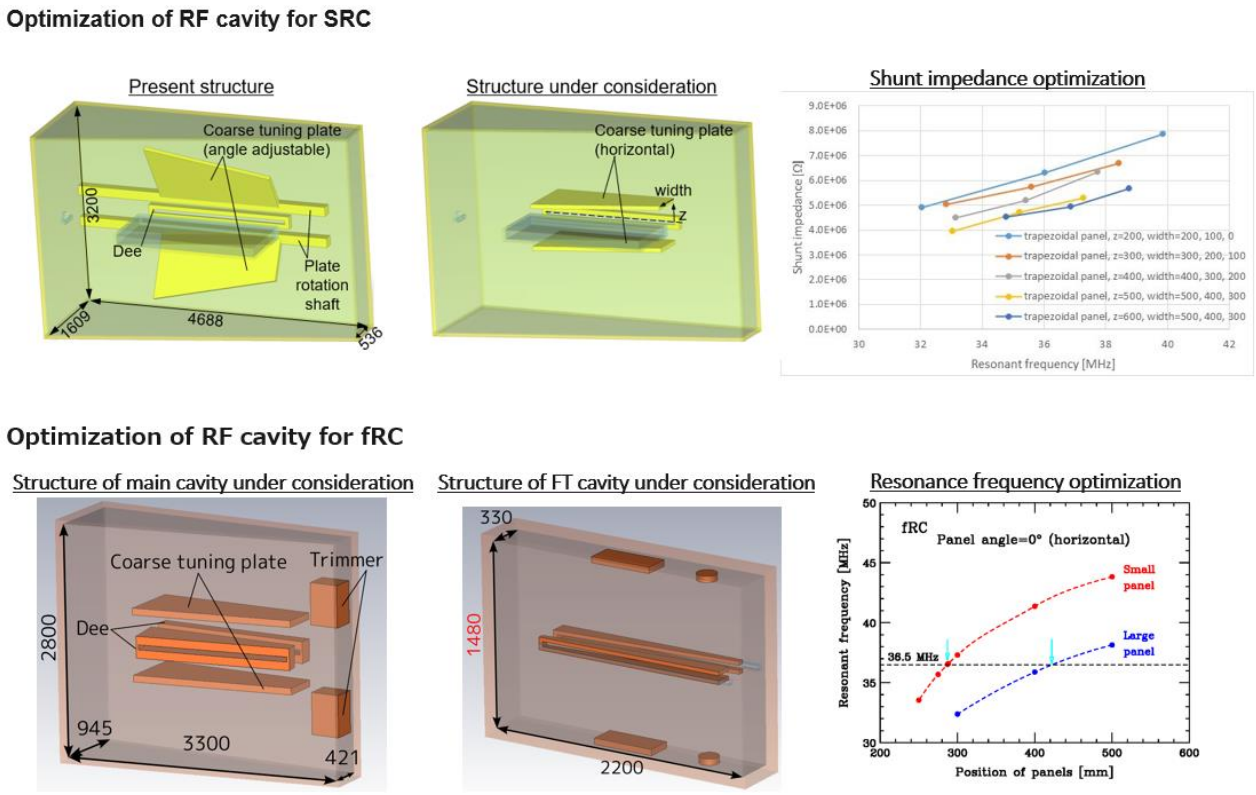

Figure 3.2.9. Calculation of new RF cavities for SRC and fRC.

Ion source upgrade

In parallel with upgrade with CSRs, the ion source (28-GHz SC-ECRIS) will be developed to further increase beam intensity. The ECR plasma is heated by a microwave of approximately 2 kW, which stably produces a U^{35+} beam of 150 μA. To obtain higher beam intensities, microwaves power must be increased. As shown in Fig. 3.2.10, the U^{35+} beam intensity has not reached its maximum with respect to the microwave power, leaving room for increasing the beam intensity by enhancing the microwave power. Therefore, we plan to increase the intensity of the U beam by increasing the microwave power (>5 kW) and enhancing the cooling capacity of the plasma chamber, which contains the high-temperature and high-density plasma generated by the high-power microwave.

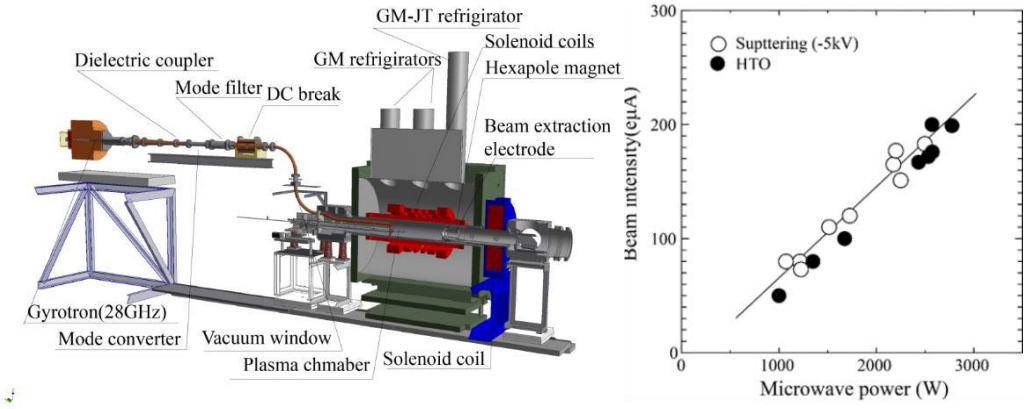

Figure 3.2.10. 28-GHz SC-ECRIS and the output intensity as a function of microwave power.

Furthermore, as the long-term development, we aim to construct a fourth-generation ECRIS (45 GHz, 20 kW) with increase of the microwave frequency and the mirror field strength to obtain higher charged ion beam with high intensity. Increasing the charge state requires high energy electrons to remove deeply bound electrons in the ions. To increase charge state of the ion beam, it is necessary to increase the microwave frequency. Since the microwave frequency (ECR frequency), will be increased, we also develop to increase the strength of the mirror field using high-temperature superconductors to optimize the performance of the ECRIS in the future.

Infrastructure upgrade

We are also studying the infrastructure development needed for the upgrade plan, including electric power, cooling water, and site organization. The total electrical power augmentation required by the upgrade plan is estimated to be approximately 6 MW (Fig. 3.2.11). The current capacity of the special high voltage substation needs to be upgraded from 25 MW to 30 MW. In coordination with the Facilities Division, the possibility of a relatively easy expansion by installing cooling fans on the current voltage transformers is being considered.

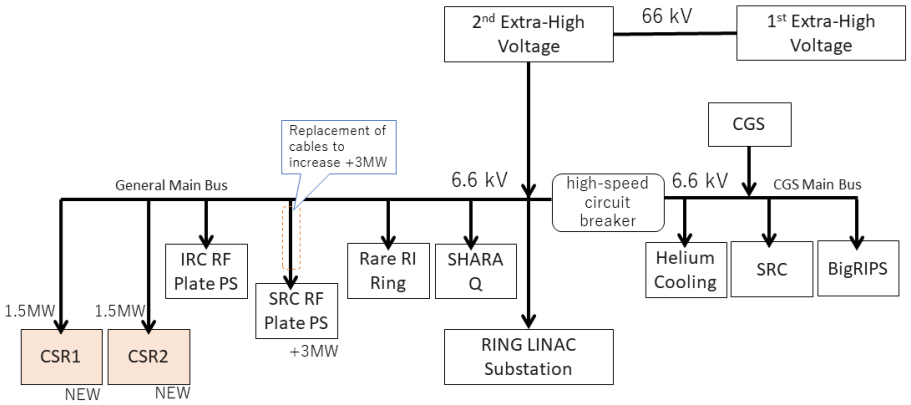

Figure 3.2.11. Electric power system diagram in the upgrade plan.

Construction Schedule

The construction of the primary accelerator-related devices described above can be divided into three packages based on the budget size such as CSR1, CSR2 and upgrade of the RF systems. The upgrading of the secondary beamlines including BigRIPS should also be kept in step. We have an annual plan as shown in Table 3.2.1.

Year	1	2	3	4	5	6	7	8	9
Injection system upgrade for IRC	design work	construction	installation						
CSR1	design work	design work	construction	construction	installation				
ECR-IS upgrade	design work	construction	construction	construction	installation				
SRC-RF upgrade	design work	construction	construction	construction	installation				
fRC-RF upgrade		design work	construction	construction	installation				
Infrastructure upgrade	design work	construction	installation						
CSR2			design work	design work	design work	construction	construction	installation	
Beam intensity						500 pnA			2000 pnA

Table 3.2.1. Construction schedule.

After the detailed design, the construction of the three packages will be completed in about five years, and the target beam intensity will be achieved three years after the completion of the construction.
The plan will proceed as follows.

Year 2: Start of IRC modification and SRC-RF upgrade.
Year 3: Start of CSR1 construction.
Year 6: Start of CSR2 construction and operation towards 500 pnA
Year 9: Operation towards 2000 pnA.

In this plan, each new CSR will increase the beam intensity by a factor of three, and existing equipment will be upgraded to match the intensity of the beam at each stage.

[3.2.1] J. Wei et al., Progress towards the Facility for Rare Isotope Beams, in Proceedings of 2013 North American Particle Accelerator Conference (NA-PAC'13), Pasadena, CA, U.S.A., September 2013, pp. 1453-1457.

[3.2.2] FAIR Baseline Technical Report. vol. 2, (2006).

[3.2.3] D. Jeon, *Status of the RAON accelerator systems*, in *Proceedings of the 4th International Particle Accelerator Conference (IPAC2013)*, Shanghai, China, May 2013, pp. 3898-3900.

[3.2.4] J.C. Yang *et al.*, *Introduction of HIAF project*, in *Proceedings of the 4th International Particle Accelerator Conference (IPAC2013)*, Shanghai, China, May 2013, WEOBB103.

[3.2.5] H. Imao *et al.*, *Charge Stripper Ring for cyclotron cascade*, in *Proceedings of the Twenty-first International Conference on Cyclotrons and their Applications (CYC2016)*, Zurich, Switzerland, September 2016, pp. 155-159.

[3.2.6] H. Imao *et al.*, *Development of gas stripper at RIBF*, in *Proceedings of the 9th International Particle Accelerator Conference (IPAC2018)*, Vancouver, BC, Canada, April 2018, pp. 41-46.

[3.2.7] H. Imao, *Charge Stripper Ring Plan at RIKEN RIBF*, J. Particle Accelerator Society of Japan, Vol. 17, No. 4, 2020. 262.

[3.2.8] H. Imao, *Charge Stripper Ring for RIKEN RI Beam Factory*, J. Inst. (2020) 15 P12036.

[3.2.9] H. Imao, *Status update of the Charge Stripper Rings project*, J. Inst. (2023) 18 P03028.

[3.2.10] Q. Zhao, *Multi-charge-state beam dynamics in FRIB*, in *Proceedings of the 54th ICFA Advanced Beam Dynamics Workshop on High-Intensity, High Brightness and High Power Hadron Beams (HB2014)*, East Lansing, MI, U.S.A., November 2014, TUO1LR01.

[3.2.11] H. Okuno et al., *Present status of and recent developments at RIKEN RI beam factory*, J. Phys.: Conf. Ser. **1401** (2020) 012005.

[3.2.12] Patent Pending, JPN 2023-128268 (Aug 7, 2023).

4 In-flight separator BigRIPS

The BigRIPS separator [KUB12], which consists of 6 dipoles and 14 superconducting triplet quadrupole magnets (STQ) [KUS04], is a tandem-type RI-beam production and separator device (Figure 4.1). Various kinds of RI-beams over a wide Z range in the nuclear chart are produced by the in-flight fission of a ^{238}U beam or projectile fragmentations of ^{238}U (70 pnA), ^{124}Xe (140 pnA), ^{78}Kr (600 pnA), ^{70}Zn (400 pnA), ^{48}Ca (500 pnA), and ^{18}O (500 pnA) beams, where the nominal intensities currently reached are shown in the parentheses. These primary beams are accelerated up to 345 MeV/u by the accelerator complex including the SRC and are irradiated to the Be production targets at F0, the entrance of BigRIPS, to produce RI beams. The RI beams are separated in the first stage equipped with an aluminum degrader by the $B\rho$-ΔE-$B\rho$ method [FUK13]. Recently, another separation method based on $B\rho$-ΔQ-$B\rho$ has been developed to remove contaminants of fission fragments for high-Z RI beams produced by the projectile fragmentation of a ^{238}U beam. The RI beams are then identified on an event-by-event basis in the second stage from F3 to F7 by the TOF-$B\rho$-ΔE method. The particle identification (PID) relies on plastic scintillators for TOF measurements, position-sensitive parallel plate avalanche counters (PPACs) [KUM01] for deducing the magnetic rigidity $B\rho$ by the track reconstruction, and the multi-sampling ionization chamber MUSIC [KIM05] to measure the energy loss ΔE. In the standard ion optics, the momentum resolution of the first and second stages are 1260 and 3440, respectively, which enable us to perform new-isotope search experiments even close to the Z = 70 region, where the fully- and partially-stripped ions are very close each other in the PID plots (Z vs. A/Q). Since the operation initiated in 2007, we have discovered a total of 156 new isotopes and made more than 500 beam settings to supply RI beams to the users of RIBF.

Other than the RI-beam production/separation, BigRIPS is also used as a spectrometer for a few experiments. One example is the spectroscopy of pionic atoms, in which the dispersion matching at F5 was achieved by changing the ion optical modes in the primary beam line and BigRIPS [TAK20]. Another example is reaction cross-section measurements. The reaction targets of carbon were installed at F5 and the PID was performed in F3-F5 and F5-F7, respectively, to assign the reaction channel.

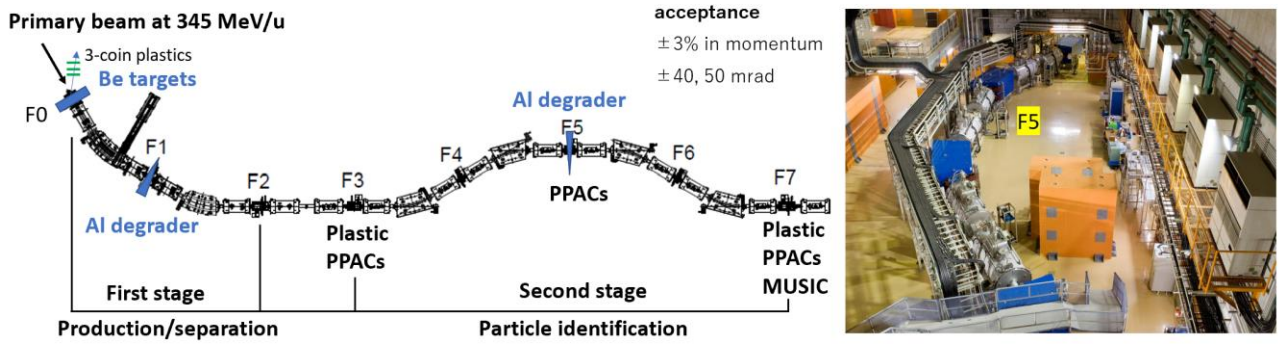

Figure 4.1 Layout of the BigRIPS separator (left) and a birdview of BigRIPS from upstream of F5 (right).

In this section, we will describe the achievement and future upgrade plans of BigRIPS. In Section 4.1, the achievements and performances of BigRIPS, such as new isotopes, since 2007 to today are summarized. In Section 4.2, the upgrade plans for BigRIPS and spectrometers are shown.

4.1 Programs FY2007 – 2022

4.1.1 Discovery of new isotopes

Since 2007, we have discovered 156 new isotopes in a wide-Z range from $_{11}$Na to $_{68}$Er. Among them, 132 RIs were produced by the in-flight fission of the ^{238}U beam. The other 24 RIs were produced by the projectile

fragmentation reaction of the ^{124}Xe (10), ^{78}Kr (4), ^{70}Zn (9), and ^{48}Ca (1) beams, where the numbers in the parentheses denote the number of new isotopes produced. The colored squares in Figure 4.2 show the new isotopes produced from each primary beams. In addition to these results, about 40 more new isotopes are currently under analysis.

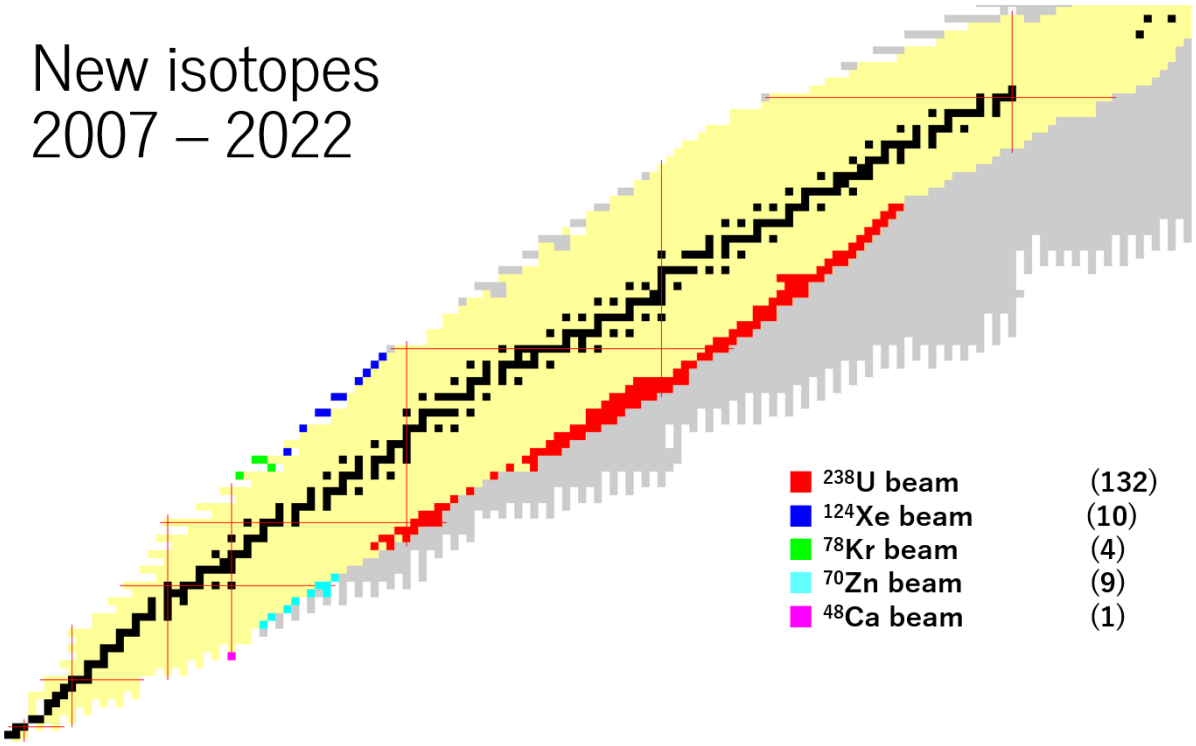

Figure 4.2 New isotopes discovered at the RIBF since 2007. In total, 156 new isotopes were reported. The numbers in the parentheses denote the number of new isotopes produced by the respective primary beams.

4.1.2 Secondary beam production

Since 2007, a total of 514 settings were made for 250 experiments, including PAC approved experiments (EXP), machine studies (MS), and director's discretionary allocations (DA). Figure 4.3 shows the chart of the RIs set as the central particle in the beam settings. Among them, the light-blue circles show the RIs supplied to users with the PID information confirmed by the isomer-tagging technique, while the dark-blue the RI beams supplied without the confirmation by the isomer-tagging technique. The most frequently visited regions include; light RIs near the neutron-dripline region produced from the ^{18}O or ^{48}Ca beams, the "island of inversion" around ^{40}Mg, and the regions near magic numbers, such as Ca, Ni, and Sn isotopes. The heaviest setting made with the PID confirmation is for an $_{68}$Er beam. This beam was used for the cross-section measurement and new-isotope search.

Efforts to produce RIs beyond $Z = 70$ by the projectile-fragmentation reaction with the ^{238}U beam are recently made in several programs of MS or DA. The magenta circles show the RIs used in the MS programs performed to test the beam production of RIs with high Z (~90).

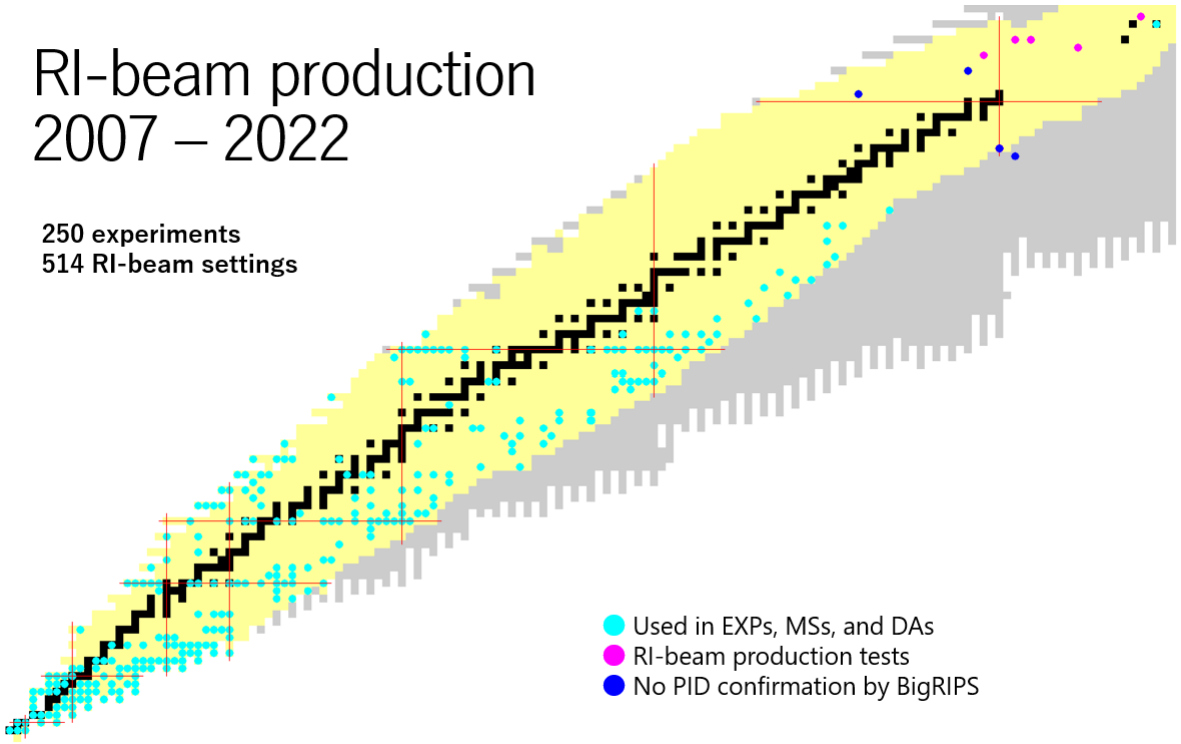

Figure 4.3 RI-beam settings of BigRIPS since 2007. All PAC approved experiments (EXP), machine studies (MS) and director's discretionary allocations (DA) are considered. The settings without the PID confirmation by the isomer-tagging technique (blue) and the settings for the RI beam production tests (magenta) were also shown. Note that the total number of the data plotted in this figure is less than the total number (514) of the settings, since some RIs were produced multiple times.

4.1.3 Development of high-performance beamline detectors

To improve the PID performance in the second stage of BigRIPS, especially toward the region for high Z RIs with Z > 70, high-performance beamline detectors are now developing.

A. The first one is a Xe-gas ionization chamber [YOS22] based on MUSIC [KIM05] to improve the Z resolution for high-Z RIs, especially for the region of $Z > 70$. In the energy range of the RIBF (~250 MeV/u at F7), charge-state fluctuations are not negligible for such heavy-Z RIs. This leads to fluctuations of the energy loss and deteriorates the Z resolution of MUSIC. With the conventional P10 gas (Ar:CH_4 90:10), the ions with $Z < 50$ stay fully stripped over the course of the travel inside MUSIC. On the other hand, the higher Z ions fluctuate its charge state (fully-stripped, H-like, etc.). Ions of $_{70}$Yb for example change the charge state twice in average inside MUSIC according to simulation studies. As this is not frequent enough to reach the charge-state equilibrium, the average charge does not converge within the travel distance inside the chamber. As a result, the average charge and the associated energy loss significantly fluctuate event-by-event. To minimize this effect, it is effective to choose a gas, which leads to the charge-state equilibrium condition as quickly as possible. We chose a Xe-based gas mixture (Xe:CH_4 70:30) for this aim. This gas changes the charge state of Yb ions about 50 times while traveling inside MUSIC. The equilibrium is thus established more quickly and the average charge converges in a shorter distance.
The arrangement of the charge sampling electrodes (12 anodes and 13 cathodes) is shown in Figure 4.4. The electrodes are arranged 2 cm apart inside the total length of 60 cm. The gas pressure is 620 Torr for both Xe-based gas and P10. The Z resolution with the Xe-based gas was evaluated to be about 0.35 in standard deviation (S.D.) for RIs with $Z = 86$ - 89 at 250 MeV/u. This is much better than the performance

with P10-gas evaluated to be about 0.50 in S.D. The improvement of the *Z* resolution is clearly seen in the comparison of the PID plots (in Z vs. A/Q) with P10 and the Xe-based gas mixture in Figure 4.4.

B. The second development is a Xe-gas scintillator [HIJ23]. This detector is an all-in-one solution for timing, position, and energy-loss measurements, currently made by different detectors; plastic scintillators, PPACs, and MUSIC, respectively. Furthermore, the Xe-gas scintillator has an excellent beam rate tolerance for more than 100-kHz RI beams, which is difficult to handle by the present detectors, especially MUSIC. This performance is thanks to a short decay constant of about 100 ns in the scintillation process of Xe gas. The lower panel of Figure 4.4 shows a photo of the Xe-gas scintillator. High purity Xe gas without mixing gas at 2-atm is enclosed in the 9-cm thick gas cell of aluminum with 4-cm openings covered by 125-mm Kapton foils. The gas cell is coupled to 4 photomultiplier tubes (Hamamatsu R6041-406) interfaced by glass windows of Shin-Etsu Quartz SUPRASIL-P310G, which efficiently transmits the 175-ns wavelength photons. The typical performances with a ^{238}U beam with Z = 92 are evaluated to be Δt = 74 ps, Δx = 0.47 mm, and ΔZ = 0.46, comparable to the current performances with the plastic scintillators (40 ps), PPACs (0.3 mm) and MUSIC with P10 (0.50), respectively. The *Z* resolution of the Xe-gas scintillator and P10-gas MUSIC are summarized in the lower panel of Figure 4.4.

It should also be noted that the detector development and commissioning were performed mainly by a group of the Kyoto University, closely collaboration with the BigRIPS team. The Xe scintillator project thus represents a good model of the partnership with universities in the area of detector developments.

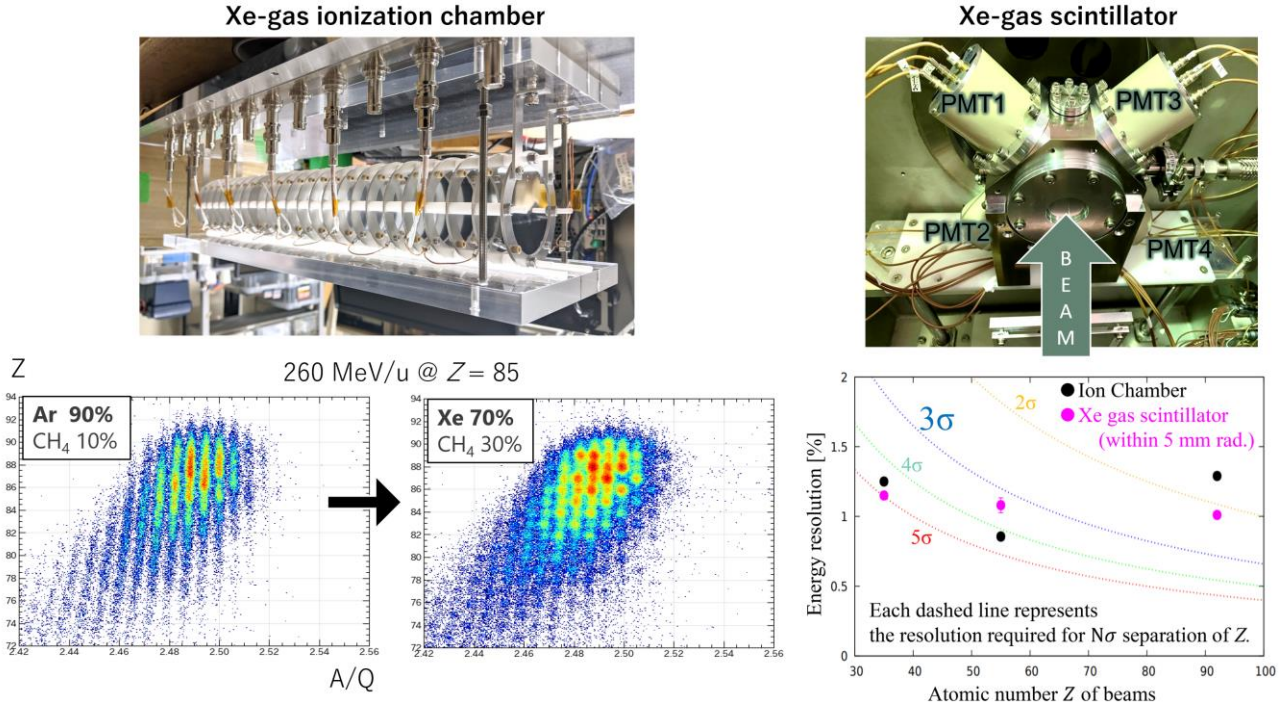

Figure 4.4 Photos of the Xe-gas ionization chamber (top left) and the Xe-gas scintillator (top right). The PID plots (Z vs. A/Q) with P10 gas (bottom left) and Xe:CH_4 70:30 (bottom right) both at 620 Torr are compared. The energy resolution of the Xe scintillator is also compared to P10 MUSIC (bottom right). The figures are taken from Refs. [HIJ23, YOS22].

4.2 Upgrade plan

Heavy element RIs (Z > ~70) will be the grand challenge in a long-term perspective of the RIBF. The projectile fragmentation reaction of a ^{238}U beam is crucial to produce RIs in the heavy element region. The upgrade project of the core facilities of the RIBF thus consists of two major items, one focused on the accelerator

complex to maximize the beam intensity of ^{238}U at 2 pμA by constructing a pair of CSRs (Chapter 2) and the other the BigRIPS separator and spectrometers to maximize the RI beam availabilities and the platform for reaction studies, described in this section. The BigRIPS separator will thus be upgrade to fully handle the high power U beam of 2 pμA. In addition, the purity will be a defining quality in RI beams of heavy element RI, where the separation is challenging. The separation power of BigRIPS will thus be strengthen. An excellent platform for reaction studies with heavy element RI beams will be a key to secure advantages of the upgraded RIBF. The SAMURAI and ZeroDegree spectrometers will be upgraded for this aim.

In this section, we will first describe the RI-beam intensities expected for the primary beam intensity of 2 pμA delivered by the upgraded accelerator complex. The second part will be focused on the upgrade plan of the BigRIPS separator and spectrometers equipped to the secondary beam delivery ports.

4.2.1 Evaluation of RI-beam intensities with 2-pμA primary beams.

The primary-beam intensities will increase to 2 pμA after the upgrade of the accelerator complex based on a pair of charge-stripper rings CSRs. The intensities of RI beams were evaluated over the whole domain of the nuclear chart for the primary beams of 2-pμA at 345 MeV/u (Figure 4.5). The isotopes denoted by colors are expected to have intensities higher than 10^{-5} particles per second (pps), which corresponds to about 1 particle per day. Listed below are examples of possible experiments at the respective intensities:

- 10^{-5} pps; new-isotope searches.
- 10^{-4} pps; β-decay lifetime measurements.
- 10^{-3} pps; β-delayed γ-ray spectroscopy.
- 10^{-2} pps; mass measurements by MRTOF-MS / R3
- 10^{-1} pps; in-beam γ-ray spectroscopy for the first 2^{+} state of even-even RIs.
- 1 pps; in-beam γ-ray spectroscopy for other channel or reaction cross-section measurements.

Candidates of new isotopes are found outside the boundary of currently known nuclei (red line). A total of about 290 new isotopes are expected to be discovered. Among them, about 160 isotopes are neutron-rich nuclei produced by the in-flight fission of the ^{238}U beam. They are spread over the region of $Z = 30 – 60$ (~30 isotopes), the region of $Z = 60 – 70$ (~30 isotopes), and $Z > 70$ (~100 isotopes). At the proton-rich side, about 110 isotopes are produced by the projectile fragmentation reaction of the ^{238}U beam. Another 20 are produced from other primary beams, such as ^{124}Xe or ^{70}Zn. The majority of new isotopes (~210) are thus concentrated in the high-Z region from $Z = 70$ to 92.

Other than the primary beam species listed above, we also evaluated the RI beam intensities for the primary beam of Pb, so far not accelerated at the RIBF. At very proton-rich and neutron-rich regions, the beam intensities of Pb do not seem to have distinct advantages over the projectile fragmentation reaction of ^{238}U. In practice, the purity could be easier to handle with a Pb beam without contaminants of fission fragments.

The beam intensities were evaluated by LISE^{++} under the conditions described below:

- The currently available primary beams, namely ^{18}O, ^{48}Ca, ^{70}Zn, ^{78}Kr, ^{86}Kr, ^{124}Xe, and ^{238}U, are considered. The beam energy is 345 MeV/u. The intensity is set to 2 pμA.
- RI-beam production reactions are the projectile fragmentation reaction for all primary beams. In-flight fission is considered for the ^{238}U beam.
- The production targets are made of beryllium with thicknesses equivalent to 0.35 in d/R.
- The measured cross sections were considered. If not available, the cross-section formula of EPAX3.1a was used for the projectile fragmentation reactions. For the in-flight fission, in the region far from the stability, the cross sections are assumed to decrease by 1/50 with one neutron added. Inside or near the stability line, the three-fissile model in the LISE^{++} ver. 8.4.1 was used.

- The transmission for the fission fragments of a ^{238}U beam. The losses due to momentum spreads and to charge state spreads are taken into account independently. For the momentum spreads, the transmission is defined as a function of *A*. It is fixed to be 5% for A < 45 and 65% for A > 195, and is gradually increased from the former to the latter. For the charge states, the transmission is expressed as a function of *Z*. It is set to be 100% for Z < 45 and 3% for Z > 65, and to constantly decrease in between.

- The transmission for the projectile fragmentation reactions. For the momentum spreads, the momentum distributions are calculated with the Goldhaber model. Note that the resulting spread sizes are multiplied by a factor of 1.2 to better reproduce the distributions calculated by LISE^{++}. For the charge states, the same procedure for the fission fragments is adopted.

- The loss due to the in-flight decay is taken into account. When the lifetime is close to or shorter than the TOF of F0 to F7 (typically 450 ns), the intensity decreases as RIs decay in flight. This effect is important for neutron-deficient RIs. The lifetime data were taken from the JAEA chart of nuclide [No127-06.pdf (aesj.or.jp)].

- The transmission loss by the exit beam dump is not included. Sometimes, the orbits of the primary beam and the RI beam are very close to each other. In such cases, a significant transmission loss results. This issue is not observed for very exotic RI beams.

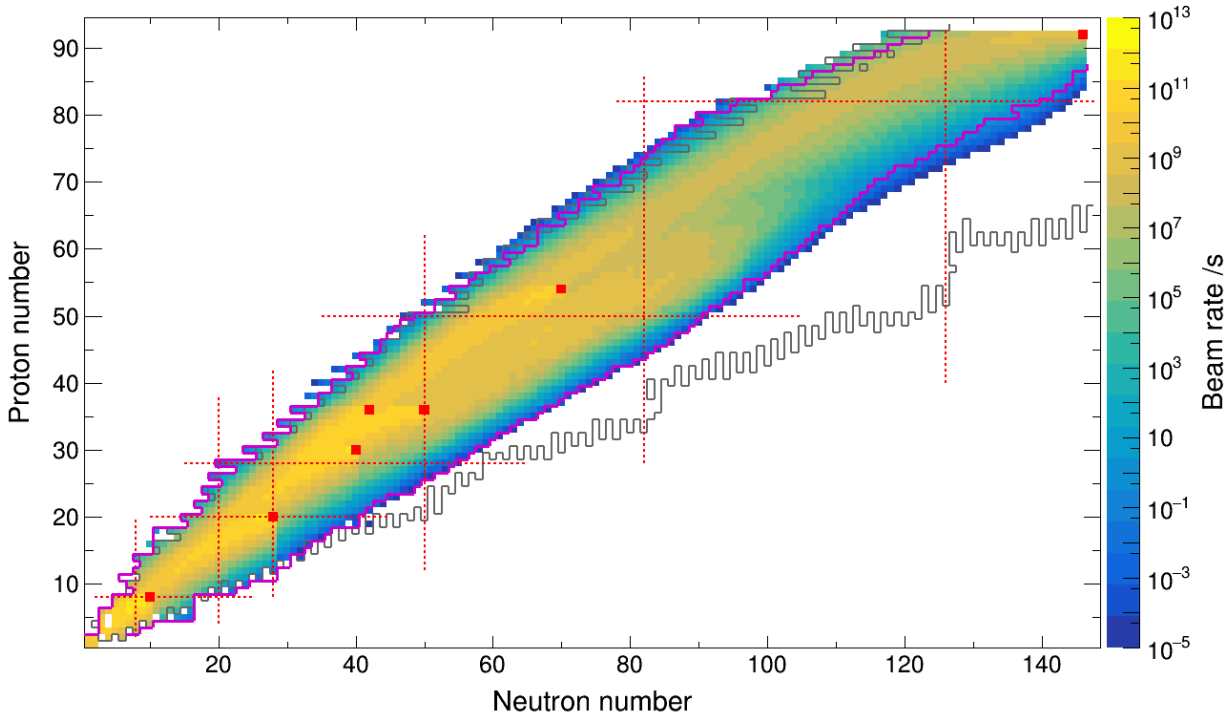

Figure 4.5 RI beam intensities evaluated for the primary beam intensity of 2,000 pnA. The color code denotes the expected intensity in the unit of particles per second (pps). The primary beam species are indicated by the red squares. The boundaries of the known nuclei (red lines) and the predicted driplines by the KTUY mass formula [KOU05] (black lines) are shown.

4.2.2 Upgrade plan for BigRIPS

The upgrade plan has three objectives as summarized below and in Figure 4.6.

(1) Upgrade of the BigRIPS first stage to handle high-power primary beams: The sustainable, efficient and safe operation of BigRIPS will be ensured for the high-power uranium beams. For this aim, the tolerance for radiation and heat loads will be improved for the first stage components irradiated by primary beams. In addition, to minimize the beam downtime, a remotely-controlled auto-exchanging system will be

developed for the maintenance and replacement works of these components.

(2) Upgrade of the BigRIPS first stage for high beam purities: The separation of RI beams is challenging in the high-Z region from Z = 70 to 92 produced by the projectile fragmentation of the ^{238}U beam. The separation power of BigRIP will be improved by implementing newly-developed superconducting quartet quadrupole magnets (SQQ) and an RF deflector (RFD) in the first stage.

(3) Upgrade of SAMURAI and ZeroDegree Spectrometer: For reaction studies with heavy element RI beams, the PID performance after the secondary reaction is crucial. The momentum resolution of the ZeroDegree Spectrometer will be improved. The SAMURAI spectrometer will also be upgraded for a higher acceptance of incoming RI beams and for an alternative dispersion matching optics.

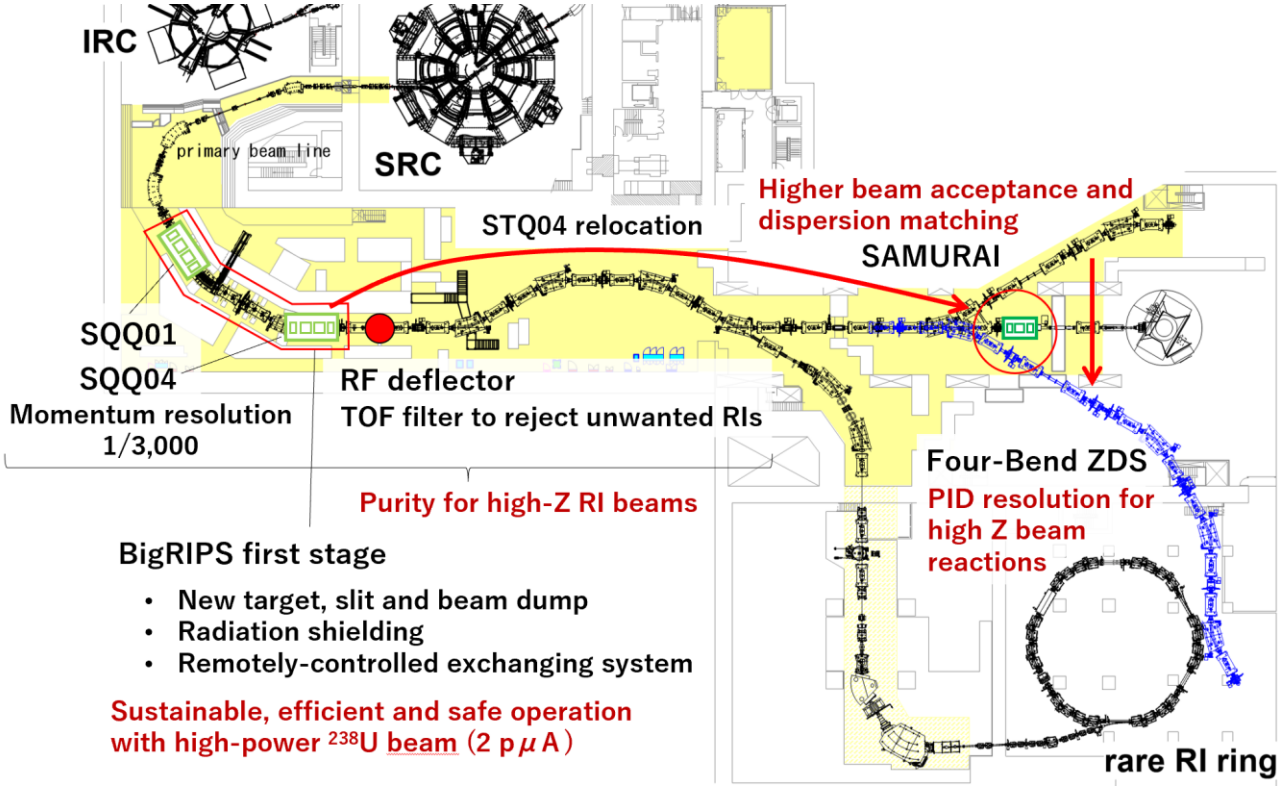

Figure 4.6 Summary of the upgrade plan for the BigRIPS and spectrometers in the secondary beam lines. Note that the layout of the four-bend ZeroDegree Spectrometer is conceptual.

Upgrade items are described for each purpose below:

(1) Upgrade of the BigRIPS first stage to handle high-power primary beams

A. The first stage with a production target and beam dump experiences the highest radiation and heat loads in BigRIPS. An improved resilience against radiation and heat loads is essential for the sustainable and efficient RI beam production by BigRIPS under the irradiation of a high power uranium beam. The current BigRIPS can accept only up to 500 pnA of the ^{238}U beam. For the final goal of 2 pμA, we will develop a new production-target system, beam dump and F1 slits.

The new target system will be a rotational carbon plate with a diameter of 1 m, which is much larger than the present beryllium target of 30 cm diameter with the intensity limit at 1 pμA. The new exit beam dump will be in a drum shape and made of copper-alloy of 30 cm in diameter. The drum is rolling under irradiation. The rotating surface will dissipate the heat more efficiently compared to the current fixed beam dumps of copper alloy, arranged in a V shape, with a limit of 500 pnA. The same rolling-drum structure will be adopted for the F1 slits. These slits will help intercept the primary beams in the F1 chamber, when the orbit of the primary beam is very close to the RI beam of interest.

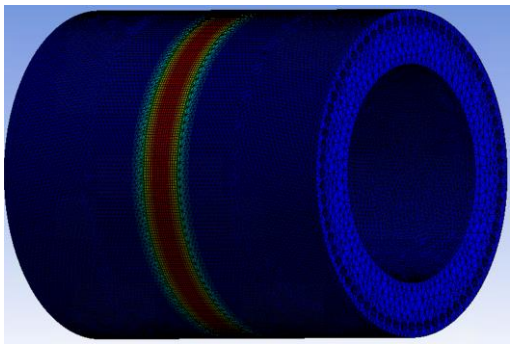

Figure 4.7 Simulation of the heat load with the beam dump with the rolling drum structure.

B. For the safety operation, a remotely-controlled auto-exchanging system will be developed for the beam line components of the first stage. Currently, all works at the first stage are made manually. The beam needs to be stopped until the radiation level becomes low enough to access the vault of the first stage. For example, to change energy degraders at F1, the downtime of BigRIPS is typically 12 to 24 hours. When the primary beam intensity reaches 2 pμA, a longer downtime will be required, causing an inefficient operation. If replacement works or light repair works can be performed remotely and without entering the vault, the downtime can be greatly minimized. We will thus develop an automated exchanging system for the beam line components of the first stage, such as the production targets or energy degraders, together with a remote monitoring system. In addition, radiation-shield concrete blocks will be added to handle the radiation for the beam intensity up to 2 pμA.

(2) Upgrade of the BigRIPS first stage for high beam purities

A. To improve the beam separation power for the high-Z region and/or more neutron-rich region, the momentum resolution of the first stage will be improved from the current value of $\Delta p/p = 1/1260$ to about 1/3000. Such a high momentum resolution could be obtained by replacing the STQ01 and STQ04 with Superconducting Quartet Quadrupole magnets (SQQ). The momentum resolution is mostly governed by the D/M ratio (D; dispersion. M; magnification). By using the current STQs, it is hard to change D or M independently to vary the D/M ratio. SQQ01 provides a more degree of freedom to the ion optics design, thus greatly helping improve the D/M ratio. For the symmetry of the first stage layout, STQ04 is also replaced by SQQ. The optimization of the ion optics with SQQs is underway.

   To increase the transmission of the RI beams, new F1 energy degraders will be developed. The material of will be chosen under the consideration that a much heavier material than aluminum, such as gold, may be useful for a faster charge-state equilibration for high Z beams. We will also design a better degrader shape. The momentum-compression mode, for instance, will be considered in the optimization of the shape.

B. For further separation, a new RF deflector (RFD) will be installed at F2.5, the middle point between F2 and F3. The RFD applies a vertical electric field at a frequency of 36.5 MHz, which transmits ions of interest passing at the moment of zero field and deflects unwanted contaminants with a different TOF. To evaluate the effects of the RFD, simulations were performed by using the existing experimental data of BigRIPS. The trajectories of ions recorded in the data are deflected in the software by a virtual RF field. The size of deflection is calculated based on the experimental TOF values from F0 to F2.5 with respect to the virtual RF phase, optimized for the transmission of the ions of interest. Figure 4.8 shows the improvement of the purities for the ^{100}Sn setting with a ^{124}Xe primary beam (top) and the $N = 126$ (^{202}Os) setting with a ^{238}U beam (bottom). In both cases, the purity is improved by a factor of six to seven with the RFD. Importantly, the latter case demonstrates that the RFD is useful not only for RI beams in the proton-rich region, as often expected, but also for the neutron-rich high-Z region, where the TOF filter serves to reject the majority of contaminants created by fission products of the ^{238}U beam. Together with other few case studies, we found that the RFD improves the purity from several factors to one oder of magnitude. The specifications required for the RFD are summarized in Table 4.1.

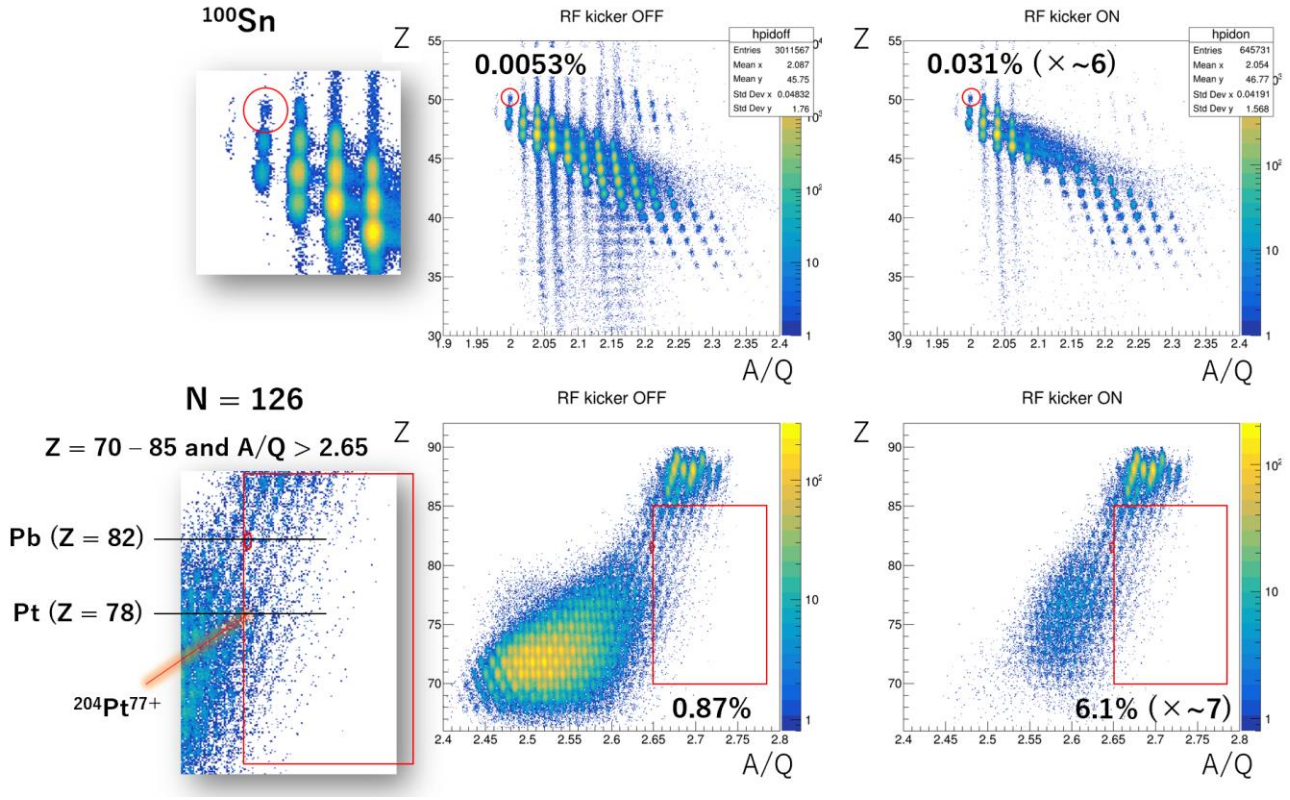

Figure 4.8 Simulation of the RF deflector as a TOF filter of the contaminants for the ^{100}Sn beam (top) and for the N = 126 beam (bottom). The experimental PID plot (Z vs. A/Q) obtained without the RF deflector (left) are filtered by TOF (right) to reflect the effects of the RF deflector. For the N = 126 setting, the purity was evaluated for the neutron-rich region with A/Q > 2.65. For reference, $^{204}Pt^{77+}$ with Z = 78, N = 126 is indicated.

	RIPS	OEDO	BigRIPS RFD
Year of installation	2002	2016	
Cavity enclosure diameter (cm)	80	150	<120
Cavity enclosure height (cm)	230	298	~150
Electrode width (cm)	12	40	~15
Electrode length (cm)	70	120	100
Electrode gap (cm)	4	20	~12
Electric field	vertical	horizontal	vertical
RF frequency (MHz)	12 ~ 19	18.25	36.5
Max voltage (kV)	150	＞350	720
Max electric field (kV/m)	3,750	1,750	6,000
Max power (kW)	20	40	170 ~ 200
Costs (1,000 JPY)	~80,000	~200,000	~500,000

Table 4.1 Summary of the specitications of the new RF deflector for BigRIPS together with the data of the existing RF deflectors at RIPS [YOS] and OEDO [MIC19].

(3) Upgrade of SAMURAI and ZeroDegree Spectrometer

A. The SAMURAI spectrometer will be upgraded for the better acceptance of RI beams. The STQ04 of the first section will be replaced by newly-developed SQQ04 for the purpose of high-resolution optics as described above. The STQ04 will be relocated to the downstream of F12 in the SAMURAI beam line. By this modification, the beam-spot size at F13 (SAMURAI target position) will be half in the normal achromatic optics. For instance, cryogenic target systems, often having a small opening of the order of 1 cm, will benefit from the smaller beam profile. An additional advantage of this modification is the new

dispersion matching optics (Figure 4.9). By using this mode, the unreacted secondary beams from the SAMURAI target can be focused into one point and isolated from reacted ions after the SAMURAI dipole magnet. A small dump can intercept the beam without shadowing the acceptance of the focal plane detectors for reacted ions. This facilitates, for instance, high beam rate experiments.

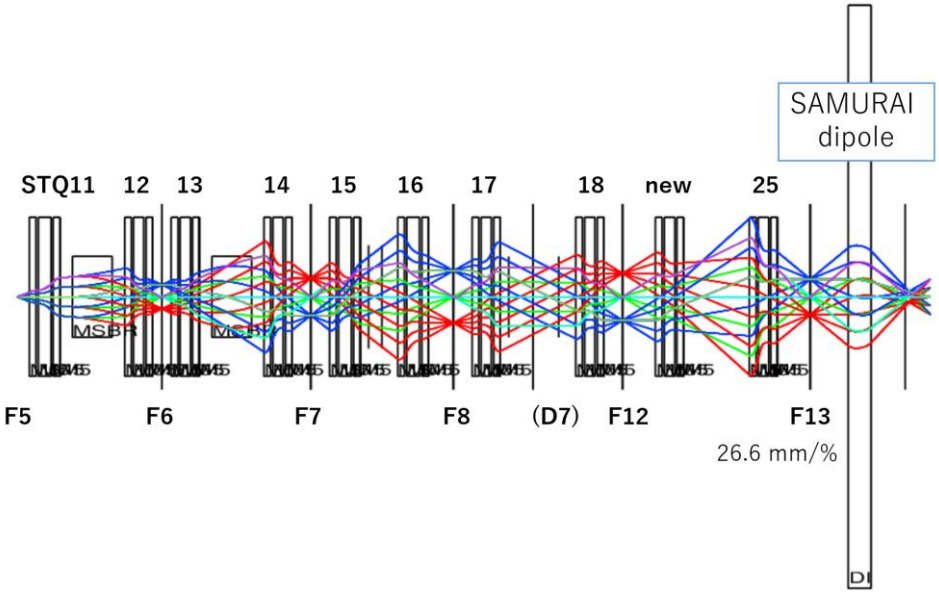

Figure 4.9 Ion optics calculation of the dispersion matching mode of SAMURAI

B. High-resolution ZeroDegree spectrometer with four-bend structure will be constructed. For reactions in inverse kinematics, the particle identification of reaction residues after the target is essential to determine the reaction channel. However, the momentum resolution of the current ZeroDegree with the two-bend structure (two bending dipole magnets) is not enough for heavy element RI beams. The present momentum resolution of 1,380 in the standard optics (Large Acceptance Achromatic mode) is much worse compared to the second stage of the BigRIPS with 3,440. To solve this problem, the four-bend structure is an effective solution as adopted for the BigRIPS second stage. For this aim, the two-bend ZeroDegree will be relocated to the east area of SAMURAI and be extended with another two-bend sector. This provides the same level of momentum resolution (~3,000) as the BigRIPS second stage and also doubles the flight length. In addition, a timing detector with a good time resolution (~5 ps) will be developed to further improve the TOF resolution. In total, the A/Q resolution will be improved from the current value of ~0.1% to ~0.03%, which achieves a similar performance with the second stage of BigRIPS.

4.2.3 Schedule and resources

The timeline of the BigRIPS upgrade is coordinated in harmony with the schedule of the accelerator complex upgrade (Table 4.2). The project is divided into two phases; the phase one covers the development of the CSR1 from Year 1 to 5 and the phase two the development of CSR2 from Year 3 to 8. In the first phase, the beam intensity is planned to reach 500 pnA in Year 6. With this intensity, the radiation and heat loads will stay manageable with the current BigRIPS. The efforts of the first phase will thus be focused on the development of a pair of SQQ and the RFD for high separation power. During the second phase, the BigRIPS first stage will be upgraded for high power beams and be preapared to receive the full beam intensity of 2,000 pnA in Year 8. In parallel, the ZeroDegree will be upgraded to the four-bend structure. The total cost related to the BigRIPS upgrade is estimated to be about 5.1 billion JPY.

The BigRIPS upgrade project will be undertaken by the BigRIPS team of the Research Instruments Group. The team currently has 10 members consisting of one PI, six permanent and three fixed-term members. Five members over 50s assisted the construction and commissioning of RIBF, while other five members under 40s are the main workfoce for the RI-beam production and development of beam line detectors at the current RIBF. The young staff members will drive the upgrade project with strong supports from the senior staff members.

The manpower should be reinforced to undertake both the upgrade task packages and the daily duties, such as the BigRIPS tuning, maintenance, trouble-shootings or data analysis. We plan to hire five new permanent staff

members under 40. Among them, two will be involved in the first phase (focused on the SQQs and RFD) and should be recruited urgently. Each recruit will be assigned a different responsibility in the upgrade workpackages, so that they are visible in the project and developed as an expert of a certain technology. They will also be assigned a related daily duty to assist the opearaiton and to smoothly slide from the development phase into the operation phase in future.

Other related developments, such as for beam line detectors, will be undertaken with close collaborations with other teams in the Research Instruments Group and research groups in universities (as in the model case of the Kyoto University commitment to the development of the Xe scintillation detector).

Year	1	2	3	4	5	6	7	8	9
Injection system upgrade for IRC	design	construction	installation						
CSR1	design	design	construction	construction	installation				
ECR-IS upgrade	design	construction	construction	construction	installation				
SRC-RF upgrade	design	construction	construction	construction	installation				
fRC-RF upgrade		design	construction	construction	installation				
Infrasstructure upgrade	design	construction	installation						
CSR2			design	design	design	construction	construction	installation	
BigRIPS first stage for high power beam			design	design	design	construction	construction	installation	
BigRIPS first stage for high purity beam	design	design	construction	construction	installation				
Spectrometer upgrade			design	design	design	construction	construction	installation	
Beam intensity						500 pnA			2000 pnA

Table 4.2 Schedule of the RIBF upgrade. The work packages describted in this section are highlighted by yellow.

4.3 References

[FUK13] N. Fukuda et al., Nucl. Instrum. Methods Phys. B 317B, 323 (2013).
https://doi.org/10.1016/j.nimb.2013.08.048
[HIJ23] Y. Hijikata et al., Nucl. Instrum. Methods Phys. B 541, 333 (2023).
https://doi.org/10.1016/j.nimb.2023.05.039
[KIM05] K. Kimura et al., Nucl. Instrum. Methods Phys. A 538, 608 (2005).
https://doi.org/10.1016/j.nima.2004.08.100
[KOU05] H. Koura et al., Prog. Theor. Phys. 113, 305 (2005).
https://doi.org/10.1143/PTP.113.305
[KUB12] T. Kubo et al., Prog. Theo. Exp. Phys. 2012, 03C003 (2012).
https://doi.org/10.1093/ptep/pts064
[KUM01] H. Kumagai et al., Nucl. Instrum. Methods Phys. A 470, 562 (2001).
https://doi.org/10.1016/S0168-9002(01)00804-X
[KUS04] K. Kusaka et al., IEEE Transactions on Applied Superconductivity 14, 310 (2004).
https://doi.org/10.1109/TASC.2004.829102
[MIC19] S. Michimasa et al., Prog. Theo. Exp. Phys. 2019, 043D01 (2019).
https://doi.org/10.1093/ptep/ptz007
[TAK20] H. Takeda, Y.K. Tanaka et al., Nucl. Instrum. Methods Phys. B 463, 515 (2020).
https://doi.org/10.1016/j.nimb.2019.03.016
[YAM04] K. Yamada et al., Nucl. Phys. A 746, 156 (2004).
https://doi.org/10.1016/j.nuclphysa.2004.09.064

[YOS22] M. Yoshimoto et al., presentation at EMIS2022 (2022).
https://indico.ibs.re.kr/event/469/contributions/3675/attachments/3379/3935/8-3%20Masahiro%20Yoshimoto.pdf

5 Experimental devices

In this chapter, we will present the instrumentation at the RIBF, its evolution since the first beam in 2007 to present and the future projects envisioned at the upgraded RIBF.

5.1 Programs FY2007 – 2022

The RIBF encompasses a fast secondary beamline based on the SRC-BigRIPS facility and a slow beamline with the AVF or RRC. The fast secondary beamline delivers RI beams produced and sepearated by the BigRIPS separator. Fast RI beams at the nominal energy range of 200 ~ 300 MeV/u create great opportunities for reaction studies in inverse kinematics. A variety of reactions at this energy range such as knockout reactions or charge exchange reactions are instrumental, for instance, in probing the magicity or in investigating the tetra neutrons. Compared to the normal kinematics, the inverse kinematics has an important advantage that the beam-like reaction residues can be momentum-analyzed and identified by a magnetic spectrometer downstream of the reaction target. Spectrometers are key to differentiate the reaction channel, identify the final quantum states, or investigate the kinematical correlations. Therefore, the fast secondary beamline of the RIBF has three different delivery ports, equipped with the ZeroDegree Spectrometer [KUB12], the SAMURAI spectrometer [KOB13] and the SHARAQ/OEDO spectrometer [MIC19, UES12], the last serving also as an injector to the storage ring R3. The three spectrometers with distinct characteristics offer strong platforms for versatile reaction studies; ZeroDegree for the high particle-identification (PID) resolution, SAMURAI for the wide acceptance, and SHARAQ/OEDO for the ultrahigh momentum resolution or energy degrading RI beams. The instrumentation of a variety of radiation devices around these spectrometers has been pivotal to exploit the full capacity of RI beams provided by BigRIPS. The evolution in types and in performances over the course of years has been behind a wide range of achievements of the RIBF. It should also be noted that most of the projects are carried out on a wide and organized international collaboration basis. The Nishina Center is committed to a total of 41 MoUs with institutions in 19 countries.

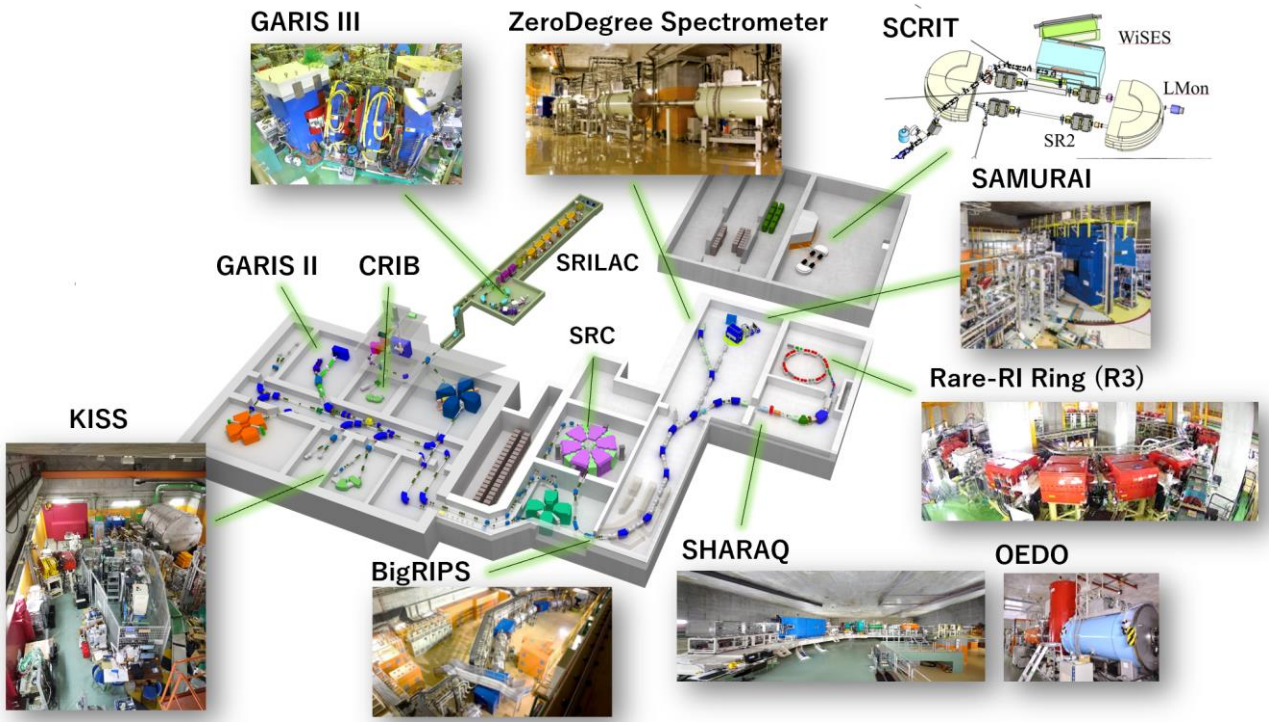

Figure 5.1 Large-scale equipement at the current RIBF.

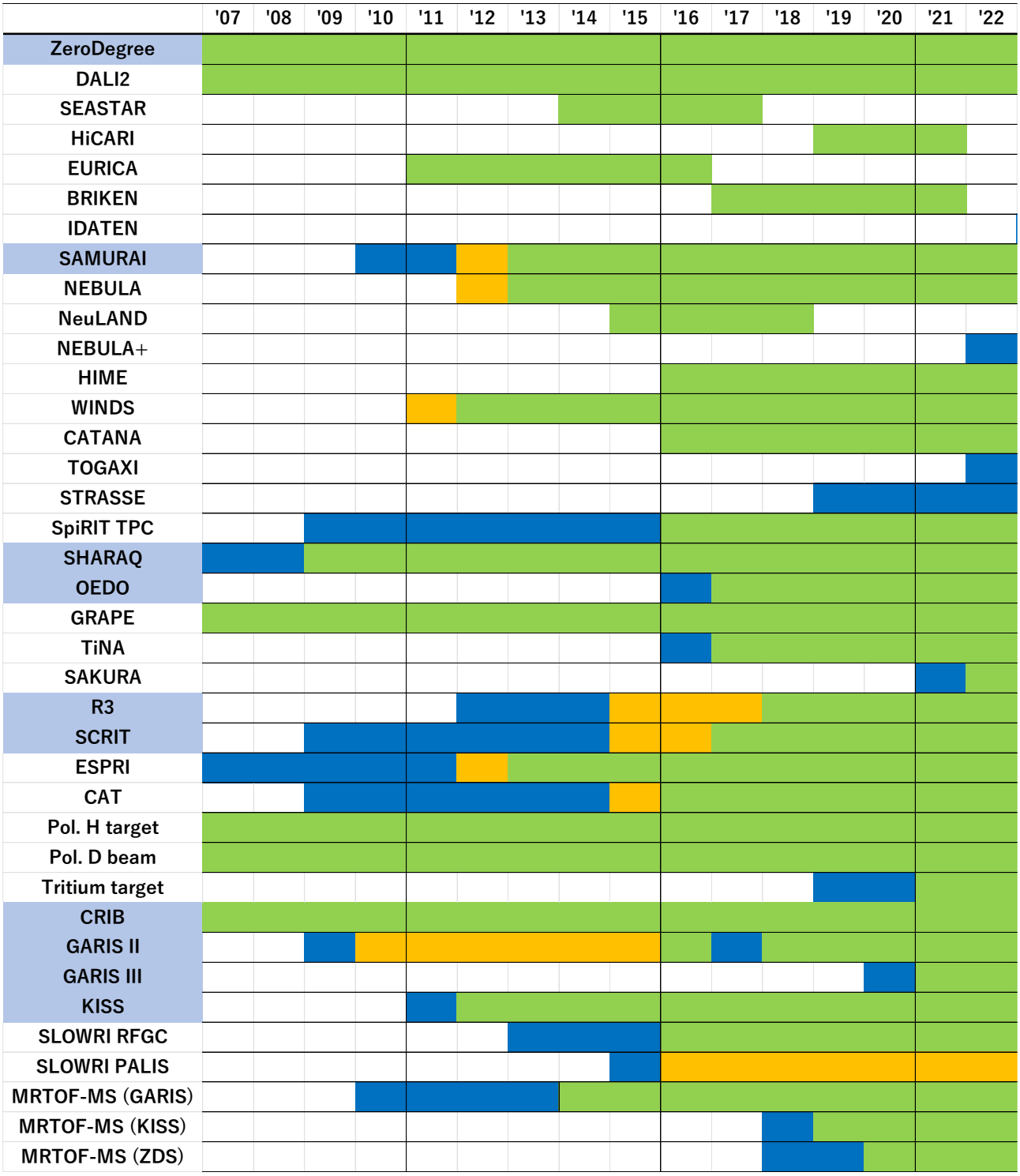

Figure 5.2 History of instrumentation at the RIBF since 2007 to present. The installation (blue), commissioning (yellow), and operation (green) phases are shown for each device. The large-scale equipment is highlighted by the light blue.

The slow beamline is hosting various studies of low-energy RI beams that complementary to the fast beam line. For the superheavy element studies, two spectrometers, GARIS II [KAJ13] at E6 and GARIS III at SRILAC, are operating. The CRIB facility [YAM23], coordinated by the CNS, is another in-flight RI beam facility that is capable of producing light RI beams at beam energies from 1 to 10 MeV/u. The HyperECR ion source and the liquid nitrogen cooled production target enable the maximum intensity of 3×10^8 pps. The KISS facility [WAT18], recently constructed by KEK, is an initiative to produce heavy element RIs in the region

from N = 126 to actinides, which has been difficult to access, by using deep-inelastic scattering.
Besides the heavy-ion-accelerator based instrumentation, a unique apparatus such as SCRIT [OHN13] for electron-RI scattering is also available.
In this section, major instrumentation projects since the arrival of the RIBF are overviewed.

5.1.1 ZeroDegree Spectrometer

The ZeroDegree [KUB12] has been a base for in-beam gamma-ray spectroscopy experiments. The NaI(Tl) scintillator array **DALI2** [TAK14] is a standard device for in-beam γ-ray spectroscopy. The excellent detection efficiency (about 36% for 1 MeV γ rays at 100 MeV/u), while providing an energy resolution of 9% and a peak-to-total ratio of 0.54, assisted the findings of the first 2^+ states in even-even nuclei at the extreme, including ^{54,56,58}Ca, ^{78}Ni, ^{52}Ar, ^{36,38,40}Mg, ^{110}Zr, ^{96,98}Kr or ^{42}Si. The coupling with the **MINOS** liquid hydrogen target system [OBE14] enhanced experimental yields for proton knockout reactions with a maximum liquid hydrogen thickness of 15 cm. The **SEASTAR** project (2014 to 2017) based on the MINOS-DALI2 setup was hosted at the ZeroDegree for the RUN1 (2014) and RUN2 (2015). The first initiative to use position-sensitive and/or tracking germanium clusters was taken in the **HiCARI** project (2019 to 2021). The HiCARI array consists of eight Miniball clusters from CERN Isolde, two GRETINA clusters of the LBNL and RCNP, and four Clover detectors of the IMP.

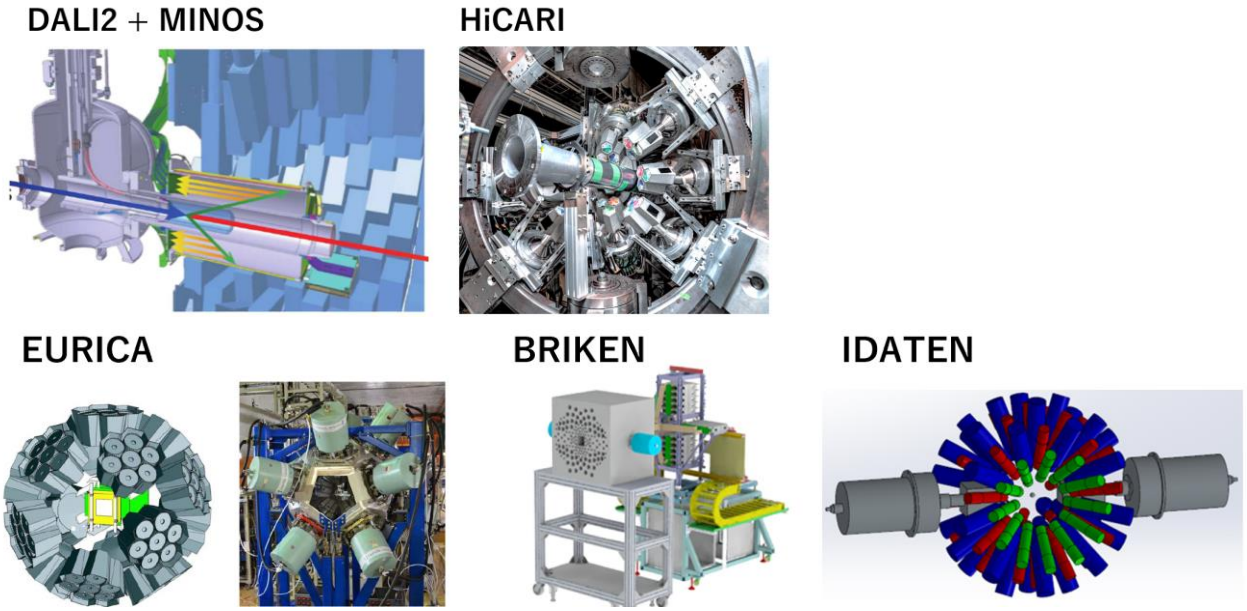

β-decay experiments have been carried out by combining in-house and outside high-performance detectors on a strong international collaboration basis. With the setup being stationed at the final focal plane F11 of the ZeroDegree, a vast amount of RI beams have been successfully measured over a wide region of the nuclear chart. The first large-scale project **EURICA** (2011 to 2016) [SOD13] was focused on β-delayed γ-ray spectroscopy by combining the position-sensitive Si detectors array WAS3ABi for the RI-beam implantation and β-ray radiations and the Ge detectors array EUROBALL (efficiency of about 25% at 200 keV). The next **BRIKEN** project (2017 to 2021) [TOL19] with a high-efficiency neutron detectors array (about 67%) is more dedicated to neutron emission probabilities P_n. β-delayed neutron measurements were performed for about 200 nuclei (with the P_n values for 83 nuclei reported). The **IDATEN** project [LEE23] is currently organized to run from 2023 onwards (until the expected completion around 2026), which couples WAS3ABi to 84 $LaBr_3$(Ce) detectors (efficiency of about 18% at 200 keV) for fast timing γ-ray measurements. The future programs also include (1) the TATAKI project based on the NaI(Tl) array DTAS for total decay energy measurements, (2) the coupling of the β-decay station to the MRTOF mass spectrograph, (3) the proton radioactivity studies by

ACTAR TPC, and a few other projects under development.

5.1.2 SAMURAI spectrometer

The wide-acceptance and multifold detection capabilities, including neutrons, of the SAMURAI spectrometer (since 2012) [KOB13] assisted a variety of reaction studies on both bound states and resonances over a range of nuclei from light RIs to medium-mass fission fragments.

The large opening at zero degrees of SAMURAI enables an efficient detection of neutrons. The neutron scintillation counters array **NEBULA** [KON20] is the core device for this purpose. It consists of two layers of 120 plastic scintillator bars, which facilitate the multifold detection of neutrons. Several efforts have been made to achieve higher efficiencies. From 2015 to 2018, the **NeuLAND** demonstrator of GSI with four double layers covering 2.5 × 2.5 m was temporarily coupled to NEBULA. In 2022, **NEBULA_Plus** with additional two layers of 90 bars was coupled to NEBULA. Both combined, the efficiency is improved to about 60% (from 35%) for 1n and 1% (from 0.2%) for 4n. Another neutron counter HIME (since 2016) is also available as a complementary solution. It has a much more granular construction than NEBULA and thus a better energy resolution (e.g. 2n relative energy resolution of 25 keV at 1 MeV).

The neutron-counter array **WINDS/PANDORA** (2011-) [YAS16, STU17], set at finite angles near the reaction target, is a device optimized for the missing mass spectroscopy by the charge exchange (p,n) reaction. It was used for studies with ^{132}Sn, ^{11}Li and ^{48}Cr. A new solid scintillation material of Eljen Technology allows for the neutron-gamma discrimination by the waveform analysis. Upgrades are planned for larger solid angles and for a better angular resolution.

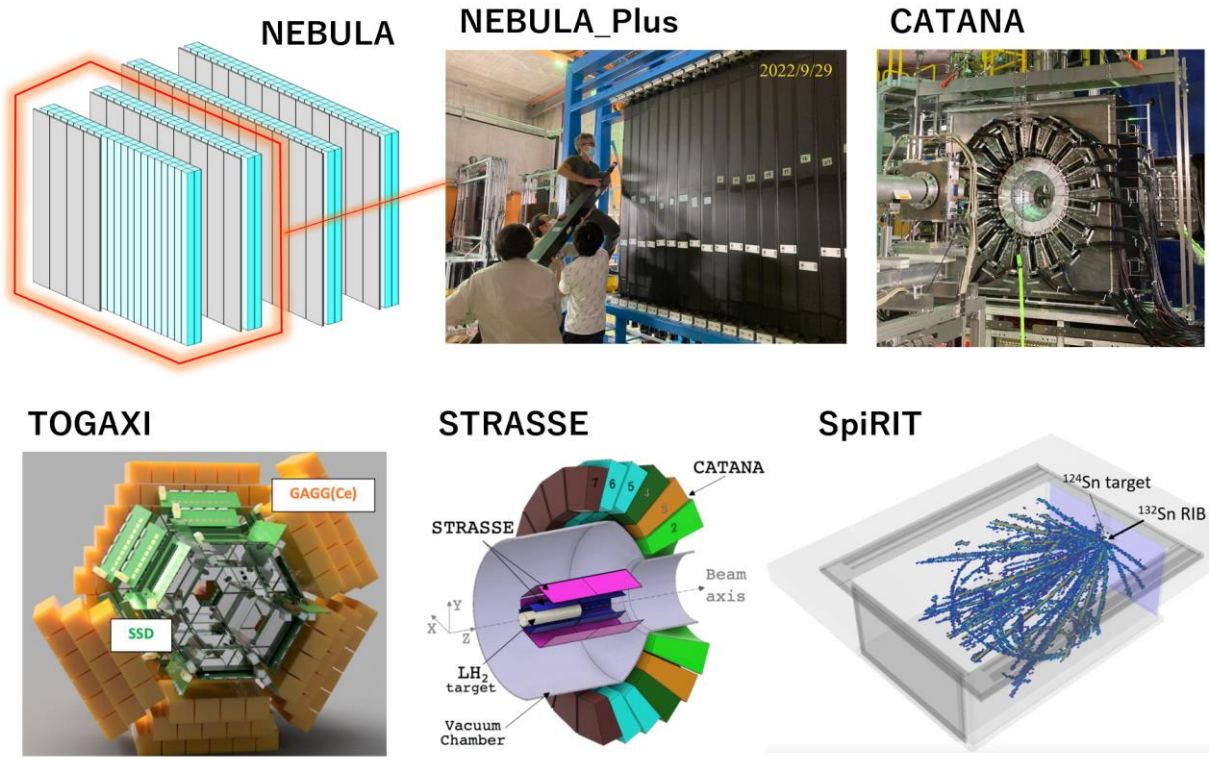

Knockout reactions are a powerful probe of nuclear structure at the typical beam energies of 200 to 300 MeV/u at the RIBF. The development of dedicated detectors was undertaken or is underway. The **MINOS** liquid hydrogen target system [OBE14] provides a thick hydrogen target equipped with a Time Projection Chamber (TPC), which tracks knockout protons to locate the reaction vertex in a very thick target. The RUN3 (2017) of the **SEASTAR** project using MINOS was carried out at SAMURAI to study the level scheme of various neutron-rich nuclei at the extreme. The CsI(Na) array **CATANA** [TOG20] (since 2016) is a calorimetric device

for knockout protons from the (p,2p) reactions. It consists of 140 crystals (and another 20 crystals in 2023) equipped with dual gain electronics, which enable the coincidence detection of de-excitation gamma-rays and knockout protons, having different energy ranges. New particle tracker systems, **TOGAXI** (under the ONOKORO project) and **STRASSE** [LIU23], are under construction. Both based on position-sensitive silicon strip detectors as tracking technologies, TOGAXI equipped with GAGG calorimeters is more adapted to alpha knockout reactions, while STRASSE is coupled to the CATANA calorimeter for (p,2p)/(p,3p) reactions as main objectives. The two detectors will soon be complete and available for physics experiments.
Another unique instrumentation at SAMURAI is **SpiRIT TPC** [BAR21] (since 2016) for heavy ion collision experiments to investigate the symmetry energy term of the nuclear equation of state. SpiRIT encompasses a TPC operated under the SAMURAI dipole magnetic field and capable of identifying light ions and pions (mass resolution of 15% FWHM for Z = 1 isotopes). The Sn+Sn collision run was performed in 2016 and another run with Xe + Sn is currently prepared for.

5.1.3 SHARAQ-OEDO beamline

The beamline serves as the high-resolution spectrometer SHARAQ [UES12] and as the energy-degrading beamline OEDO [MIC19]. The SHARAQ and OEDO modes can be switched by reconfiguring the arrangement of beamline magnets.
The **SHARAQ** beamline (since 2009) is a high resolution beam line optimized to use an RI beam as a reaction probe. The beam monitoring system based on low-pressure MWDC and diamond detector technologies realizes high rate tolerance (about 1 MHz), position resolution (about 100 μm FWHM) and time resolution (about 10 ps r.m.s.). Various charge exchange reactions (t,^{3}He), (^{10}C, ^{10}Be+γ), (^{12}N,^{12}C) or (^{8}He,^{8}Be) have been studied, best known for the study on a tetra neutron resonance. The SHARAQ beamline is also used for mass measurements by the TOF technique over the flight length all the way from BigRIPS down to SHARAQ.
The **OEDO** energy-degrading beam line (2017-), equipped with an angle-tunable energy degrader at FE9 for the energy compression and with a horizontal RF deflector (RFD) for the focusing, provides energy-degraded RI beams in-flight down to 10 MeV/u. The first experiment was performed in 2017 to collect low-energy reaction data at about 20 MeV/u for Long-Lived Fission Products (LLFP), such as ^{79}Se, ^{93}Zr, or ^{107}Pd. The SAKURA project for (d,p) reactions based on the Si-CsI recoil particle array TiNA was initiated in 2022. The minimum beam energy of 15 ± 1 MeV/u was so far achieved with a spot size of about 12 mm SD on target.

5.1.4 Rare-RI Ring (R3)

The isochronous storage ring **R3** [YAM13] is a device for high-precision mass measurements. It features a trim coil system for high precision isochronism (ΔT/T ~1 ppm) over a wide momentum acceptance (Δp/p ~±0.5%), a fast kicker system for the isotope-selectable self-triggered injection and a resonant cavity schottky system. After the construction (2012 – 2014) and machine studies (2015 – 2017), R3 was put into physics experiments in the region of ^{132}Sn and neutron-rich Ni isotopes in 2018 and 2021. In parallel, the development to improve the efficiency and precision continues. Especially the kicker system was upgraded to realize a flat-

top magnetic field for the duration equivalent to one revolution.

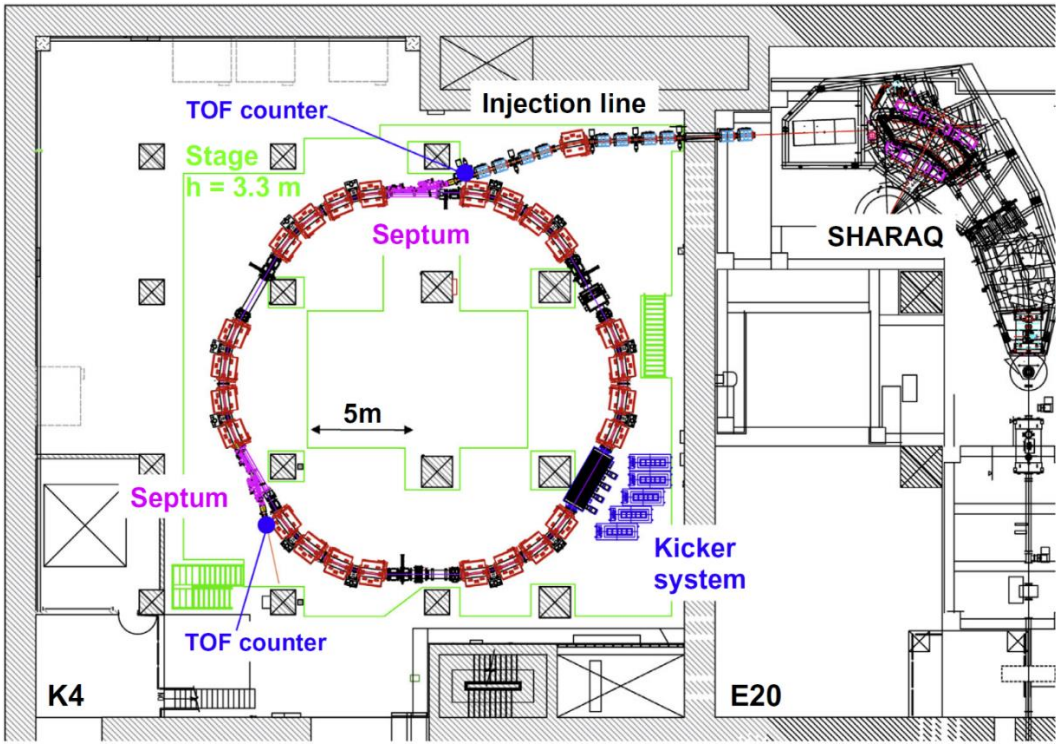

Figure 5.3 Schematic layout of the storage ring R3. The figure is taken from Ref. [YAM13].

5.1.5 Devices for (in)elastic scattering: SCRIT, ESPRI, and CAT-M

SCRIT [OHN13] is a facility for electron-RI scattering measurements based on the self-confining RI target technology. After the construction of SCRIT (2009), ISOL(ERIS) (2011) and the electron spectrometer WiSES (2014), the first measurement was performed with stable ^{132}Xe in 2015 to 2016, demonstrating the validity of the method. Measurements with radioactive ^{137}Cs isotopes produced online were achieved in 2022. Studies of Xe isotopes are currently underway. The machine has so far achieved the luminosity of 3.2 $\times 10^{27}$ /cm^2/s (250 mA e-beam of 250 MeV, 2.5 $\times 10^8$ ^{136}Xe ions/pulse), which will further increase as the development continues. The RI production performance is rated to be 3 $\times 10^5$ cps for ^{132}Sn at 10 W onto a U target of 15 g, which will be upgraded to 1 kW and 30 g in future.

The **ESPRI** system [SAK17] is a device dedicated to measure proton elastic scattering of RIs with high precisions. The neutron and proton density distributions extracted from the elastic data are invaluable information to constrain the equation of state. The ESPRI telescope for recoiling protons encompasses two modules of RPS each having an MWDC, a plastic scintillator and seven NaI(Tl) calorimeters. The telescope is coupled to a solid hydrogen target (SHT) of 1 mm in thickness with an opening of 30 mm in diameter. The ESPRI system was first used at the RIBF in 2013. It is routinely used for elastic measurements or applied to alpha knockout reactions. The next-generation ESPRI project was recently initiated as part of the ONOKORO project.

The active target time projection chamber **CAT-M** [OTA15] is a device of inelastic scattering with RI beams to measure giant monopole resonances for the nuclear incompressibility. A small prototype with deuteron gas served to measure the ^{132}Sn(d,d') reaction in 2016. The CAT-M (2017 -) has a larger active volume of 28 (W) $\times$ 20 (H) $\times$ 32 (D) cm^3. A permanent magnet of 0.3 T is set in the active volume along the beam path to suppress delta rays, which is a huge background source in measurements at the RIBF. The signal-to-noise ratio is by about 400 times better with this magnet.

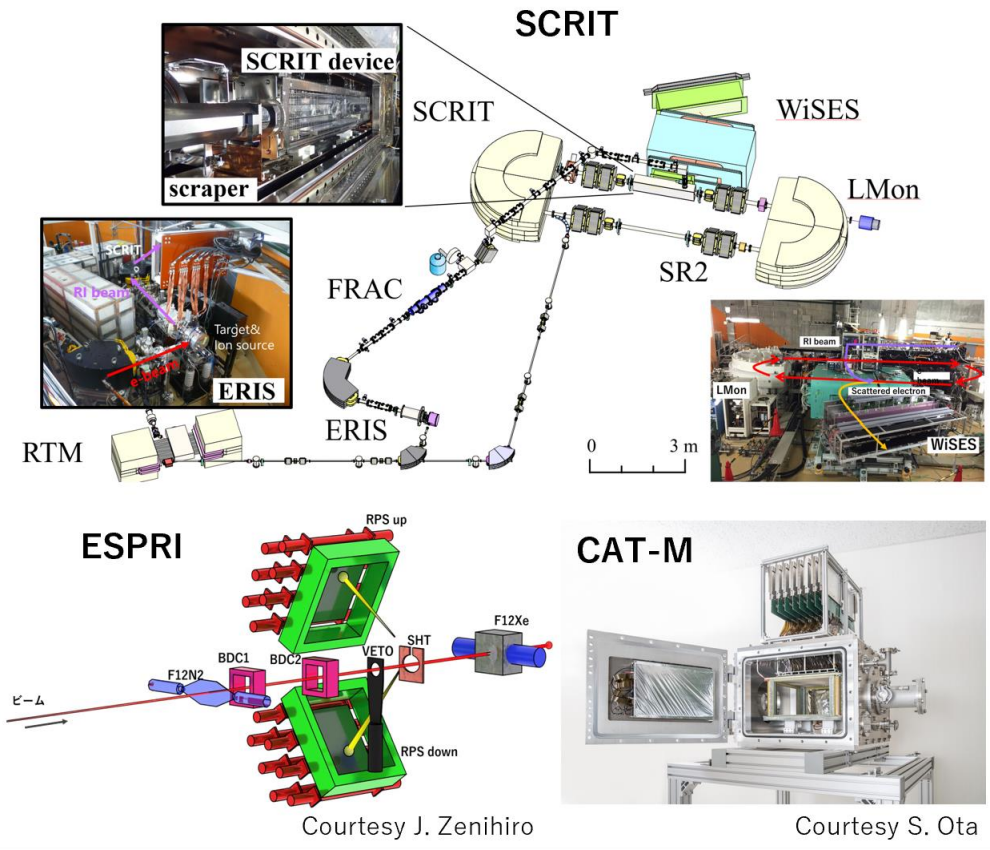

5.1.6 Spin-polarized target and beam; tritium-loaded Ti target

A **spin-polarized proton target system** [WAK05] consists of a naphthalene C_8H_{10} target with a thickness of 1 – 4 mm and a diameter of 10 – 24 mm. A special laser pumping technique provides a high polarization (about 20% at 0.1 T and 20% at 0.3 T) under a relatively low magnetic field at around 100 K, thus facilitating the coupling to detectors for recoiling particles. The target was used for elastic scattering with a ^{6}He beam at SAMURAI and also for the (p,2p) reactions of O, F isotopes at SHARAQ to investigate the spin-orbit potential with neutron-rich nuclei. Upgrade efforts to replace the target material from naphthalene to p-Terphenyl ($C_{18}H_{14}$) are underway to polarize the target at room temperatures without cooling. About 20% polarization is expected under 0.4 T.

The target system has also been upgraded for a larger opening aperture (±60°). This is intended for the future study of the three-body nucleon force (3NF) by scattering with a **polarized deuteron beam** [OKA94] delivered by the AVF-RRC-SRC acceleration scheme. The beam was used for previous studies on 3NF by non-polarized proton elastic scattering in the energy ranges from 200 to 300 MeV/u (2009 to 2015). The beam excels in polarization (about 80%), intensity (100 pnA), and full controllability of the spin axes.

A tritium-loaded Ti target [MIK23] is another unique target developed for the search of tri-neutron by the ^{3}H(t,^{3}He)3n reaction at SHARAQ in 2021. The Ti foil of the targets is loaded with 1.6TBq of tritium, equivalent to 3.5 mg/cm^2, with a high ^{3}H/Ti atomic ratio of 1.54. The tritium thickness is much greater (by about 100 times) than typical Ti-^{3}H targets used in RI beam experiments.

5.1.7 SSRI-PNS (Stop and Slow RI-Precise Nuclear Spectroscopy)

SSRI-PNS is a unified body of collaboration for KISS, SLOWRI, GARIS and MRTOF-MS, each based on low-energy RI beam techniques at the RIBF.

KISS (KEK Isotope Separation System) [WAT18] is an RI beam production beamline developed and

coordinated by KEK. The KISS facility uses deep inelastic scattering to produce neutron-rich RIs in the region from N = 126 to actinides that are important for r-process but hard to study in conventional ISOL or in-flight facilities. A combination of an Ar gas cell, laser resonant ionization, and dipole magnet mass separator, allows to deliver a beam of previously challenging isotopes of refractory elements or of actinide for β-decay and laser spectroscopy or mass measurements. Since 2012, measurements were performed for $_{73}$Ta, $_{74}$W, $_{75}$Re, $_{76}$Os, $_{77}$Ir, or $_{78}$Pt isotopes, and most recently for $_{92}$U and $_{93}$Np, including the new ^{241}U isotope.

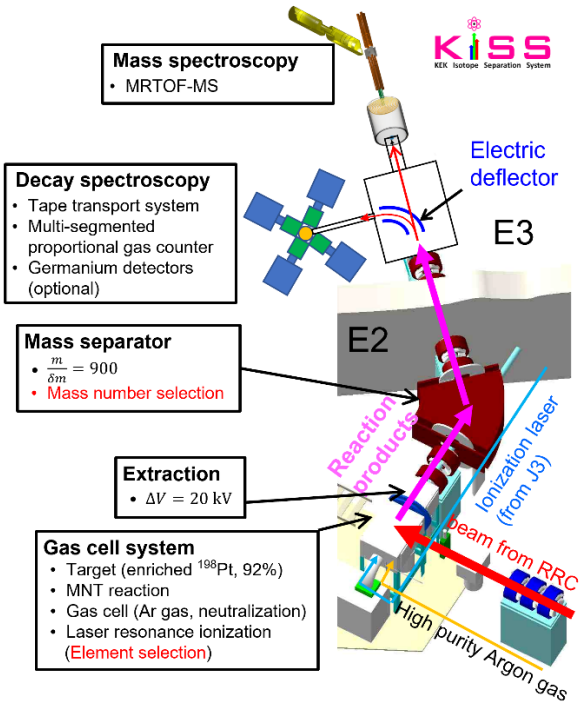

Figure 5.4 Schematic layout of KISS.

The **SLOWRI** project [WAD03] is to provide a low-energy RI beam by the gas catcher technology. It encompasses two types of gas cell, one the RF-carpet type cryogenic He gas catcher (**RFGC**) and the other a parasitic Ar gas catcher with resonant laser ionization (**PALIS**) [SON18]. The RFGC is capable of extracting ions with less elemental dependence than the ISOL technique. The device is presently used to feed ions to MRTOF-MS. For a higher stopping efficiency, it is planned to size up the cell (about 1 m length) and increase the gas pressure (about 300 Torr). PALIS was installed at the F2 terminal of the first stage of BigRIPS in 2015. The online extraction of RI beams was confirmed in 2021 with alpha emitters produced by BigRIPS. A quadrupole mass separator (QMS) and TOF spectrometer are under development for the laser ionization.

GARIS is a gas-filled separator for superheavy element studies. The original GARIS-I was used for the discovery of Nh. GARIS-II [KAJ13] dedicated to hot fusion reactions has been installed in 2009. When the upgrade construction of the SRILAC started in 2017, GARIS-II was relocated to the E6 vault. The new SRILAC beamline was equipped with GARIS-III in 2020. The search for Z = 119 by the ^{51}V+^{248}Cm reaction started in 2018 with GARISS II and is currently underway at the SRILAC + GARIS-III facility. The GARIS-II was equipped with an MRTOF-MS in 2014. The first high-precision direct mass measurement of a superheavy nuclide was recently achieved with ^{257}Db. Since the E6 vault will be a site for the CSR1, the relocation of the GARIS-II to elsewhere, including other vaults, is under consideration to keep the current activity of superheavy mass measurements.

MRTOF-MS (Multi-Reflection Time-Of-Flight Mass Spectrograph) [ROS23] is an instrument for mass spectroscopy. It consists of a drift tube with a pair of mirror electric fields at both ends, which reflect ions to

make multiple laps for the duration of ms range. The mass of an ion is deduced from the TOF over the total distance traveled. A total of three devices are operating at the fast (ZeroDegree since 2018) and slow (GARIS II since 2014 and KISS since 2018) beam lines. The first online application at ZeroDegree was performed during the HiCARI campaign in 2020 in parasitic experiments. More than 70 masses were measured with the mass resolving power better than 500,000. The MRTOF-MS at KISS was instrumental in the recent finding of new isotope ^{241}U. MRTOF-MS is constantly upgraded for higher performances. Examples include a beta-TOF detector for decay-correlated mass measurements or an in-MRTOF deflector (IMD), which deflects unwanted ions by switching on the field at selected times.

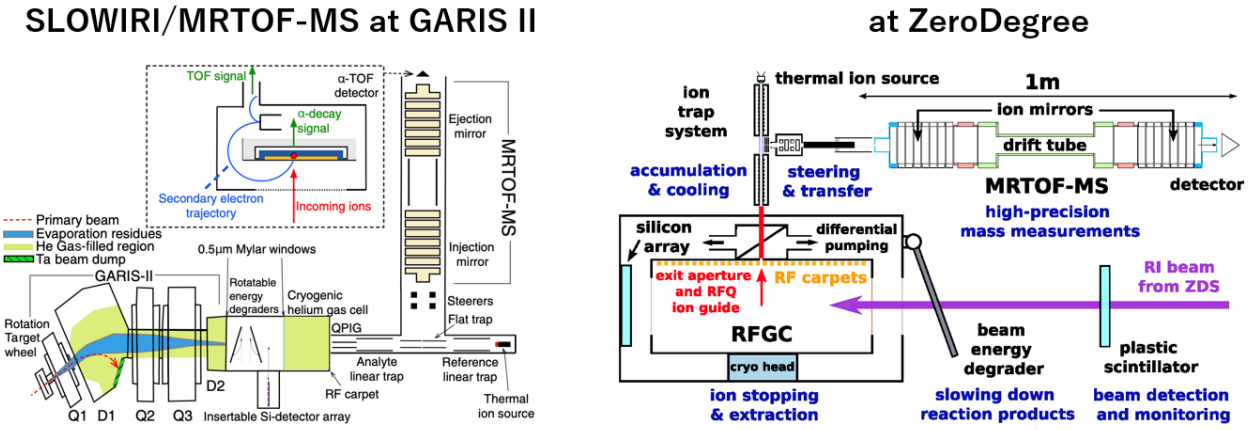

Figure 5.5 Schematic layout of the SLOWRI/MRTOF-MS setup at GARIS II (left) and at ZeroDegree (right).

5.2 Upgrade plan

The region of heavy elements will be the new frontier for the upgraded RIBF in a long-term perspective. This will also be a challenge for the instrumentation. While the existing devices will continuously be upgraded, new initiatives are envisioned or have already been taken to support, especially, reaction studies in inverse kinematics.

In-beam γ-ray spectroscopy will stay as an important method for reactions in inverse kinematics with RI beams. Detectors for γ-ray from fast RI beams constitute an important part of instrumentation. **A new scintillators array of GAGG and/or $CeBr_3$** with a higher energy resolution (5% instead of 9% at 1 MeV) will be developed to replace the DALI2 array. In addition, **the GT-5 project** has recently started to develop tracking germanium detectors with a higher energy resolution (about 2%), position sensitivity (about 3 mm FWHM), and the γ-ray tracking capability.

Experiments related to isomeric states are a promising area of future studies. **The R3 isomer beam filter** is an innovative platform to realize reaction studies with isomeric beams. The isochronous storage ring R3 will serve to tag and/or physically filter isomeric states based on direct mass measurements by TOF. Ions extracted from the ring are delivered in-flight to a reaction station.

Optical model potentials are a fundamental element in reaction analyses. The global potentials currently available are not calibrated with elastic scattering data of RI beams. **The MESA project** has been initiated to establish a global potential for RI beams. The project will deliver a parasitic data taking system for elastic scattering of RI beams, operated anytime with main physics experiments.

RUNBA is another application of the storage ring technology for reaction studies in future. The storage ring of RUNBA encompasses a reaction target inside. Revolving RI beams in the ring are allowed to hit this target multiple times during the revolutions. As a result, RUNBA serves as a luminositiy booster. In addition, RI + RI collisions are envisioned by integrating a self-confining RI target of SCRIT.

KISS II is a major upgrade plan from the KISS facility. KISS II will significantly improve the efficiency of RI beam production and extraction to establish an efficient access to the region from N =126 to the actinide, which includes the region beyond ^{238}U inaccessible by BigRIPS.

As a common infrastructure to all experimental devices, t**he data acquisition system** will be upgraded to be much faster than the present. The expected tolerable trigger rates of about 100 kHz will essentially make it a triggerless system for many cases.

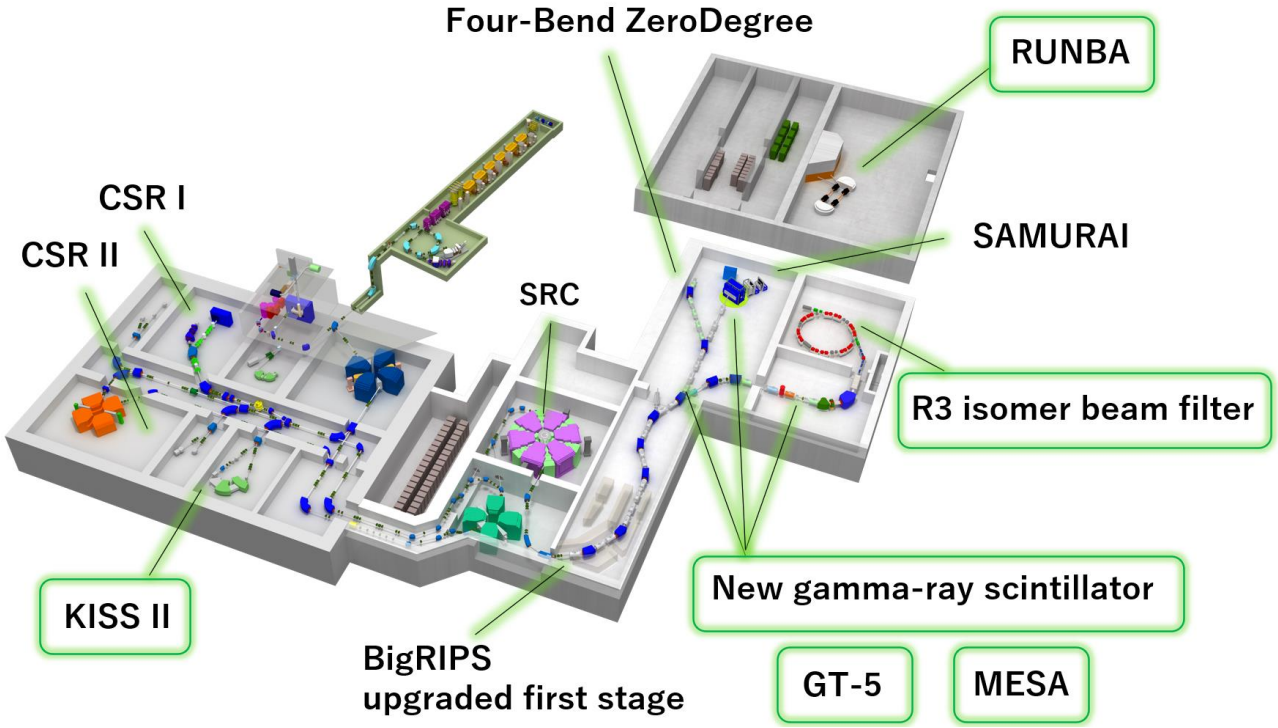

Figure 5.6 Summary of the upgrade plans for the instrumentation. The highlighted instruments are described in this section.

5.2.1 New-generation scintillator array project

Since advent of the RIBF, the NaI(Tl) based scintillation array DALI2 [TAK14] has been the workhorse for in-beam γ-ray spectroscopy experiments. Due to its modest energy resolution, caused by large opening angles and intrinsic energy resolution of NaI(Tl) scintillators, long absorption lengths of the scinitllation material, as well as modest time resolution, the long-term potential is limited. Furthermore, limited available budget makes low cost alternatives to 4π Ge tracking arrays with superior features, except energy resolution, desirable. Consequently, **a new-generation scintillator array for in-beam γ-ray experiments** is being devised for the near future. Here, the scintillation materials HR-GAGG(Ce) ($Gd_3(Ga,Al)_5O_{12}(Ce)$) and $CeBr_3$ have been identified as the most promising choices. Key advantages for the former include its high density, low radiation length, and that it's neither hygroscopic nor self-emissive, while the latter offers a better intrinsic resolution and extremely fast decay time.

It is envisioned that a hybrid array, composed of HR-GAGG(Ce) and $CeBr_3$ crystals, will be employed at different experimental stations of the RIBF (ZeroDegree, SAMURAI, SHARAQ), each having different performance requirements and constraints. In design studies carried out so far, the number of different crystal shapes is minimized. Only two shapes seem sufficient for an entire array, arranged in a configuration combining a forward wall with annular rings, as shown in Figure 5.7 (left). Envisioned detector sizes are 25 × 100 mm^3 for the forward wall and 30 × 8 mm^3 for the rings. A few prototype HR-GAGG(Ce) crystals have been purchased by RIKEN, showing an energy resolution of 4–4.5 % (FWHM) at 1.33 MeV with APD or SiPM as readout, while about 3 % are expected for the $CeBr_3$ crystals.

Using these numbers, an array of ~1000 crystals yields 5 % energy resolution, 53 % efficiency, and 0.72 P/T in GEANT4 simulations of a 1 MeV γ ray emitted at 100 MeV/nucleon. These values need to be compared with 9 % resolution, 36 % efficiency and 0.54 P/T for DALI2, highlighting the potential of the new γ-ray calorimeter. Since 2022, a collaboration comprising several European and Asian institutes has formed with the aim of gradual replacement of $DALI2^+$ crystals.

Key experiments to be carried out in the future at the RIBF at intermediate energies involve inelastic scattering

on high-Z targets to induce Coulomb excitation, as well as inelastic scattering and quasi-free scattering on liquid hydrogen. An example of the performance of the array is shown in Figure 5.7 (right) for inelastic scattering of ^{32}Mg at 50 MeV/nucleon on liquid hydrogen.

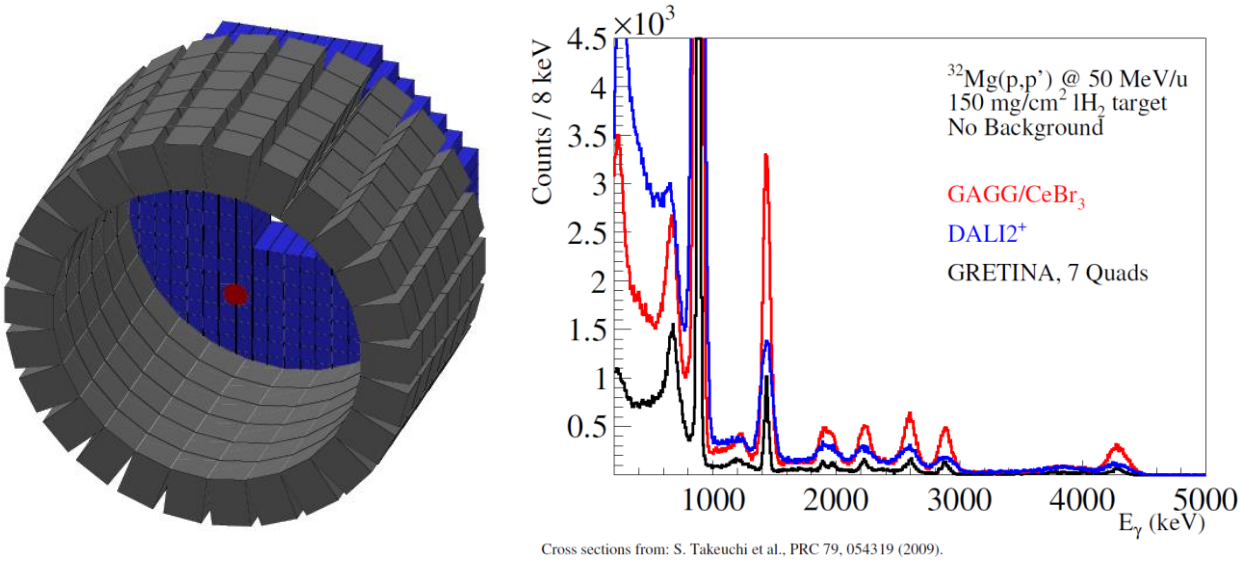

Figure 5.7 (left) Layout of scintillation-based γ-ray spectrometer containing 384 HR-GAGG and 624 $CeBr_3$ detectors. The latter are packed in common housing of 2×2 crystals and arranged in anannular configuration with an inner radius of ~250 mm. (right) GEANT4 simulation of inelastic scattering of ^{32}Mg on liquid hydrogen for new scintillation array, DALI2$^+$, and the GRETINA setup containing 7 quads. Note that background was not included into the simulation.

5.2.2 GT-5: Gamm-ray Tracking in R5 for germanium clusters array

The GT-5 project is a new initiative to develop a tracking germanium clusters array for the next generations of in-beam γ-ray experiments. The array will be a crucial platform for future reaction studies at the upgraded RIBF that will be steered toward heavier mass regions with a higher level density. The effectiveness of tracking germanium clusters is demonstrated in the preliminary results of HiCARI, where the GRETINA clusters of LBNL and RCNP are instrumental to differentiate complex levels in medium-heavy RIs, especially odd nuclei, and also to measure lifetimes down to 10 ps with fast RI beams at 200 ~ 300 MeV/u.

It is envisioned that the GT-5 array will be coupled to auxiliary devices, such as the knockout particle tracker STRASSE (for the precise reaction vertex in a thick cryogenic target) or to the new scintillator array. The high vertex resolution of the former can be capitalized with the high position sensitivity of GT-5. The latter provides a high efficiency for γ-ray detections. The integration of the two arrays will help the γ-γ coincidence analysis beyond the first 2^+ state.

The Nishina Center envisions to procure two quad-type GRETINA clusters under the framework of the TRIP (Transformative Research Innovation Platform of RIKEN platforms) starting in FY2023 (R5). The first cluster (T1) has been ordered in April 2023 with a delivery date set at the end of March 2024, while the second (T2) is planned after 5 years. The first cluster will be commissioned in 2024 and used to collect high-quality data with RI beams to fulfill the mission of the TRIP project. The detector will also be put into physics programs. A campaign-type project can be considered with other clusters in the RCNP and in other laboratories.

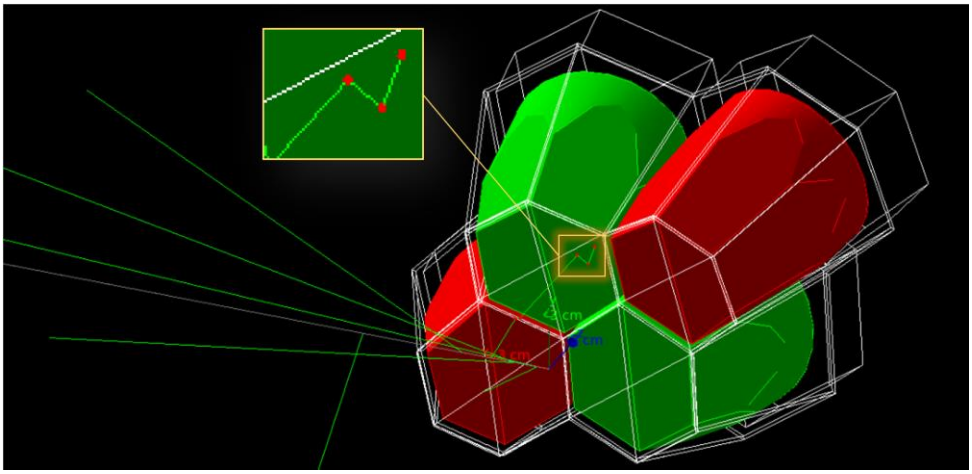

Figure 5.8 GEANT4 simulation of γ-ray interactions in a GRETINA cluster. In this specific event, the γ-ray interacts multiple times in a crystal by Compton scattering.

5.2.3 R3 isomer beam filter

The R3 isomer beam filter is a new application of the isochronous storage ring to provide isomeric beams tagged or filtered by the mass-TOF information. The R3 is capable of measuring the mass of an ion from TOF while revolving inside the ring. Isomeric states are thus tagged by the mass (or excitation energy) information, after minimum 50 μs of revolution. The fast kicker system (currently having 100 ns for the rise and fall, and also for the flat-top duration) can handle the extraction of a single ion from the ring. Extracted ions are then delivered to a reaction station downstream and scattered by a reaction target. The reaction events recorded at this station will be correlated with the tagging information provided by the R3, thus enabling to sort out the events associated with an isomeric state. Furthermore, a physical filtering of isomeric states is feasible if the lifetime is long (> 50 ms). When the revolutions build a sufficient time gap between an isomeric state and the ground state, the kicker system can exclusively filter the isomeric state ions by shuting down the kicker field for the ground state ions.

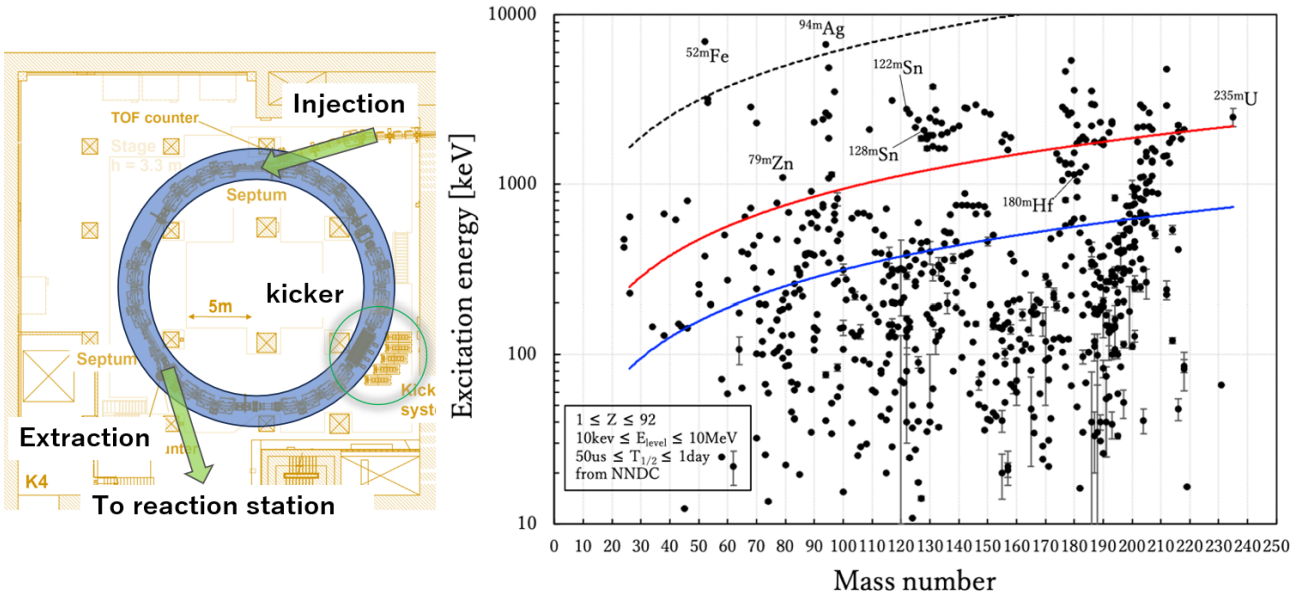

Figure 5.9 (Left) Concept of the isomer beam filtering with the R3. (right) The limits of isomer tagging by the TOF-mass measurement method. The curves denote the minimum excitation energies required to differentiate an isomeric state from the ground state. The known isomer data with lifetimes longer than 50 μs (necessary for TOF measurements at the R3) are compared to the limits with the present (red line) and upgraded R3 (blue

line). For reference, the non-storage measurement for the flight from BigRIPS F3 to SHARAQ S0 (about 500 ns) is compared by the dashed line.

With the current performances of the R3, isomers at energies higher than 1 MeV and with a lifetime longer than 100 ms are only feasible for the filtering. In addition, the extraction efficiency is limited to 1 pps by the kicker, which constrains the application to reaction studies. To enhance the performance of the isomer beam filter, two major upgrades are planned. One is to improve the isochronism level. This will help improve the mass precision, and thus the excitation energy resolution. The isochronism is currently limited to 3 ppm r.m.s. by the fluctuation of the magnetic field, which comes from the instability of the power supply current. The control system of the power supply will be upgraded to eliminate this instability to achieve the isochronous level of 1 ppm. The other upgrade is related to the kicker system. A new power supply module will be able to drive the kicker more frequently, improving the extraction efficiency by roughly 100 times (from 1 pps to 100 pps). It also enables a more instant rise and fall of the magnetic field (about 30 ns with respect to the present system with 100 ns) and a shorter flat top duration (about 30 ns compared to 100 ns). A narrower window (~90 ns) allows to extract the isomer of interest more efficiently. With these upgrades, it will be possible to extract an isomeric state (A~125) at 1 MeV for a lifetime down to 10 ms (currently 100 ms). If the lifetime is about 40 ms, the excitation energy range is expected to go down to as low as 300 keV.

Other necessary developments include a vacuum baking system for better vacuum pressures and a more sensitive schottky device.

5.2.4 MESA: Measurement of Elastic Scattering Anytime, anywhere, any beam

The MESA project is an initiative to collect elastic scattering data systematically over the nuclear chart to ultimately establish a global optical model potential that can reliably be used for RI beam-induced reactions. The global optical model potentials presently available are tuned with stable targets data. It is desirable to calibrate the potentials with data of various RI beams. In addition, it is also interesting in terms of reaction mechanisms how RIs would alter optical model potentials. To collect systematic data of elastic scattering for various RI beams, the idea of MESA is to deploy dedicated setups consisting of telescopes and a thin CH_2 target (about 100 μm) to several locations on the secondary beamlines. The MESA stations will always collect elastic scattering data in parallel with the main experiments running downstream of the beam line. The idea of such a parallel data taking existed in the past, but the implementation has been difficult due to the limited efficiency of data acquisition (DAQ) systems. The new DAQ system described in Section 5.2.7 is expected to tremendously improve the efficiency, thus facilitating the parallel data taking.

The project has been initiated in 2023 under the framework of the TRIP. A pilot study is planned in 2023 and 2024 by three compact telescopes of the Si-Si-CsI/GAGG three detector layer configuration.

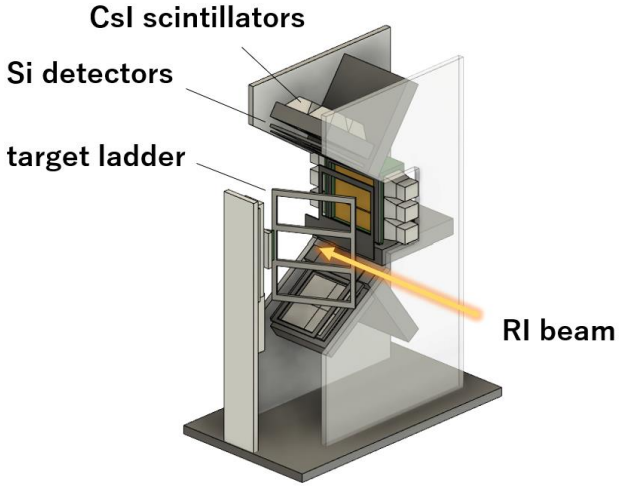

Figure 5.10 MESA prototype for elastic scattering measurements. The prototype consists of a target ladder and three telescopes, each consisting of a pair of Si detectors in stack for ΔE, followed by CsI/GAGG

calorimeters.

5.2.5 RUNBA: Recycled-Unstable-Nuclear Beam Accumulator

RUNBA is a storage ring of RI beams to boost the lumnisity for low-enegy reaction studies and a test bench for RI + RI reaction measurements in future. In a conventional setup, an RI beam delivered by BigRIPS is bombarded onto a reaction target only once, having most of the beam particles left unreacted and discarded. RUNBA is a solution to enhance the luminosity by revolving RI beams in its ring to allow multiple interactions with an internal target (10^{18} /cm^2). To address the emittance growth and energy loss due to the interactions with the target, RUNBA will correct for the deviation from the central trajectory on an event-by-event basis based on the monitoring of each particle passage position on the target and will also compensate the energy loss by an RF accelerating field. As a result, RUNBA is expected to revolve beam particles at 1 MHz and realize the luminosity of 10^{24} /cm^2/s even for less than 10 particles. The development is ongoing under the collaboration with the Kyoto University Institute for Chemical Research. The storage ring sLSR was relocated from Kyoto to the E21 room of the RIBF to develop a prpototpye. It is planned to deliver RI beams from the ISOL facility of SCRIT and to measure astrophysical reactions or particle transfer reactions. In future, RUNBA will be coupled to the SCRIT target to realize RI + RI reaction studies.

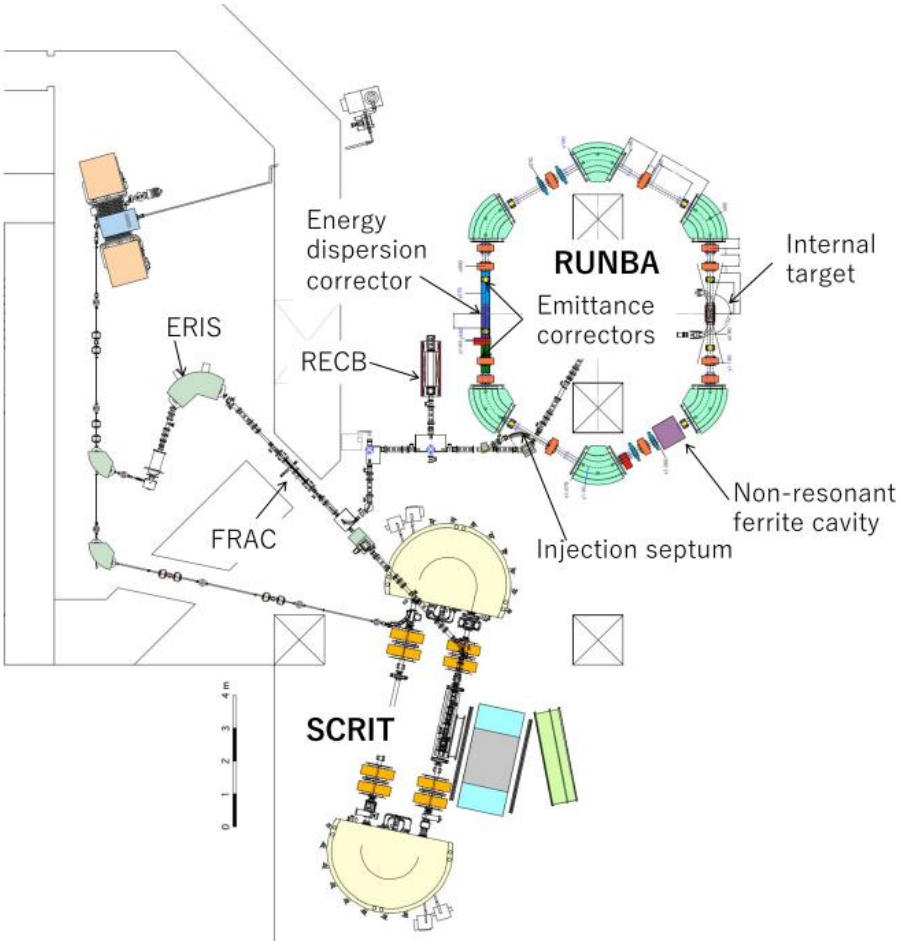

Figure 5.11 Schematic layout of RUNBA installed in the experimental vault of SCRIT.

5.2.6 KISS-II

The KISS-II project is aimed at constructing an upgraded facility based on the KISS technologies to expand the RI production area from the neutron-rich $N = 126$ region towards actinide isotopes. The KISS-II facility consists of four key components: a gas-filled superconducting solenoid filter, a large helium gas cell, a variable mass range separator and MRTOF-MS. Heavy element RIs are produced by deep-inelastic scattering, as it is adopted in KISS. The gas-filled solenoid filter transmits outgoing RIs at large angles into the helium gas cell, while intercepting the primary beam at zero degrees before the cell. This allows to increase the primary a

plasma and realizes an extraction efficiency of 1% or higher, which is ten times better than the present Ar gas cell of KISS. The variable mass range separator can select five different masses at the mass dispersive mid-focal plane between the two dipole magnets and transmit various ions to the MRTOF-MS, which identifies the ions based on precise mass measurements. The tagged ions are then available for decay spectroscopy. The total efficacy of KISS II is about 10,000 times higher than KISS. The upgraded performance will open the access to the region from N = 126 to the actinides previously unavailable for experimental studies, and yet highly important for the r-process nucleosynthesis.

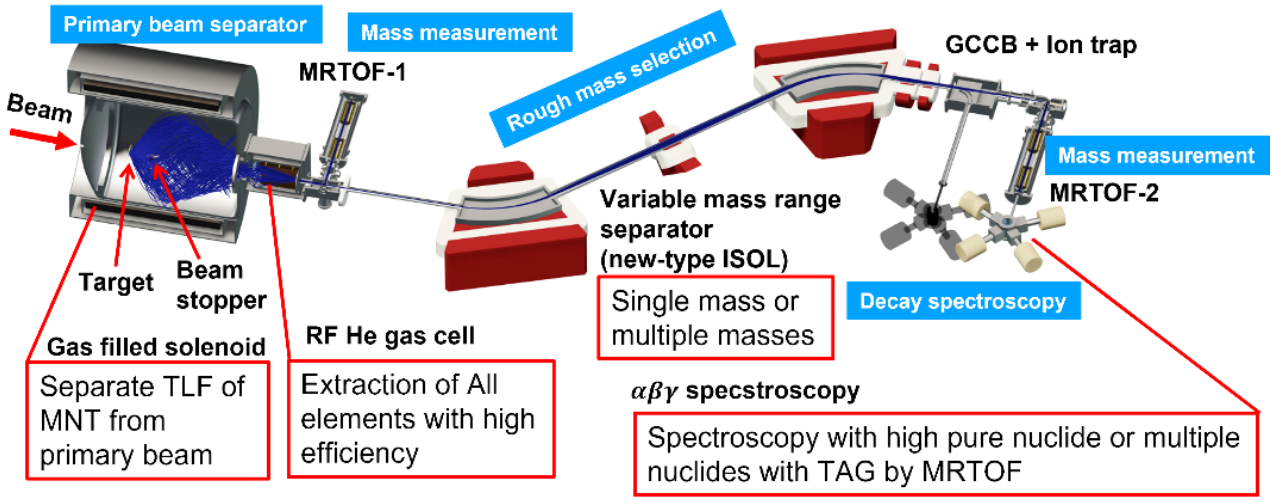

Figure 5.12 Schematic layout of KISS II.

5.2.7 Upgrade of the RIBF data acquisition system

The DAQ system of the RIBF has progressively been upgraded since 2007. A network-distributed system based on the CAMAC technology was developed in 2007. This system supports the trigger rate up to about 1 kHz. Around 2018, the MPV system was developed for the parallel readout of multiple VME crates. This system can handle the trigger rate up to about 10 kHz.

An upgrade project is currently underway with the completion planned around 2025. The goal is to establish a DAQ system adapted to the trigger rate of about 100 kHz. With this new system, all data can be recorded up to the beam intensity of 100 kHz without event selections on a hardware basis. The front-end electronics are under development in-house since this performance cannot be realized with commercial ADC/TDC modules. The developing items include (1) a high energy and time resolution system based on a 4GHz ADC (Xilinx RFSoC) module for plastic and diamond detectors, (2) a medium resolution multi-channel TDC on a FPGA basis for PPAC and drift chambers, (3) a 125 MHz digitizer system for ion chambers, NaI(Tl) detectors and silicon semiconductor detectors, (4) a high precision clock distributor, which ensures precise clock synchronization (about 20 ps in r.m.s.) among sub-DAQ systems deployed in several experimental vaults at distance. This enables the functionalities that are not feasible with the conventional trigger-based DAQ, for instance, the determination of TOF based on synchronized clocks, or the free-streaming data collection.

5.3 References

[BAR21] J. Barney et al., Rev. Sci. Instrum. 92, 063302 (2021).
https://doi.org/10.1063/5.0041191
[KAJ13] D. Kaji et al., Nucl. Instrum. Methods Phys. B 317B, 311 (2013).
https://doi.org/10.1016/j.nimb.2013.05.085
[KOB13] T. Kobayashi et al., Nucl. Instrum. Methods Phys. B 317B, 294 (2013).
https://doi.org/10.1016/j.nimb.2013.05.089
[KON20] Y. Kondo et al., Nucl. Instrum. Methods Phys. B 463, 173 (2020).
https://doi.org/10.1016/j.nimb.2019.05.068

[KUB12] T. Kubo et al., Prog. Theor. Exp. Phys. 2012, 03C003 (2012).
https://doi.org/10.1093/ptep/pts064
[LIU23] H.N. Liu et al., Nucl. Instrum. Methods Phys. A 59, 121 (2023).
https://doi.org/10.1140/epja/s10050-023-01018-3
[LEE23] J. Lee et al., Nucl. Instrum. Methods Phys. B 540, 259 (2023).
https://doi.org/10.1016/j.nimb.2023.04.023
[MIC19] S. Michimasa et al., Prog. Theor. Exp. Phys. 2019, 043D01 (2019).
https://doi.org/10.1093/ptep/ptz007
[MIK23] K. Miki et al., Nucl. Instrum. Methods Phys. A 1056, 168583 (2023).
https://doi.org/10.1016/j.nima.2023.168583
[OBE14] A. Obertelli et al., Eur. Phys. J. A 50, 8 (2014).
https://doi.org/10.1140/epja/i2014-14008-y
[OKA94] H.Okamura et al., AIP Conf. Proc. 293, 84 (1994).
https://doi.org/10.1063/1.45151
[OHN13] T. Ohnishi et al., Nucl. Instrum. Methods Phys. B 317B, 357 (2013).
https://doi.org/10.1016/j.nimb.2013.07.029
[OTA15] S. Ota et al., J. Rad. and Nucl. Chem. 305, 907 (2015).
https://doi.org/10.1007/s10967-015-4130-5
[ROS23] M. Rosenbusch et al., Nucl. Instrum. Methods Phys. A 1047, 167824 (2023).
https://doi.org/10.1016/j.nima.2022.167824
[SAK17] H. Sakaguchi and J. Zenihiro, Prog. Part. Nucl. Phys. 97, 1 (2017).
https://doi.org/10.1016/j.ppnp.2017.06.001
[SOD13] P.-A. Söderström et al., Nucl. Instrum. Methods Phys. B 317B, 649 (2013).
https://doi.org/10.1016/j.nimb.2013.03.018
[SON18] T. Sonoda et al., Nucl. Instrum. Methods Phys. A 877, 118 (2018).
https://doi.org/10.1016/j.nima.2017.09.055
[STU17] L. Stuhl et al., Nucl. Instrum. Methods Phys. A 866, 164 (2017).
https://doi.org/10.1016/j.nima.2017.06.015
[TAK14] S. Takeuchi et al., Nucl. Instrum. Methods Phys. A 763, 596 (2014).
https://doi.org/10.1016/j.nima.2014.06.087
[TOG20] Y. Togano et al., Nucl. Instrum. Methods Phys. B 463, 195 (2020).
https://doi.org/10.1016/j.nimb.2019.05.049
[TOL19] A. Tolosa-Delgado et al., Nucl. Instrum. Methods Phys. A 925, 133 (2019).
https://doi.org/10.1016/j.nima.2019.02.004
[UES12] T.Uesaka et al. Prog. Theor. Exp. Phys. 2012, 03C007 (2012).
https://doi.org/10.1093/ptep/pts042
[WAD03] M. Wada et al., Nucl. Instrum. Methods Phys. B 204, 570 (2003).
https://doi.org/10.1016/S0168-583X(02)02151-1
[WAK05] T. Wakui et al., Nucl. Instrum. Methods Phys. A 550, 521 (2005).
https://doi.org/10.1016/j.nima.2005.05.062
[WAT18] Y. Watanabe et al., Nuclear Physics News 28, 25 (2018).
https://doi.org/10.1080/10619127.2018.1529984
[YAM13] Y. Yamaguchi et al., Nucl. Instrum. Methods Phys. B 317, 629 (2013).
https://doi.org/10.1016/j.nimb.2013.06.004
[YAM23] H. Yamaguchi et al., Nuclear Physics News 30, 21 (2023).
https://doi.org/10.1080/10619127.2020.1717263
[YAS16] J. Yasuda et al., Nucl. Instrum. Methods Phys. B 376, 393 (2016).
https://doi.org/10.1016/j.nimb.2016.02.007

6 Role of RIBF upgrade in the regional and international community

The experimental programs accompanied with the RIBF upgrade are internationally unique and competitive with the newly constructed inflight facility in US, FRIB (https://frib.msu.edu/) and new other facilities under construction, FAIR (Germany) (https://fair-center.eu/), RAON (Korea) (https://risp.ibs.re.kr/html/risp_en/) and HIAF (China) (https://hiaf.impcas.ac.cn/hiaf_en/public/). It should be noted that part of programs with the RIBF upgrade can encourage the nuclear engineering community. From now on these facilities are compared with the upgraded RIBF in terms of primary beam energy and intensity, and reaction-study setup.

These facilities are categorized into two parts in terms of heavy-ion accelerator: synchrotron and linac.

The synchrotron inflight facilities are FAIR and HIAF. The FAIR facility is consisted of the S100 synchrotron and super-FRS separator. The maximum energy of heavy ions accelerated at S100 is 2.7 GeV/u for uranium ions with intensity of 5×10^{11}/cycle. One cycle composes of acceleration period of 1 sec and slow extraction period. A typical extraction period of 1sec leads to a duty factor of 50%, and hence the intensity is 2.5×10^{11}/sec on average. At present, the RIBF facility has delivered a 345 MeV/u uranium beam with intensity of 6×10^{11}/sec. The intensity will be increased by a factor of 20 at the upgraded RIBF facility to be 1.2×10^{13}/sec, which is about 50 times higher than that of FAIR. Concerning a spectrometer for analyzing secondary reaction products, FAIR has only one spectrometer proposed, the R3B spectrometer which is an open-geometry spectrometer. In general, momentum resolution of such an open-geometry spectrometer is limited up to 0.1% level, which could be compared with momentum resolution of 0.01% at ZeroDegree and SHARAQ spectrometers at RIBF.

The new facility, HIAF is under construction in China. One superconducting linac and one synchrotron is being constructed. The linac coupled with a powerful ion source can accelerate heavy ions up to an energy of 17-22 MeV/u, which are utilized for low-energy nuclear reaction studies. The synchrotron will boost up the energy of heavy ions injected with the linac, up to a few GeV/u. Energy and intensity of a uranium beam at the synchrotron is about 1 GeV/u and 5×10^{11}/cycle, respectively. These are the same as those of FAIR. The beams accelerated at the synchrotron will be utilized for inflight production of RI beams. The physics programs with the fast RI beams are still under discussion and spectrometers newly constructed are to be funded.

The brand-new facility in US, FRIB started in operation in 2022. The FRIB facility is consisted of a super-conducting linac and the ARIS inflight separator. The ARIS separator was uniquely designed to have a large momentum acceptance and also to have three stages of pre-separation, post-separation and particle identification. The energy of a uranium beam is about 200 MeV/u, and the goal intensity is 5×10^{13}/sec. The goal intensity is about 4 times larger than that of the upgraded RIBF. By considering thickness of primary and secondary targets, total luminosity for reaction study at RIBF is a few times higher than that of FRIB. A new spectrometer system HRS is being constructed and will be completed in 2027. Before HRS completed, the S800 spectrometer can serve for analyzing reaction products, but the magnetic rigidity of S800 is limited up to 4 Tm; the luminosity for reaction study with neutron-rich RI beams is limited because of the limitation of the magnetic rigidity.

The RAON facility in Korea is consisted of three sets of accelerators: K70 cyclotron as a driver for ISOL with a beam power of 70 kW at maximum, two sets of superconducting linac (SCL3 and SCL2). Energy of heavy ions accelerated at SCL3 is a few 10 MeV/u, and that at SCL2 is a few 100 MeV/u. Two inflight separators are coupled with SCL3 and SCL2, respectively. The separator coupled with SCL3, “KoBRA” was designed to produce relatively light RI with A<40. The separator for SCL2 beams, “IF” was optimized for fission products with a 200 MeV/u uranium beam with intensity of 5×10^{13}/sec. The goal energy and intensity are the same as those of FRIB. One of the unique features of RAON is that RIs produced at the ISOL can be post-accelerated up to a few 10 MeV/u at SCL3 and a few 100 MeV/u at SCL2, and ^{140}Xe at 222 MeV/u with an intensity of 10^7/sec can produce neutron-rich isotopes with Z<50. Spectrometers coupled with the IF

separator are under discussion.

As discussed above, the upgraded RIBF facility will play a leading role in both the regional and international community, especially for experimental programs with reaction study. The RIBF upgrade aims to maximize research potentials of inflight RI beams in terms of reaction study as well as a variety of radioactive isotopes toward a heavy mass region.

7 Cost, Schedule, and Status

The cost and schedule for the RIBF upgrade are shown in Table 7.1. This project is eight-year plan. The first five years are devoted to achieving 500 pnA intensity of a uranium beam and high purification of the RI beams. At the end of eighth year, the intensity will reach to 2000 pnA and the BigRIPS will be upgraded for high power beam. Total cost necessary for the facility upgrade is 22.4 B¥ (224 M$ in case of 1$=100¥). Subtotal for the accelerator upgrade and the BigRIPS and ZeroDegree upgrade are 17.3 B¥ and 5.1 B¥, respectively. Additionally required manpower for the accelerator staff and the inflight-separator staff are 12 and 5 permanent staff members, respectively.

This proposal of RIBF upgrade has been submitted to “Science Council of Japan” (Japanese Academy) and MEXT (Ministry of Education, Culture, Sports, Science and Technology), respectively, under collaboration with Univ. of Tokyo (CNS), KEK (WNSC), and Osaka Univ. (RCNP). Science Council of Japan is discussing a long-range plan of academic activities in Japan and defining the role of the RIBF upgrade. MEXT will review proposals of large-scale project/facility, prioritize the proposals and summarize a short list of promising proposals as a “roadmap” in 2023. The operation cost including 8-month machine time is requested, too. The RIBF upgrade proposal has been strongly supported by the nuclear experimental physics community in Japan and RIBF User-Executive-Committee and endorsed by the RIKEN management.

Table 7.1 Cost and Schedule of the RIBF upgrade

Year	1	2	3	4	5	6	7	8	9
Total Cost	22.4 BYen								
Accelerator System	17.3 BYen								
Injection system upgrade for IRC	design	construction	installation						
CSR1	design	design	construction	construction	installation				
ECR-IS upgrade	design	construction	construction	construction	installation				
SRC-RF upgrade	design	construction	construction	construction	installation				
fRC-RF upgrade		design	construction	construction	installation				
Infrasstructure upgrade	design	construction	installation						
CSR2			design	design	design	construction	construction	installation	
BigRIPS and ZeroDegree	5.1 BYen								
BigRIPS first stage for high power beam			design	design	design	construction	construction	installation	
BigRIPS first stage for high purity beam	design	design	construction	construction	installation				
Spectrometer upgrade			design	design	design	construction	construction	installation	
Achievement Goal									
Beam intensity						500 pnA			2000 pnA

8 About this document

This document is a report on the RIBF facility upgrade project. It was submitted to the Nishina Center Advisory Committee for the review meeting held in July 2023.

The report was authored by the following members of the RNC:
Hiroshi Imao, Osamu Kamigaito, Masaaki Kimura, Hiroyoshi Sakurai, Daisuke Suzuki, Hiroshi Suzuki, Hideki Ueno, and Tomohiro Uesaka.

The future plan outlined in the report also owes much to the members of the RIBF Future Plan Working Group:
The theory subgroup with Yoshihiro Aritomo, Shuichiro Ebata, Tokuro Fukui, Nobuo Hinohara, Wataru Horiuchi, Futoshi Minato, Takayuki Miyagi, Tomoya Naito, Nobuya Nishimura, Kazuyuki Sekizawa, Hajime Sotani, Hiroyuki Tajima, Kota Yanase, Kenichi Yoshida, Sota Yoshida, and Masaaki Kimura as a coordinator.
The experiment subgroup with Hidetada Baba, Pieter Doornenbal, Naoki Fukuda, Shintaro Go, Tadaaki Isobe, Daiya Kaji, Yue Ma, Sarah Naimi, Megumi Niikura, Tetsuya Ohnishi, Masaki Sasano, Tetsu Sonoda, Toshiyuki Sumikama, Hiroshi Suzuki, Aiko Takamine, Kenichiro Tateishi, Yoshitaka Yamaguchi, and Daisuke Suzuki as a coordinator.
The accelerator subgroup with Taihei Adachi, Yoshihide Higurashi, Yasuto Miyake, Yasuyuki Morita, Takashi Nagatomo, Takahiro Nishi, Kazutaka Ozeki, Glynnis Mae Quinones Saquilayan, Kenji Suda, Akito Uchiyama, Kazunari Yamada, and Hiroshi Imao as a coordinator.

The other RNC members who contributed to this report include:
Yuto Hijikata, Hironobu Ishiyama, Koji Morimoto, Shunji Nishimura, Hideaki Otsu, Yohei Shimizu, Yasuhiro Togano, Ken-ichiro Yoneda, Koichi Yoshida and Masahiro Yoshimoto.

The inputs from the following external colleagues are gratefully acknowledged.
Nobuaki Imai (CNS, University of Tokyo)
Shin'ichiro Michimasa (CNS, University of Tokyo)
Kenjiro Miki (Tohoku University)
Shinsuke Ota (RCNP, Osaka University)
Kimiko Sekiguchi (TITECH)
Yutaka Watanabe (KEK)
Hidetoshi Yamaguchi (CNS, University of Tokyo)
Juzo Zenihiro (Kyoto University)